

On Model Selection Criteria for Climate Change Impact Studies*

Xiaomeng Cui[†] Bulat Gafarov[‡] Dalia Ghanem[§] Todd Kuffner[¶]

December 15, 2024

Abstract

Climate change impact studies inform policymakers on the estimated damages of future climate change on economic, health and other outcomes. In most studies, an annual outcome variable is observed, e.g. agricultural yield, annual mortality or gross domestic product, along with a higher-frequency regressor, e.g. daily temperature. While applied researchers tend to consider multiple models to characterize the relationship between the outcome and the high-frequency regressor, a choice between the damage functions implied by the different models has to be made to inform policy. This paper formalizes the model selection problem and the policy objective in this empirical setting in light of current empirical practice. We then show that existing model selection criteria are only suitable for the policy objective under specific conditions. These conditions include a requirement that one of the models under consideration nests the true model. To overcome this restriction, we propose a new criterion, the proximity-weighted mean-squared error (PWMSE) of predicting climate change impacts. The PWMSE targets the policy objective of predicting the impact of projected climate change directly by giving higher weight to prior years with weather closer to the projected scenario. We show that our approach selects the best approximate regression model that has the smallest weighted error of predicted impacts for a future climate scenario. A simulation study and an application revisiting the impact of climate change on agricultural production illustrate the empirical relevance of our theoretical analysis.

Keywords: mixed frequency data, Monte Carlo cross-validation, information criteria, aggregation

**Corresponding Author:* Dalia Ghanem, dghanem@ucdavis.edu. The authors are grateful to Felix Pretis, Zack Miller, Ariel Ortiz-Bobea and Glenn Rudebusch for helpful comments and suggestions. We also thank participants at the World Congress of the Econometric Society 2020 and the Climate Econometrics Virtual Seminar.

[†]Jinan University, cuixiaomeng@jnu.edu.cn.

[‡]UC Davis, bgafarov@ucdavis.edu

[§]UC Davis, dghanem@ucdavis.edu.

[¶]Washington University, St. Louis, kuffner@wustl.edu.

1 Introduction

Using panel data, impacts of climate change have been extensively studied on aggregate economic productivity (Burke et al. 2015; Dell et al. 2012; Hsiang 2010), micro-level productivity and economic returns (Addoum et al. 2020; Deryugina and Hsiang 2017; Somanathan et al. 2021; Zhang et al. 2018), agricultural profits and crop production (Aragón et al. 2021; Burke and Emerick 2016; Cui 2020; Deschênes and Greenstone 2007; Schlenker and Roberts 2009), energy consumption (Auffhammer et al. 2017; Li et al. 2019; Wenz et al. 2017), migration and labor allocation (Cattaneo and Peri 2016; Feng et al. 2010; Jessoe et al. 2018; Mueller et al. 2014), human capital (Garg et al. 2020; Graff Zivin et al. 2018; Park et al. 2020), health and mortality (Barreca et al. 2016; Burke et al. 2018; Deschênes and Greenstone 2011; Heutel et al. 2021), and conflicts (Harari and Ferrara 2018; Hsiang et al. 2011, 2013).

While researchers tend to consider multiple models in their analysis of the relationship between the outcome and temperature, both researchers and policymakers have to choose between the implied damage functions. These chosen functions not only inform policy design regarding climate adaptation in specific sectors and locations, but they also serve as empirical foundations for quantifying the social cost of carbon and influence decision-making on mitigating and adapting climate change at the regional and global scale (Dell et al. 2014; Diaz and Moore 2017; Ricke et al. 2018). This paper formalizes the model selection problem and policy objective in climate change impact studies, evaluates the suitability of existing criteria and proposes a new model selection criterion that directly targets the policy objective.

In typical climate change impact studies, for $i = 1, 2, \dots, n$, $t = 1, 2, \dots, T$, we observe an outcome Y_{it} and a regressor W_{ith} , which is observed at a higher frequency $h = 1, 2, \dots, H$. Practitioners tend to present results for a set of models $\{\mathbf{M}_\alpha\}_{\alpha=1}^A$, where each model uses different summary statistics of the higher-frequency weather variable as a model of the response function, $\mu_\alpha(\mathcal{W}_{it})$, of the outcome to the high-frequency regressor time series, $\mathcal{W}_{it} \equiv \{W_{ith}\}_{h=1}^H$. Among the most commonly used summary statistics of temperature are the annual average (e.g., Dell et al. 2012), various degree day measures (e.g., Burke and Emerick 2016), seasonal averages (e.g., Mendelsohn et al. 1994) as well as temperature bins (e.g., Deschênes and Greenstone 2011). To capture nonlinearities in the annual average temperature, a quadratic function has also been employed (e.g., Burke et al. 2015). For a given α , \mathbf{M}_α specifies a linear model,

$$Y_{it} = \mu_\alpha(\mathcal{W}_{it}) + a_{i,\alpha} + u_{it,\alpha}. \quad (1)$$

Here, $a_{i,\alpha}$ is a fixed effect and $u_{it,\alpha}$ constitutes idiosyncratic shocks. In practice, additional covariates, year fixed effects and flexible time trends are included. To simplify our presentation, we do

not include these additional features. However, our analysis extends in a straightforward manner to accommodating them as we illustrate in our empirical applications.

Our first contribution is to formalize the model selection problem and policy objective in the climate change impacts literature. To do so, we first provide a review of recent work published in leading economics journals with a focus on modeling the response function between an outcome and temperature. Building on the review, we show that the response functions used in this literature can be characterized as follows,

$$\mu_\alpha(\mathcal{W}_{it}) = X'_{it,\alpha}\beta_\alpha, \quad (2)$$

$$X_{it,\alpha} = \psi_\alpha \left(\sum_{h=1}^H f_\alpha(W_{ith})' \phi_{\alpha,h} \right), \quad (3)$$

where $f_\alpha(\cdot)$ is a possibly nonlinear transformation of the high-frequency regressor, W_{ith} , $\phi_{\alpha,h}$ is a weight given to $f_\alpha(W_{ith})$, and $\psi_\alpha(\cdot)$ is a transformation of the aggregated transformed weather variable, where f_α , $\phi_{\alpha,h}$ and ψ_α are all finite-dimensional and known given the regressor.¹ Formalizing the class of models in the empirical literature allows us to define nested, non-nested overlapping and strictly non-nested models as well as formalize the policy objective of climate projections.

The policy objective can be specifically represented as forecasting the impact of the change in climate in period T from \mathcal{W}_{iT} to $\mathcal{W}_{i,T+\tau}^f$, the projected climate in a future period $T + \tau$, for an outcome of interest in the set of cross-sectional units in a given study, $i = 1, \dots, n$. Suppose that the outcome is given by the true model, \mathbf{M}_\star ,

$$Y_{it} = \mu_\star(\mathcal{W}_{it}) + a_i + u_{it}, \quad (4)$$

where $\mu_\star(\cdot)$ is the true response function. To fulfill the policy objective in climate change impact studies, the prediction should be based on a causal parameter, specifically the change in the true response function, $\mu_\star(\cdot)$, due to the projected climate change. However, since the true model, \mathbf{M}_\star , corresponding to the causal parameter is unknown, policymakers tend to consider different models and have to rely on a criterion to choose between them.

With the formal expression of the policy objective, we proceed to define the ideal mean-squared error (MSE) target for this policy problem, specifically

$$E[(\mu_\alpha(\mathcal{W}_{i,T+\tau}^f) - \mu_\alpha(\mathcal{W}_{iT}) - (\mu_\star(\mathcal{W}_{i,T+\tau}^f) - \mu_\star(\mathcal{W}_{iT})))^2], \quad (5)$$

which is the mean of squared errors in predicting the climate change impact using the model \mathbf{M}_α . This ideal target allows us to assess the suitability of existing criteria, such as Monte Carlo cross-validation (MCCV) and Generalized Information Criteria (GICs), for this policy objective. A formal

¹In Appendix B, we define f_α , $\phi_{\alpha,h}$ and ψ_α for the models in our literature review.

analysis of the asymptotic properties of these criteria illustrates that consistent model selection criteria are suitable for this policy objective *if* at least one of the models under consideration nests the true model.² To do so, we extend results from the classical literature on MCCV and GICs (Shao 1993, 1997; Sin and White 1996; Vuong 1989) to the mixed-frequency panel data setting in the climate change impacts literature. We show that MCCV with a vanishing training-to-full sample ratio and the criteria proposed in Sin and White (1996) are model selection consistent in the context of climate change impact studies assuming that one of the models under consideration nests the true model.³ While this assumption is plausible for outcomes with a clear and well-studied physical relationships with weather, it is not plausible for a wide range of economic outcomes of interest. If none of the models under consideration nest the true model, however, consistent model selection criteria are not guaranteed to select models that perform well in terms of the ideal MSE target for the policy objective given in (5).⁴ We therefore proceed to propose an alternative criterion suitable for the policy objective regardless of the models under consideration.

Building on our formal definition of the policy objective, we propose a new criterion that mimics the (infeasible) ideal MSE target in (5). The criterion we propose is based on a proximity-weighted mean squares of the errors (PWMSE) in predicting the impact of the change in climate between year T relative to prior years available in the data $T - r$ for $r = 1, \dots, T - 1$,

$$PWMSE_{\alpha} = \sum_{r=1}^{T-1} E[(\mu_{\alpha}(\mathcal{W}_{i,T-r}) - \mu_{\alpha}(\mathcal{W}_{iT}) - (\mu_{\star}(\mathcal{W}_{i,T-r}) - \mu_{\star}(\mathcal{W}_{iT})))^2 \pi(\mathcal{W}_{i,T-r}, \mathcal{W}_{i,T+\tau}^f)]. \quad (6)$$

The weighting function in the PWMSE is designed to give higher weight to prior years in the sample that are more similar to the projected future climate at $T + \tau$. The weighting function therefore ensures that the selected model performs well in terms of predicting the impacts of projected climate change from \mathcal{W}_{iT} to $\mathcal{W}_{i,T+\tau}^f$ in line with the policy objective.

To estimate the PWMSE, we propose an MCCV procedure and show that the model that minimizes the estimated PWMSE minimizes the population PWMSE with probability approaching one as the sample size grows. We demonstrate numerically that the simulated ideal MSE target is minimized by the true model as well as models that nest it in our simulation examples. We also conduct a simulation study to examine the finite-sample performance of the estimated PWMSE. Our simulations demonstrate that the PWMSE criteria tend to select the true model or models that nest it with high probability when these models are under consideration. When all models

²Let \mathbf{M}_{\star} denote the true model and $\widehat{\mathbf{M}}_C$ denote the model selected by criterion C , a criterion is said to be model selection consistent if $P(\widehat{\mathbf{M}}_C = \mathbf{M}_{\star}) \rightarrow 1$ as sample size grows. For additional discussion see Section 3.1.

³Appendix D provides a detailed simulation study on the finite sample behavior of these criteria.

⁴The criteria proposed in Sin and White (1996) retain the property of pseudo-model selection consistency, whereas the MCCV with vanishing training-to-full sample ratio is not. For a definition of pseudo-model selection consistency and related discussions see Section 3.1.

are misspecified, it is more likely to select the model that minimizes the simulated ideal MSE target. We also examine the finite-sample performance of the PWMSE with different choices for the weighting function and provide guidance to practitioners on the choice of weighting function in Appendix F.

To illustrate the empirical relevance of our results, we compare the behavior of existing criteria and our proposed PWMSE in the context of an application revisiting the relationship between temperature and agricultural yield. In this application, while different criteria select different models, the associated damage functions are qualitatively similar — rising temperature becomes detrimental at high temperatures. Consistent with our theoretical predictions, the Sin and White (1996) criteria (SW) choose the smallest among those models. Our proposed criteria of PWMSE, which incorporates the HadCM3-B1 climate scenario in the weighting function, selects a less parsimonious model that provides flexible estimates of the nonlinear relationship consistent with the agronomic literature. Although the models selected by SW and PWMSE criteria result in qualitatively similar damage functions, the quantitative differences between their predicted outcomes matter for policy arrangements on adaptation toward the specific climate scenario projected by HadCM3-B1. This application highlights the value of the PWMSE criterion in terms of ensuring that the selected model targets the policy objective for a given climate change projection.

This paper has practical implications for the use of model selection criteria in climate change impact studies. We show that the existing model selection criteria, although useful, have important limitations in their application to climate change impact studies. The usefulness of consistent model selection criteria is limited to the case when the true model is nested in one of the models under consideration. While this is plausible in applications where the relationship between temperature and the outcome of interest is well-studied, such as for agricultural outcomes, it is restrictive for many other economic outcomes of interest. Therefore, the PWMSE serves as a useful addition to the existing criteria as it ensures improved performance for the policy objective of climate change projections. We emphasize, however, that rather than reporting the results of a particular model selection criterion, applied researchers should report the results of the different model selection criteria we consider, MCCV, GIC and PWMSE. The reasoning behind this recommendation stems from the fact that if the true response function is nested in one or more of the models under consideration, then the different model selection criteria *should* select models that have similar response functions, albeit different numbers of parameters, which is consistent with our theoretical and simulation analysis. The usefulness of reporting the different criteria in interpreting the empirical results is also clearly illustrated in our empirical application.

This paper builds on the literature on the asymptotic properties of model selection criteria (e.g. Arlot and Celisse 2010; Claeskens and Hjort 2008). We build on the literature on the asymptotic

behavior of MCCVs in linear models (Shao 1993, 1997) as well as nonlinear model selection based on GICs (Hong and Preston 2012; Sin and White 1996). The latter strand of the literature builds on the seminal work in Vuong (1989) which shows that the convergence rate of the quasi-likelihood ratio depends on whether the models under consideration are nested or not.⁵

The analysis of model selection consistency in the context of the mixed-frequency panel data models is of independent interest and relates to an important body of work on aggregation in mixed-frequency time series. While the goal in this literature is starkly different from the climate change impacts literature, both share a common theme which is the need to aggregate regressors due to the mixed-frequency nature of the empirical setting. There is a large body of work in the mixed-frequency time series literature providing different aggregation schemes (Andreou and Ghysels 2006; Chambers 2016; Ghysels et al. 2006, 2007; Miller 2016, 2018).⁶ One promising direction for future work that complements existing work on specification testing (Andreou et al. 2010; Groenvik and Rho 2018; Kvedaras and Zemlys 2012; Liu and Rho 2019; Miller 2018) is to adopt the proposed model selection framework to examine the aggregation problem in mixed-frequency time series from the perspective of optimal selection of an approximate model.

The remainder of the paper is organized as follows. Section 2 provides the policy motivation behind the present paper, summarizes current empirical practice, and formalizes the model selection problem and policy objective. Section 3 evaluates the suitability of existing criteria for the policy objective of climate change projections and introduces the PWMSE criterion. Section 4 illustrates the empirical relevance of our theoretical analysis in the context of an empirical application revisiting the relationship between temperature and agricultural yields.

2 Why Model Selection in Climate Change Impact Studies?

Panel estimates of climate change impacts have served as critical inputs for policy making on climate change mitigation and adaptation. In this section, we first briefly introduce the rationale behind the existing empirical studies and review existing methods in recent work. We then formalize the model selection problem and the policy objective in this context, which also provides a foundation for understanding the behavior of existing criteria as well as the rationale behind our proposed PWMSE criteria in Section 3.

⁵Recent work in this literature develops approaches to uniformly valid testing and post-selection inference for non-nested models (Liao and Shi 2020; Shi 2015).

⁶We point to some interesting connections between notions of misspecification bias in this paper and the literature on aggregation in cointegration models (Chambers 2003, 2011; Chambers and McCrorie 2007; Miller 2014, 2016) in Appendix C.

2.1 Damage functions as policy parameters

Designing cost-effective policy on climate change mitigation and adaptation requires a precise and thorough understanding on how the key climatic factor (e.g., temperature) affects human society. In responding to this mission, extensive efforts have been made to properly estimate the economic damage functions, which characterize the quantitative relationship between certain economic outcomes and climatic factors, especially temperature.

The estimated damage functions serve two purposes. From a micro perspective, they help improve the design of regulatory and adaptation policies that target specific contexts. Using agricultural production as an example, Figure 1 shows sharply contrasted warming implications on corn yields in the United States under two distinct but reasonable damage functions. Both panels reflect predicted warming-induced yield losses by 2050 under future temperatures projected by the HadCM3-B1 model. Panel A relies on a damage function empirically estimated based on a specification of monthly average temperatures, while panel B relies on that of linear spline with an endogenously determined knot.⁷ It is clear that the chosen damage function would directly influence policy arrangements on where and how corn production needs to be adapted to mitigate potential losses under future warming.

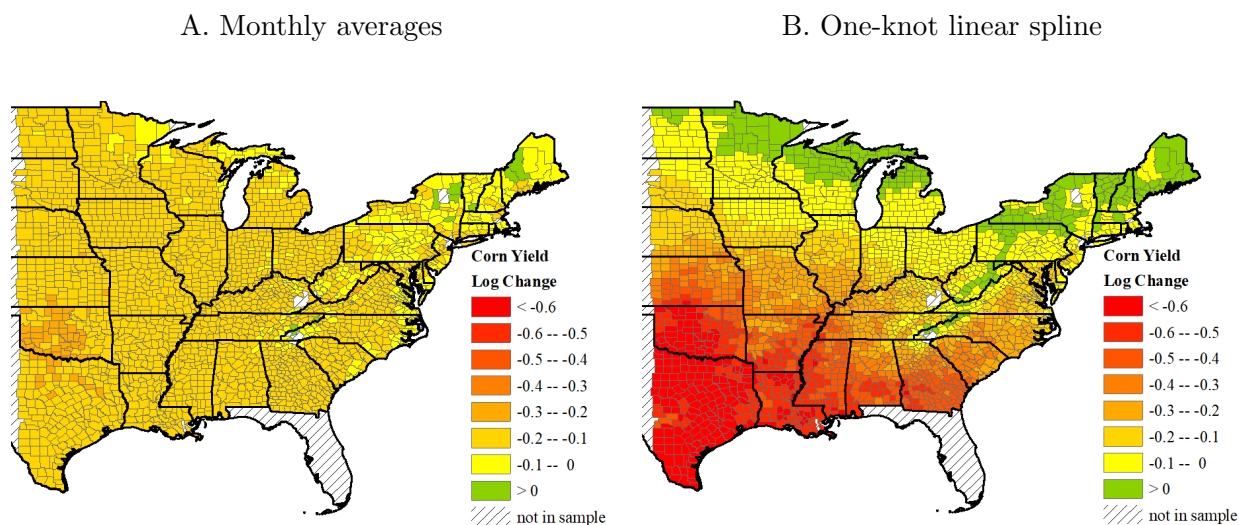


Figure 1: Yield Impacts Projected under Future Climate

Notes: The county-level log changes in corn yields are obtained by applying different empirically estimated damage functions to the temperature of 2050 projected under HadCM3-B1. The damage functions are estimated based on monthly average temperatures in panel A and linear spline with one endogenously determined knot in panel B.

The policy relevance of damage functions is not restricted to policies targeting specific outcomes

⁷We describe the precise steps for obtaining these estimates and projections in Section 4.

and sectors. From a macro perspective, the cost-benefit evaluation of a host of domestic policies as well as international agreements is directly influenced by the estimated social cost of carbon (SCC). Improving this estimate hinges on those damage functions as critical inputs (National Academies of Sciences, Engineering, and Medicine 2017). This point is epitomized in Moore et al. (2017) as they show that the SCC is doubled by simply updating the damage functions of agriculture with the most recent empirical estimates in the FUND model.⁸

2.2 Current Empirical Practice

The empirical studies for pinning down the damage functions typically rely on panel data with large n and relatively small T . For example, the empiricist may observe some economic outcomes at the county level for more than a thousand counties, and the outcomes are observed annually over a period of a few decades. This practice was first initiated in the seminal work of Deschênes and Greenstone (2007) on identifying temperature impacts on agriculture, it then became popular and widely adopted in understanding climatic impacts on many dimensions of the human society.

In this empirical literature, researchers commonly use a panel fixed effects model where, conceptually, the location fixed effects control for impacts of the time-invariant factors like county characteristics.⁹ With this setup, identifying the damage function would mostly rely on year-to-year within-county variation in weather that is arguably exogenous.¹⁰ This empirical approach rests on the validity of the strict exogeneity assumption. To focus our attention on the model selection problem in this literature, we therefore maintain this assumption here.

A critical component in these econometric examinations is to estimate the particularly damaging effects associated with high temperatures, commonly referred to as the nonlinear temperature effects. With raw temperature data observed at a higher frequency than that for the panel regressions, identifying this nonlinearity would require the empiricist to first summarize the high-frequency regressor data in certain ways such that the variables with summarized temperature information can support estimating nonlinear temperature effects.

There is no consensus or best practice on how to implement this process. Empiricists usually make decisions on how they summarize high-frequency temperature information to eventually obtain the estimates on the nonlinearity. In Table 1, we summarize temperature models considered in recent empirical studies in leading economics journals, including the “Top 5” journals, Amer-

⁸The FUND model is a widely used integrated assessment model (IAM) developed by Richard Tol and David Anthoff. See more details at: <http://www.fund-model.org>.

⁹To the best of our knowledge, there are no studies in this literature relying on random effects models.

¹⁰The literature has acknowledged that this year-to-year weather variation is different from long-run climate change, but utilizing the arguably exogenous weather variation for pinning down damage functions is still regarded as highly useful for policy purposes (Auffhammer 2018).

Table 1: Summary of Temperature Models Appeared in Leading Economics Journals since 2015

Article	Journal	Temperature Models Considered						
		mean temp.	max temp.	degree days	bins	poly- nomials	splines	heat index
Levinson (2016)	<i>AER</i>			✓				
Barreca et al. (2016)	<i>JPE</i>				✓			
Somanathan et al. (2021)	<i>JPE</i>			✓	✓	✓		
Busse et al. (2015)	<i>QJE</i>		✓		✓			
Heyes and Saberian (2019)	<i>AEJ-App</i>	✓			✓			✓
Colmer (2021)	<i>AEJ-App</i>	✓		✓	✓			
LoPalo (Forthcoming)	<i>AEJ-App</i>				✓			
Burke and Emerick (2016)	<i>AEJ-Pol</i>			✓				
Park et al. (2020)	<i>AEJ-Pol</i>	✓			✓			
Aragón et al. (2021)	<i>AEJ-Pol</i>			✓	✓			
Cohen and Dechezleprêtre (Forthcoming)	<i>AEJ-Pol</i>				✓			
Liu et al. (Forthcoming)	<i>AEJ-Pol</i>	✓						
Anderson et al. (2017)	<i>EJ</i>	✓						
Jessoe et al. (2018)	<i>EJ</i>			✓	✓			
Jagnani et al. (2021)	<i>EJ</i>			✓	✓			
Adhvaryu et al. (2020)	<i>REStat</i>					✓	✓	
Heutel et al. (2021)	<i>REStat</i>				✓			
Novan et al. (Forthcoming)	<i>REStat</i>	✓					✓	

Notes: This survey covers empirical studies on the Top 5 journals, AEJs, EJ, and REStats since 2015. We focus on studies for which identifying the response function to temperatures is of critical importance. The temperature models are broadly categorized. Within each model category, the specific formulation of the model still varies across different articles. Formal definitions of these models are provided in Appendix B.

ican Economic Journals (*AEJ*), Economic Journal (*EJ*), and Review of Economics and Statistics (*REStat*). We limit our attention to the studies for which identifying the response function to temperature fluctuations is of critical importance for the research question.¹¹

The chosen models vary across different studies, and none of the listed empirical studies adopt a selection rule for determining which model should be used to inform policy.¹² Even though many studies favor the use of degree days and bins, the specific ways of constructing these variables as well as the critical thresholds involved are determined by the empiricists.¹³ It is important to note, however, that the revealed nonlinearity (or the absence of it) obtained from the econometric estimation is shaped or at least indirectly influenced by the decision made on how to summarize the high-frequency regressor data, as we have illustrated in Figure 1. If empiricists improperly summarize the information and adopt a poorly specified model, they could potentially reach biased conclusions on climate change impacts.

In the following subsection, we make precise definitions and formalize the model selection problem and policy objective for these empirical studies on identifying climate change impacts.

2.3 Formalizing the Model Selection Problem and Policy Objective

2.3.1 Class of Models in Empirical Practice

In the setting of climate change impact studies, researchers observe an annual outcome Y_{it} and a vector of regressors observed at a higher frequency, such as daily or hourly, $\mathcal{W}_{it} = \{W_{ith}\}_{h=1}^H$. In this mixed-frequency panel data setting, the models considered in the literature as presented in Section 2.2 are fixed effects models that differ in terms of the response functions used to model the relationship between the outcome, Y_{it} , and the high-frequency regressor time series, \mathcal{W}_{it} . For a given model \mathbf{M}_α , the outcome equation is thus given by the following

$$Y_{it} = \mu_\alpha(\mathcal{W}_{it}) + a_{i,\alpha} + u_{it,\alpha}. \quad (7)$$

While control variables and additional fixed effects can be included, we omit them in our analysis to simplify the exposition and to focus our analysis on the main issue we consider here which is the potential misspecification of the response function.

The class of response functions considered in the empirical literature can be formally represented

¹¹Under this criterion, this survey does not include articles where response to temperature is only a first-stage or temperatures are simply considered as control variables.

¹²While not included this review, we note that the influential study in Schlenker and Roberts (2009), which we revisit in Section 4, relies on Monte Carlo cross-validation to select between the models under consideration.

¹³We note one exception in Burke and Emerick (2016) where the authors rely on in-sample fits (i.e., R^2) to determine the whole-number cutoff degree for separating growing and heat degree days.

as follows,

$$\mu_\alpha(W_{it}) = X'_{it,\alpha}\beta_\alpha \quad (8)$$

$$X_{it,\alpha} = \psi_\alpha \left(\sum_{h=1}^H f_\alpha(W_{ith})' \phi_{\alpha,h} \right). \quad (9)$$

where $f_\alpha(\cdot)$ is a $d_{f_\alpha} \times 1$ vector of linear and/or nonlinear transformations of the high-frequency regressor, W_{ith} , and $\phi_{\alpha,h}$ is a $d_{f_\alpha} \times 1$ vector of h -specific weights. Once the weighted transformations of W_{ith} are aggregated over h , the $d_{\psi_\alpha} \times 1$ transformation $\psi_\alpha(\cdot)$ is applied to them. For the purposes of this paper, we assume that d_{f_α} , d_{ϕ_α} and d_{ψ_α} are finite, such that $k_\alpha = \dim(X_{it,\alpha}) < \infty$.

While the class of models considered in the literature preserves linearity in the parameters and separability between observables and unobservables, it can allow for nonlinearities in the high-frequency regressor. To illustrate this, we provide a few examples to illustrate the different roles played by f_α , $\phi_{\alpha,h}$ and ψ_α . The annual mean model, where $X_{it,\alpha} = \bar{W}_{it} = \sum_{h=1}^H W_{ith}/H$, can be obtained by letting $f_\alpha(W_{ith}) = W_{ith}$, $\phi_{\alpha,h} = \frac{1}{H}$, and $\psi_\alpha(\bar{W}_{it}) = \bar{W}_{it}$, where $\bar{W}_{it} = \sum_{h=1}^H W_{ith}/H$. The quadratic in annual mean model, where $X_{it,\alpha} = (\bar{W}_{it}, \bar{W}_{it}^2)'$, relies on the same f_α and $\phi_{\alpha,h}$ as the annual mean model, but uses a second-order polynomial function ψ_α , such that $\psi_\alpha(W_{ith}) = (W_{ith}, W_{ith}^2)'$. To obtain the quarterly mean model, we set $f_\alpha(W_{ith}) = W_{ith}(1, 1, 1, 1)'$,

$$\phi_{\alpha,h} = (1\{h \in Q_1\}/|Q_1|, 1\{h \in Q_2\}/|Q_2|, 1\{h \in Q_3\}/|Q_3|, 1\{h \in Q_4\}/|Q_4|)',$$

and ψ_α is the identity function. For $j = 1, \dots, 4$, Q_j denotes the subset of indices $\{1, \dots, H\}$ that are in the j^{th} quarter and $|\mathcal{A}|$ denotes the cardinality for a set \mathcal{A} . Finally, the model with temperature bins, where $\dim(W_{ith}) = 1$, can be obtained by setting

$$f_\alpha(W_{ith}) = (1\{W_{ith} \in [l_1, u_1]\}, 1\{W_{ith} \in [l_2, u_2]\}, \dots, 1\{W_{ith} \in [l_{d_{f_\alpha}}, l_{d_{f_\alpha}}]\})',$$

$\phi_{\alpha,h} = (1, 1, \dots, 1)'$, ψ_α is the identity function and $\{[l_j, u_j]\}_{j=1}^{d_{f_\alpha}}$ is a set of intervals. In Appendix B, we also provide formal definitions for other commonly used models in the literature, such as degree days, polynomials, splines, etc.

2.3.2 Defining Nested and Non-nested Models

Since all models considered rely on different aggregated transformations of the same underlying high-frequency regressor, the models are likely to be overlapping. However, we would like to differentiate between different cases of overlapping models. Assume without loss of generality $k_\alpha < k_\gamma$. Let $\omega = \{\omega_h\}_{h=1}^H$ denote a realization of \mathcal{W}_{it} . For a fixed realization ω , the realizations of $X_{it,\alpha}$ and $X_{it,\gamma}$ are given by $x_{\omega,\alpha} = \psi_\alpha \left(\sum_{h=1}^H f_\alpha(\omega_h) \phi_{\gamma,h} \right)$ and $x_{\omega,\gamma} = \psi_\gamma \left(\sum_{h=1}^H f_\gamma(\omega_h) \phi_{\gamma,h} \right)$, respectively. Let \mathcal{B}_α denote the parameter space of β_α and β_α^k the k^{th} element of β_α .

We next provide formal definitions for when two models, \mathbf{M}_α and \mathbf{M}_γ , are nested, non-nested overlapping or strictly non-nested. In the following, let $\mathbf{0}_{k_\alpha}$ denote a k_α -dimensional column vector of zeros.

- Definition 1.** (i) \mathbf{M}_α is nested in \mathbf{M}_γ iff $x'_{\omega,\alpha}\beta_\alpha = R_{\alpha,\gamma}x'_{\omega,\gamma}\beta_\gamma$ for all ω and $\beta_\alpha \in \mathcal{B}_\alpha$, where $\beta_\gamma \in \mathcal{B}_\gamma$ and $R_{\alpha,\gamma}$ is a $k_\alpha \times k_\gamma$ non-random matrix with full row rank,
- (ii) \mathbf{M}_α and \mathbf{M}_γ are non-nested, overlapping iff \mathbf{M}_γ does not nest \mathbf{M}_α , but $x'_{\omega,\alpha}\beta_\alpha = x'_{\omega,\gamma}\beta_\gamma$ for all ω and some $\beta_\alpha \in \mathcal{B}_\alpha \setminus \{\mathbf{0}_{k_\alpha}\}$ and $\beta_\gamma \in \mathcal{B}_\gamma \setminus \{\mathbf{0}_{k_\gamma}\}$,
- (iii) \mathbf{M}_α and \mathbf{M}_γ are strictly non-nested iff they are not nested and $x'_{\omega,\alpha}\beta_\alpha \neq x'_{\omega,\gamma}\beta_\gamma$ for all ω , $\beta_\alpha \in \mathcal{B}_\alpha$ and $\beta_\gamma \in \mathcal{B}_\gamma$.

Note that according to (i), a model contains another if the regressors in the latter can be expressed as a linear combination of the regressors in the former. This is different from the typical linear regression framework where a model contains another if the regressors in the latter are a subset of the regressors in the former, i.e. the elements in $R_{\alpha,\gamma}$ can only be zero or one. We illustrate the above definitions with the following example.

Example 1. (*Annual Mean, Quarterly Mean, Quadratic in Annual Mean and Temperature Bin Models*)

Let \mathbf{M}_α denote the annual mean model, with outcome equation

$$Y_{it} = X'_{it,\alpha}\beta_\alpha + a_{i,\alpha} + u_{it,\alpha}, \quad (10)$$

where $X_{it,\alpha} = \bar{W}_{it} \equiv \sum_{h=1}^H W_{ith}/H$. The quarterly mean model uses instead the quarterly means of W_{it} as regressors. In the quarterly mean model, $X_{it,\gamma} = (\sum_{h \in Q_1} W_{ith}/|Q_1|, \dots, \sum_{h \in Q_4} W_{ith}/|Q_4|)$. Then \mathbf{M}_γ prescribes the outcome equation

$$Y_{it} = X'_{it,\gamma}\beta_\gamma + a_{i,\gamma} + u_{it,\gamma}. \quad (11)$$

Note that for all $\beta_\alpha \in \mathcal{B}_\alpha$ $X'_{it,\alpha}\beta_\alpha = R_{\alpha,\gamma}X'_{it,\gamma}\beta_\gamma$, where

$$R_{\alpha,\gamma} = \frac{1}{H} \begin{pmatrix} |Q_1| & |Q_2| & |Q_3| & |Q_4| \end{pmatrix},$$

$$\beta_\gamma = \beta_\alpha(1, 1, 1, 1)'.$$

Hence, \mathbf{M}_α is nested in \mathbf{M}_γ .

The quadratic in annual mean model, \mathbf{M}_δ , uses $X_{it,\delta} = (\bar{W}_{it}, \bar{W}_{it}^2)$ as regressors. Even though the quadratic in annual mean and the quarterly mean models are not nested, if $\beta_\delta^2 = 0$ and $\beta_\gamma^k = \beta_\gamma^{k'}$

for $k \neq k'$, with $k, k' \in \{1, 2, 3, 4\}$, then both models yield the annual mean model given \mathcal{W}_{it} . Hence, they are overlapping, non-nested.

To complete the example, note that annual mean model is both non-nested and non-overlapping with the temperature bin model \mathbf{M}_ρ with regressor $X_{it,\rho} = \frac{1}{H} \sum_{h=1}^H 1\{W_{ith} \geq 0\}/H$ as long as W_{ith} has continuous support. Indeed, one can construct multiple examples of elementary events ω such that the number of the days with positive values W_{ith} being equal, but the annual average being different and vice versa. Thus the only overlapping submodel of \mathbf{M}_α and \mathbf{M}_ρ is an empty model.

2.3.3 Policy Objective: Climate Change Projections

Consider a set of locations $i = 1, \dots, n$, for which we observe an annual outcome and daily temperature time series over T time periods, $\{Y_{it}, \mathcal{W}_{it}\}_{t=1}^T$.¹⁴ We would like to forecast the impact of climate change on the outcome between period T and $T + \tau$. The location is projected to experience the daily weather time series in $T + \tau$ periods ahead, $\mathcal{W}_{i,T+\tau}^f$. In this setting, $\{\mathcal{W}_{i,T+\tau}^f\}_{i=1}^n$ is obtained from a forecast model for a given climate change scenario.

Our goal is to predict the impact of this change in climate on an outcome of interest. One of the unique features of this policy objective is that the goal of the prediction exercise here is a causal parameter. As a result, to make progress here, we have to define a true model that generates the outcome. For the purposes of this paper, we assume that the outcome, Y_{it} , is given by the following model, \mathbf{M}_\star ,

$$Y_{it} = \mu_\star(\mathcal{W}_{it}) + a_i + u_{it}. \quad (12)$$

Similar to the models imposed in the literature, \mathbf{M}_\star imposes separability between unobservables and observables. As a result, the potential source of misspecification of a given model \mathbf{M}_α would stem from the misspecification of the true response function, $\mu_\star(\cdot)$.

Assuming strict exogeneity, $E[u_{it} | \mathcal{W}_{i1}, \dots, \mathcal{W}_{i,T+\tau} = \mathcal{W}_{i,T+\tau}^f, a_i] = 0$, which imposes the mean independence of u_{it} not only of $\{\mathcal{W}_{it}\}_{t=1}^T$ but also $\mathcal{W}_{i,T+\tau} = \mathcal{W}_{i,T+\tau}^f$, we can formally define the object of interest for each location i

$$E[Y_{i,T+\tau} | \mathcal{W}_{i,T+\tau} = \mathcal{W}_{i,T+\tau}^f, a_i] - E[Y_{iT} | \mathcal{W}_{iT}, a_i] = \mu_\star(\mathcal{W}_{i,T+\tau}^f) - \mu_\star(\mathcal{W}_{iT}). \quad (13)$$

Let us define $Supp\mathcal{W}_t$ as the support of \mathcal{W}_{it} . Our object of interest is a functional of $\omega_1 \in Supp\mathcal{W}_T$ and $\omega_2 \in Supp\mathcal{W}_{T+\tau}^f$

$$\mu_\star(\omega_2) - \mu_\star(\omega_1). \quad (14)$$

¹⁴Note that our setting can allow for a vector of high-frequency regressors, but to fix ideas and to remain consistent with the policy question, we motivate this section with \mathcal{W}_{it} as the temperature time series.

We are therefore interested in estimating the function with the highest precision in a specific set of values that correspond to the support of $\mathcal{W}_{i,T+\tau}^f$ and \mathcal{W}_{iT} , respectively.

In practice, researchers and policymakers do not know the true functional form of μ_* , they rely on a set of models $\{\mathbf{M}_\alpha\}_{\alpha=1}^A$ to estimate the impact of projected climate change. The question that arises here is what criterion policymakers should use to choose between the different models and their implied projections. For instance, in Figure 1, how should a policymaker decide between the two models considered which give substantially different climate change projections and therefore have very different policy implications? We tackle this question in the following section, evaluating the usefulness of existing criteria and proposing a new criterion tailored to the policy objective in climate change impact studies. We then illustrate the empirical relevance of our theoretical analysis in the context of the empirical application that corresponds to Figure 1.

3 Model Selection Criteria for Climate Change Impact Studies

Given the policy objective of climate change projections, an ideal criterion to choose between a set of models under consideration would be to minimize the following mean-squared error (MSE) criterion,

$$E[(\mu_\alpha(\mathcal{W}_{i,T+\tau}^f) - \mu_\alpha(\mathcal{W}_{iT}) - (\mu_*(\mathcal{W}_{i,T+\tau}^f) - \mu_*(\mathcal{W}_{iT})))^2]. \quad (15)$$

This MSE criterion is based on the error of predicting the impact of the projected climate change from \mathcal{W}_{iT} to $\mathcal{W}_{i,T+\tau}^f$. A challenge here, as in other forecasting problems, is of course that this ideal target is infeasible. Given the use of MCCV in practice, we first examine the asymptotic properties of this criterion as well as GICs (Section 3.1). Since our theoretical analysis of these existing criteria underscores the importance of at least one of the models in the set $\{\mathbf{M}_\alpha\}_{\alpha=1}^A$ nesting \mathbf{M}_* for these criteria to minimize the ideal MSE target in (15), we proceed to propose a class of alternative criteria that minimize feasible counterparts of the ideal target whether or not the models under consideration are correctly specified (Section 3.2).

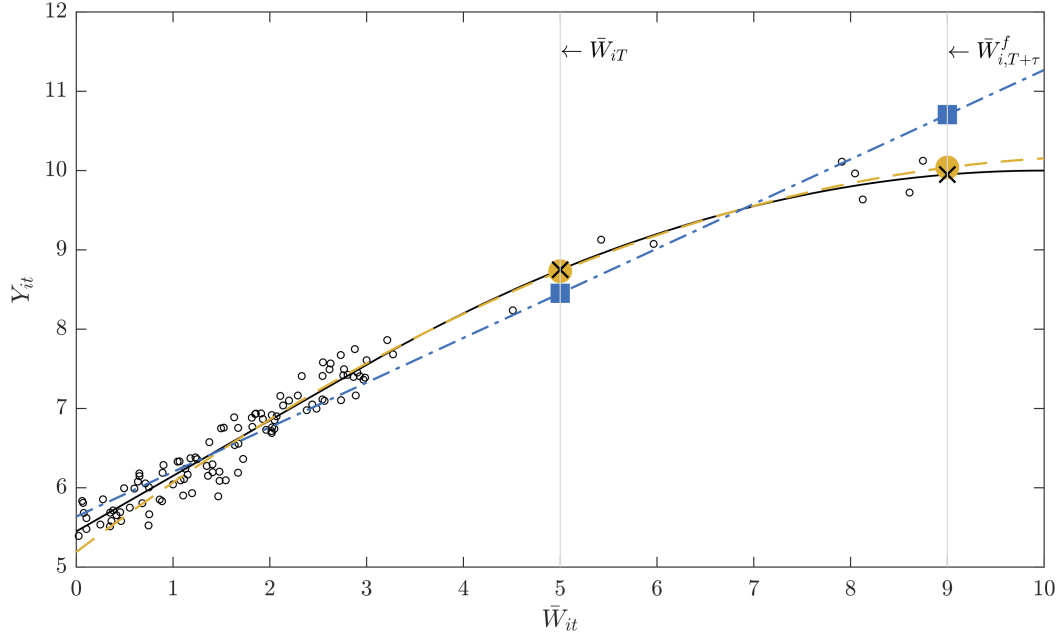
In the following, we consider asymptotics that let $n \rightarrow \infty$ while holding T fixed. Given the observational nature of the panel data under consideration in this setting, we do not restrict the conditional mean of a_i given $\{\mathcal{W}_{it}\}_{t=1}^T$, but maintain the strict exogeneity assumption, $E[u_{it}|\mathcal{W}_{i1}, \dots, \mathcal{W}_{iT}, a_i] = 0$. As a result, we focus our attention on fixed effects estimators that rely on the within-group transformation.¹⁵ For a random variable V_{it} , $\tilde{V}_{it} = V_{it} - \sum_{t=1}^T V_{it}/T$ and $\tilde{V}_i = (\tilde{V}_{i1}, \dots, \tilde{V}_{iT})$.

¹⁵Our results can be extended to the first-difference estimator in a straightforward manner.

3.1 Asymptotic Properties of Existing Model Selection Criteria

When examining the asymptotic behavior of MCCV and GICs, there are two properties that have been examined in the literature, model selection efficiency (optimality) as well as model selection consistency (e.g., Claeskens and Hjort 2008; Shao 1993, 1997).¹⁶

Figure 2: Illustrating the Difference between Minimizing the MSE of Impacts and Levels



Notes: The black solid line corresponds to the true model $\mu_*(W_{it})$ (non-linear in \bar{W}_{it}); blue dot-dashed line corresponds to the best approximating model that minimizes the in-sample MSE (linear in \bar{W}_{it}), the gold dashed line corresponds to the best approximating model that minimizes the impact MSE (quadratic in \bar{W}_{it}). The small black circles correspond to a random sample of (Y_{it}, \bar{W}_{it}) for a given i .

A model selection criterion is said to be efficient (Claeskens and Hjort 2008; Shao 1997) if the ratio of the mean squared error (MSE) of the model selected by these criteria and the theoretical minimizer among those under consideration will converge in probability to one. Formally, a criterion C is said to be model selection efficient in our context relying on fixed effects estimators, if the following ratio converges to one

$$\frac{L_{nT}(\widehat{\mathbf{M}}_C)}{L_{nT}(\mathbf{M}_m)} \xrightarrow{p} 1, \quad (16)$$

¹⁶See Yang (2005), for an interesting analysis that poses the question of whether these two objectives can be combined and points to a clear trade-off between the two objectives.

where $\widehat{\mathbf{M}}_C$ is the model selected by the criterion C , \mathbf{M}_m is the theoretical minimizer of the loss function, $E_{\widehat{\mathbf{M}}_C}$ integrates over all random quantities except for $\widehat{\mathbf{M}}_C$,

$$L_{nT}(\widehat{\mathbf{M}}) = \sum_{i=1}^n \sum_{t=1}^T E_{\widehat{\mathbf{M}}_C}[(\tilde{Y}_{it} - \hat{\mu}_{\widehat{\mathbf{M}}_C}(\mathcal{W}_{it}))^2],$$

$$L_{nT}(\mathbf{M}^m) = \sum_{i=1}^n \sum_{t=1}^T E[(\tilde{Y}_{it} - \tilde{\mu}_{\mathbf{M}^m}(\mathcal{W}_{it}))^2].$$

As a result, while such a criterion selects models that minimize the MSE of the within-group transformed outcome, they are not guaranteed to perform well for the ideal target for climate change projections in (15). These two criteria can in fact result in substantially different best approximate models, even in settings where the true impact model μ_\star depends only on a scalar \bar{W}_{it} . To illustrate this point, consider the prediction of the impact of project climate change for a unit i illustrated in Figure 2. In this graphical illustration, both linear and quadratic in \bar{W}_{it} models are misspecified, but the quadratic model predicts the impact of the projected change from \bar{W}_{iT} to $\bar{W}_{i,T+\tau}^f$ better. To see this, compare the gold circles with the blue squares, noting that the black crosses correspond to the true impact. In this diagram, most observations are far away from the projected climate $\bar{W}_{i,T+\tau}^f$ and lie in the domain where the true impact function is linear. As a result, minimizing the MSE in levels results in a linear-in- \bar{W}_{it} model, which has a larger bias at the projected climate. Alternatively, using only data for period T and the periods with weather “close” to $\bar{W}_{i,T+\tau}^f$ for model selection would result in the choice of the better approximate model, quadratic in \bar{W}_{it} . This insight will guide our proposal of the PWMSE criterion to be introduced later in Section 3.2.

Next, we consider the suitability of consistent model selection for the policy objective in climate change impact studies. If one of the models under consideration nests the true model, a consistent model selection criterion C chooses \mathbf{M}_\star with probability approaching one asymptotically, $P(\widehat{\mathbf{M}}_C = \mathbf{M}_\star) \rightarrow 1$ as $n \rightarrow \infty$. As a result, consistent model selection criteria minimize the ideal target in (15)

$$E[(\mu_\alpha(\mathcal{W}_{i,T+\tau}^f) - \mu_\alpha(\mathcal{W}_{iT}) - (\mu_\star(\mathcal{W}_{i,T+\tau}^f) - \mu_\star(\mathcal{W}_{iT})))^2] \quad (17)$$

and particularly attain zero by selecting \mathbf{M}_\star with probability one asymptotically. As a result, we next provide conditions on the tuning parameter choices for the MCCV and GIC that ensure consistent model selection.

3.1.1 Monte Carlo Cross-Validation

Cross-validation is a very popular method in practice, because it directly measures out-of-sample prediction error and seems “model-free”. It has been used in Schlenker and Roberts (2009) to

justify their model selection choice. In this section, we establish conditions under which Monte Carlo cross-validation (MCCV) yields consistent model selection.

Let $Y_i = (Y_{i1}, \dots, Y_{iT})$ and $X_i = (X_{i1}, \dots, X_{iT})$. Given observations $\{Y_i, X_i\}_{i=1}^n$, to compute the MCCV mean squared error, we randomly draw a collection \mathcal{R} of b subsets of $\{1, \dots, n\}$ with size n_v (test sample size) and select a model $\widehat{\mathbf{M}}_{cv}$ that minimizes, among $\alpha = 1, \dots, A$, the criterion given by

$$\hat{\Gamma}_{\alpha, nT}^{MCCV} = \frac{1}{n_v T b} \sum_{s \in \mathcal{R}} \|\mathbb{Y}_s - \hat{\mathbb{Y}}_{\alpha, s^c}\|^2. \quad (18)$$

Here $\mathbb{Y}_s = (Y'_i)_{i \in s}$ is an $nT \times 1$ vector that vertically stacks Y'_i for all $i \in s$ and $\hat{\mathbb{Y}}_{\alpha, s^c} = \tilde{\mathbb{X}}_{s, \alpha} \hat{\beta}_{\alpha}^{s^c}$, where $\tilde{\mathbb{X}}_{s, \alpha}$ denotes the within-demeaned version of $\mathbb{X}_{s, \alpha} = (X'_{i, \alpha})_{i \in s}$ and $\hat{\beta}_{\alpha}^{s^c}$ is the estimator of the parameter vector of \mathbf{M}_{α} using the training data set $\{Y_i, \mathcal{W}_i\}_{i \in s^c}$, where s^c denotes the complement of s , i.e. the remaining $b - 1$ subsets in the collection \mathcal{R} after removing subset s .

To proceed, we need to express the within-demeaned model in matrix form, $\tilde{\mathbb{Y}} = (\tilde{V}_1, \dots, \tilde{V}_n)'$. Further, write U_i , $i = 1, \dots, n$, to denote the error terms in the true DGP, which are assumed to be conditionally mean zero. Then we can express the within-demeaned version of model \mathbf{M}_{α} in matrix form as

$$\tilde{\mathbb{Y}} = \tilde{\mathbb{X}}_{\alpha} \beta_{\alpha} + \tilde{\mathbb{U}}_{\alpha}.$$

Similarly to Shao (1993), we study the mean squared prediction error (MSPE) of \mathbf{M}_{α} , which is estimated using $\{Y_i, X_i\}_{i=1}^n$, in predicting out-of-sample observations of Y_i , which we will refer to as Z_i . Assume that the conditional variance of the error terms in the true DGP (which are conditionally mean zero) is equal to $E[U_i U'_i | \mathcal{W}_i] = \sigma^2 I_T$, and also assume that $\{Y_i, X_i\}$ are i.i.d. across i . The expectation operators $E[\cdot | \mathcal{W}_i]$ in the preceding sentence and $E[\cdot | \{\mathcal{W}_i\}_{i=1}^n]$ in the following displayed equation refer to the conditional distribution derived from the true joint distribution of Y_i and \mathcal{W}_i . The MSPE of the fitted model \mathbf{M}_{α} is given by

$$\begin{aligned} \Gamma_{\alpha, nT} &= \frac{1}{nT} E \left[\sum_{i=1}^n \sum_{t=1}^T (\tilde{Z}_{it} - \tilde{X}'_{it, \alpha} \hat{\beta}_{\alpha})^2 \middle| \{\mathcal{W}_i\}_{i=1}^n \right] \\ &= \frac{T-1}{T} \sigma^2 + \underbrace{\frac{1}{nT} \sigma^2 k_{\alpha}}_{\text{model dimension}} + \underbrace{\Delta_{\alpha, nT}}_{\text{"misspecification" error}}, \end{aligned}$$

where $\Delta_{\alpha, nT} = \frac{1}{nT} \beta'_{\star, o} \tilde{\mathbb{X}}'_{\star} (I_{nT} - P_{\alpha}) \tilde{\mathbb{X}}_{\star} \beta_{\star, o} \geq 0$ and P_{α} is the projection matrix onto the column space of the design matrix $\tilde{\mathbb{X}}_{\alpha}$. The derivation of the above equality is included in Section A of the Appendix for the reader's convenience. Several remarks are in order. The homoskedasticity

and serial uncorrelatedness of the idiosyncratic shocks are crucial to obtain a component of the MSPE that depends on the model dimension. As in Shao (1993), it is convenient to consider two categories of models,

- Category I: $\Delta_{\alpha,nT} > 0$,
- Category II: $\Delta_{\alpha,nT} = 0$, when $X_{it,\star} = R_{\star,\alpha}X_{it,\alpha}$.

The following standard conditions correspond to conditions in Shao (1993) which we have adapted to the fixed effects model with stochastic regressors.

Condition 1. (*MCCV Consistency*)

1. (*DGP and Models*) For $i = 1, 2, \dots, n$, $t = 1, 2, \dots, T$, $Y_{it} = X_{it,\star}\beta_{\star,o} + a_i + u_{it}$, where $u_{it}|\mathcal{W}_{i1}, \dots, \mathcal{W}_{iT}, a_i \stackrel{i.i.d.}{\sim} (0, \sigma^2)$ across i and t . For some $\alpha = 1, \dots, A$, $\mathbf{M}_\alpha = \mathbf{M}_\star$.
2. (*Restriction on Category I Models*) $\text{plim}_{n \rightarrow \infty} \Delta_{\alpha,nT} > 0$ for \mathbf{M}_α in Category I.
3. (*Regularity Conditions*)

$$i. \quad \tilde{\mathbf{X}}_\alpha' \tilde{\mathbf{X}}_\alpha = O_p(n) \text{ and } \left(\tilde{\mathbf{X}}_\alpha' \tilde{\mathbf{X}}_\alpha \right)^{-1} = O_p(n^{-1}) \text{ for } \alpha = 1, 2, \dots, A,$$

$$ii. \quad \text{plim}_{n \rightarrow \infty} \max_{i \leq n, t \leq T} w_{it,\alpha} = 0 \quad \forall \alpha = 1, 2, \dots, A, \text{ where } w_{it,\alpha} \text{ is the } it^{\text{th}} \text{ diagonal element of } P_\alpha,$$

$$iii. \quad \max_{s \in \mathcal{R}} \left\| \frac{1}{n_v} \sum_{i \in s^c} \sum_{t=1}^T \tilde{X}_{it,\alpha} \tilde{X}_{it,\alpha}' - \frac{1}{n_c} \sum_{i \in s} \sum_{t=1}^T \tilde{X}_{it,\alpha} \tilde{X}_{it,\alpha}' \right\| = o_p(1) \text{ for } \alpha = 1, 2, \dots, A.$$

Condition 1.1 imposes the i.i.d. assumption on the idiosyncratic shocks conditional on the time series of the high-frequency regressor $\{\mathcal{W}_{it}\}_{t=1}^T$ and a_i across i and t .¹⁷ Note that the i.i.d. assumption is not imposed on the joint distribution of (Y_{it}, X_{it}) . In fact, the regularity condition in 1.3(i) is a high-level condition that ensures the applicability of a law of large numbers for $\tilde{\mathbf{X}}_\alpha' \tilde{\mathbf{X}}_\alpha/n$, and that it converges to an invertible matrix in probability for any $\alpha = 1, \dots, A$. If we assume the cross-sectional i.i.d. assumption on X_{it} , then the existence of $E[\tilde{X}_{it} \tilde{X}_{it}']$ as well as its inverse would suffice. These conditions would also be sufficient for Condition 1.3(ii)-(iii) (see Section 4.5, Shao 1993, for additional discussion). As for Condition 1.2, it is a restriction that ensures that models in Category I are well-separated from models in Category II. Note that $\Delta_{\alpha,nT}$ is the sum of squares

¹⁷The derivation of $\Gamma_{\alpha,nT}$ in Appendix A.1 illustrates the crucial role of this condition in obtaining the term that depends on model dimension, $\frac{1}{nT} \sigma^2 k_\alpha$.

of the elements of the vector of misspecification errors of \mathbf{M}_α , $(I - P_\alpha)\mathbb{X}_*\beta_{*,0}$. Since Category I models do not nest \mathbf{M}_* , $\Delta_{\alpha,nT}$ will be greater than zero assuming $(\tilde{\mathbb{X}}_\alpha\tilde{\mathbb{X}}'_\alpha)^{-1}$ exists.¹⁸

Proposition 1. *Assume Condition 1, and $n_v/n \rightarrow 1$ and $n_c = n - n_v \rightarrow \infty$, $b^{-1}n_c^{-2}n^2 \rightarrow 0$.*

(i) *If \mathbf{M}_α is in Category I, then for some $R_n \geq 0$,*

$$\hat{\Gamma}_{\alpha,nT}^{MCCV} = \frac{1}{n_v T b} \sum_{s \in \mathcal{R}} \tilde{\mathbf{U}}'_s \tilde{\mathbf{U}}_s + \Delta_{\alpha,nT} + o_p(1) + R_n, \quad (19)$$

where $\tilde{\mathbf{U}}_s = \tilde{\mathbf{Y}}_s - \tilde{\mathbb{X}}_s \beta$.

(ii) *If \mathbf{M}_α is in Category II, then*

$$\hat{\Gamma}_{\alpha,nT}^{MCCV} = \frac{1}{n_v T b} \sum_{s \in \mathcal{R}} \tilde{\mathbf{U}}'_s \tilde{\mathbf{U}}_s + \frac{k_\alpha \sigma^2}{n_c T} + o_p(n_c^{-1}). \quad (20)$$

(iii) *It follows that*

$$\lim_{n \rightarrow \infty} P(\widehat{\mathbf{M}}_{cv} = \mathbf{M}_*) = 1. \quad (21)$$

The proof is given in Appendix A. The above proposition establishes that if \mathbf{M}_* is under consideration, then MCCV with $n_v/n \rightarrow 1$ and $n_c \rightarrow \infty$, hereinafter MCCV-Shao, will select this model with probability tending to one in large samples. Suppose \mathbf{M}_* is not considered, however some models that contain it (Category II) are in the set of candidate models. Then the above proposition implies that the most parsimonious among those models in Category II will be selected with probability tending to one as $n \rightarrow \infty$ by the MCCV-Shao procedure. However, the above does not ensure that if the models considered are all in Category I, i.e. none of the models considered contain \mathbf{M}_* , that the most parsimonious model with the smallest $\lim_{n \rightarrow \infty} \Delta_{\alpha,nT}$ will be selected with probability tending to one. We will explore this issue in simulations in Section D.

In the absence of homoskedasticity and serial uncorrelatedness, it is well-known that it is very difficult to formally justify MCCV. We will, however, examine its performance under weaker conditions in the numerical experiments.

3.1.2 Generalized Information Criteria

Here we introduce the generalized information criterion (GIC) for this problem. In the linear fixed effects model, we do not need to specify a parametric family for the errors to define the estimator.

¹⁸By contrast, for models in Category II, $X_{it,*} = R_{*,\alpha} X_{it,\alpha}$ and therefore $\tilde{\mathbb{X}}_* = \tilde{\mathbb{X}}_\alpha R_{*,\alpha}$. As a result, for Category II models, $P_\alpha \tilde{\mathbb{X}}_* \beta_{*,0} = \tilde{\mathbb{X}}_\alpha (\tilde{\mathbb{X}}'_\alpha \tilde{\mathbb{X}}_\alpha)^{-1} \tilde{\mathbb{X}}'_\alpha \tilde{\mathbb{X}}_\alpha R_{*,\alpha} \beta_{*,0} = \tilde{\mathbb{X}}_\alpha R'_{*,\alpha} \beta_\alpha = \tilde{\mathbb{X}}_* \beta_{*,0}$. As a result, $\Gamma_{nT,\alpha} = 0$ for models in Category II.

However, it is computationally convenient to use the result that the linear fixed effects estimator is identical to the conditional maximum likelihood estimator under the additional assumption of Gaussian errors, and the conditioning is on $\bar{Y}_i = \sum_{t=1}^T Y_{it}/T$, which is a sufficient statistic for the individual fixed effect (Arellano 2003). To be clear, we do not require the Gaussianity assumption or conditional maximum likelihood estimator for our theoretical results, but we take advantage of this equivalence with the linear fixed effects estimator for convenience. We will use $f(\cdot)$ to denote the relevant density function. Let $Y_i = (Y_{i1}, \dots, Y_{iT})'$ and $X_{i,\alpha} = (X_{i1,\alpha}, \dots, X_{iT,\alpha})$, the i^{th} contribution to the conditional log-likelihood for \mathbf{M}_α is given by $\log(f(Y_i|X_{i,\alpha}, a_{i,\alpha}, \bar{Y}_i; \beta_\alpha, \sigma_\alpha^2)) = \log(f(\tilde{Y}_i|\tilde{X}_{i,\alpha}; \beta_\alpha, \sigma_\alpha^2)) \propto -(T-1)\log(\sigma_\alpha^2) - \sum_{t=1}^T (\tilde{Y}_{it} - \tilde{X}'_{it,\alpha}\beta_\alpha)^2/\sigma_\alpha^2$. The log-likelihood function is hence given by

$$\ell_{nT}^\alpha(\beta_\alpha, \sigma_\alpha^2) = -n(T-1)\log(\sigma_\alpha^2) - \frac{\sum_{i=1}^n \sum_{t=1}^T (\tilde{Y}_{it} - \tilde{X}'_{it,\alpha}\beta_\alpha)^2}{\sigma_\alpha^2}. \quad (22)$$

In the following, we will work with the conditional profile likelihood function

$$\ell_{nT}^\alpha(\beta_\alpha, \hat{\sigma}_\alpha^2(\beta_\alpha)) \propto -n(T-1)\log(\hat{\sigma}_\alpha^2(\beta_\alpha)),$$

where

$$\hat{\sigma}_\alpha^2(\beta_\alpha) = \frac{1}{n(T-1)} \sum_{i=1}^n \sum_{t=1}^T (\tilde{Y}_{it} - \tilde{X}'_{it,\alpha}\beta_\alpha)^2 \quad (23)$$

is the maximum likelihood estimator for σ_α^2 given a fixed value of β_α . Hereinafter, we let $\hat{\ell}_{nT}^\alpha \equiv \ell_{nT}^\alpha(\hat{\beta}_\alpha, \hat{\sigma}_\alpha^2(\hat{\beta}_\alpha)) = -n(T-1)\log(\hat{\sigma}_\alpha^2(\hat{\beta}_\alpha))$, where

$$\hat{\beta}_\alpha = \arg \max_{\beta \in B} \ell_{nT}^\alpha(\beta_\alpha, \hat{\sigma}_\alpha^2(\beta_\alpha)).$$

The generalized information criterion (GIC) is given by the following

$$GIC_{\alpha, \lambda_{nT}} = \hat{\ell}_{nT}^\alpha - \lambda_{nT} k_\alpha. \quad (24)$$

The term λ_{nT} penalizes model dimension. The choice of $\lambda_{nT} = 2$ corresponds to the AIC, whereas the choice $\lambda_{nT} = \log(nT)$ corresponds to the BIC, since nT is the total number of observations. One of the attractive features of information criteria is that we can formally justify their behavior under heteroskedasticity, spatial and/or time series dependence by viewing them as a misspecification of the above log-likelihood. Since we will deal with misspecification in this section, we introduce another definition, which is pseudo-consistency of a model selection procedure following Sin and White (1996).

Definition 2. (Pseudo-Consistency of Model Selection) Let $\mathbb{M} = \{\mathbf{M}_\alpha\}_{\alpha=1}^A$ and \mathbf{M}_\star is not nested in \mathbf{M}_α for any $\alpha = 1, \dots, A$. Then a model selection criterion \mathbf{C} is said to be pseudo-consistent

if $\lim_{n \rightarrow \infty} P(\widehat{M}_{\mathbf{C}} = \mathbf{M}_{\mathbf{P}}) = 1$, where $\widehat{M}_{\mathbf{C}}$ is the model selected by criterion \mathbf{C} and $\mathbf{M}_{\mathbf{P}}$ is the most parsimonious model with the smallest Kullback-Leibler divergence (Claeskens and Hjort 2008, Chapter 2) from the true data-generating distribution among all models in \mathbb{M} .

Building on previous results on the behavior of the quasi-log-likelihood ratio statistic (Sin and White 1996; Vuong 1989), we can establish conditions for GIC's consistency and pseudo-consistency in the context of climate change impact studies. Without loss of generality, consider the choice between two models \mathbf{M}_{α} and \mathbf{M}_{γ} with $k_{\alpha} < k_{\gamma}$. Let $LR_{nT}^{\alpha, \gamma} = \hat{\ell}_{nT}^{\alpha} - \hat{\ell}_{nT}^{\gamma}$. Furthermore, write $\widehat{\mathbf{M}}_{\lambda_{nT}}$ to denote the model that minimizes the GIC given λ_{nT} ,

$$P(\widehat{\mathbf{M}}_{\lambda_{nT}} = \mathbf{M}_{\alpha}) = P(GIC_{\alpha, \lambda_{nT}} > GIC_{\gamma, \lambda_{nT}}) = P(LR_{nT}^{\alpha, \gamma} > \lambda_{nT}(k_{\alpha} - k_{\gamma})).$$

Vuong (1989) establishes that the rate of convergence of the quasi-likelihood ratio statistic under the null hypothesis differs depending on whether the conditional densities under \mathbf{M}_{α} and \mathbf{M}_{γ} agree at the pseudo-true parameter values or not. In our setting, this is determined by whether the predicted values of the outcome at the pseudo-true parameters of the two models differ or coincide.

Since we allow for the possibility for misspecification in this section, we introduce the pseudo-true parameter value for a model \mathbf{M}_{α} ,

$$\beta_{\alpha}^* = \left(\bar{E}[\tilde{X}_{i,\alpha} \tilde{X}_{i,\alpha}'] \right)^{-1} \bar{E}[\tilde{X}_{i,\alpha} \tilde{Y}_i],$$

where $\tilde{X}_{i,\alpha} = (\tilde{X}_{i1,\alpha}, \tilde{X}_{i2,\alpha}, \dots, \tilde{X}_{iT,\alpha})$ and $\tilde{Y}_i = (\tilde{Y}_{i1}, \dots, \tilde{Y}_{iT})'$. We also introduce $\tilde{u}_{it,\alpha} = \tilde{Y}_{it,\alpha} - \tilde{X}_{it,\alpha}' \beta_{\alpha}^*$, $\hat{u}_{it,\alpha} = \tilde{Y}_{it,\alpha} - \tilde{X}_{it,\alpha}' \hat{\beta}_{\alpha}$, $\tilde{u}_{i,\alpha} = (\tilde{u}_{i1,\alpha}, \dots, \tilde{u}_{iT,\alpha})'$ and $\hat{u}_{i,\alpha} = (\hat{u}_{i1,\alpha}, \dots, \hat{u}_{iT,\alpha})'$. For a random variable W_i , $\bar{E}[W_i] = \lim_{n \rightarrow \infty} \frac{1}{n} \sum_{i=1}^n E[W_i]$. We use $\sigma_{\alpha}^2(\beta_{\alpha}^*) = \bar{E}[\tilde{u}_{i,\alpha}' \tilde{u}_{i,\alpha}]$ to denote the population MSE for a model \mathbf{M}_{α} .

$$\begin{aligned} \hat{D}_{\alpha} &= \frac{1}{n} \sum_{i=1}^n \tilde{X}_{i,\alpha} \tilde{X}_{i,\alpha}', & D_{\alpha} &= \bar{E}[\tilde{X}_{i,\alpha} \tilde{X}_{i,\alpha}'], \\ \hat{C}_{\alpha} &= \frac{1}{n} \sum_{i=1}^n \tilde{X}_{i,\alpha} \tilde{Y}_i, & C_{\alpha} &= \bar{E}[\tilde{X}_{i,\alpha} \tilde{Y}_i], \\ \hat{b}_{\alpha} &= \frac{1}{n} \sum_{i=1}^n \tilde{X}_{i,\alpha} \tilde{u}_{i,\alpha}', & b_{\alpha} &= \bar{E}[\tilde{X}_{i,\alpha} \tilde{u}_{i,\alpha}']. \end{aligned}$$

For two models \mathbf{M}_{α} and \mathbf{M}_{γ} , let

$$\begin{aligned} B_{\alpha, \gamma} &= \bar{E}[\tilde{X}_{i,\alpha} \tilde{u}_{i,\alpha} \tilde{u}_{i,\gamma}' \tilde{X}_{i,\gamma}'], \\ V_{\alpha, \gamma} &= \bar{E}[(\tilde{u}_{i,\alpha}' \tilde{u}_{i,\alpha} - \bar{E}[\tilde{u}_{i,\alpha}' \tilde{u}_{i,\alpha}]) (\tilde{u}_{i,\gamma}' \tilde{u}_{i,\gamma} - \bar{E}[\tilde{u}_{i,\gamma}' \tilde{u}_{i,\gamma}])]. \end{aligned}$$

Note that by definition the matrix $B_{\gamma, \alpha} = B'_{\alpha, \gamma}$ and the scalar $V_{\alpha, \gamma} = V_{\gamma, \alpha}$. With a slight abuse of notation, we will use B_{α} and V_{α} to denote $B_{\alpha, \alpha}$ and $V_{\alpha, \alpha}$, respectively.

Condition 2. *The following conditions hold as $n \rightarrow \infty$ holding T fixed:*

1. $\hat{D}_\alpha \xrightarrow{p} D_\alpha$ and $\hat{D}_\gamma \xrightarrow{p} D_\gamma$, where D_α and D_γ are finite, symmetric positive definite matrices.

2. $\hat{C}_\alpha \xrightarrow{p} C_\alpha < \infty$ and $\hat{C}_\gamma \xrightarrow{p} C_\gamma < \infty$.

3.

$$\sqrt{n} \begin{pmatrix} \hat{b}_\alpha \\ \hat{b}_\gamma \end{pmatrix} \xrightarrow{d} N \left(0, \begin{pmatrix} B_\alpha & B_{\alpha,\gamma} \\ B_{\gamma,\alpha} & B_\gamma \end{pmatrix} \right).$$

4. $\hat{\sigma}_\alpha^2(\hat{\beta}_\alpha) \xrightarrow{p} \sigma_\alpha^2(\beta_\alpha^*)$ and $\hat{\sigma}_\gamma^2(\hat{\beta}_\gamma) \xrightarrow{p} \sigma_\gamma^2(\beta_\gamma^*)$, where $0 < \sigma_\alpha^2(\beta_\alpha^*) < \infty$ and $0 < \sigma_\gamma^2(\beta_\gamma^*) < \infty$.

5.

$$\sqrt{n} \begin{pmatrix} \hat{\sigma}_\alpha^2(\beta_\alpha^*) - \sigma_\alpha^2(\beta_\alpha^*) \\ \hat{\sigma}_\gamma^2(\beta_\gamma^*) - \sigma_\gamma^2(\beta_\gamma^*) \end{pmatrix} \xrightarrow{d} N \left(0, \begin{pmatrix} V_\alpha & V_{\alpha,\gamma} \\ V_{\gamma,\alpha} & V_\gamma \end{pmatrix} \right).$$

Conditions 2.1 and 2.2 ensure the consistency of $\hat{\beta}_\alpha$ and $\hat{\beta}_\gamma$ for their respective well-defined pseudo-true parameter values, β_α^* and β_γ^* . Conditions 2.1 and 2.3 ensure the joint asymptotic normality of $\hat{\beta}_\alpha$ and $\hat{\beta}_\gamma$. Note that this condition does not require the variance-covariance matrix to be nonsingular. This is by design, since this condition is used to show the asymptotic distribution of the QLR statistic when the two models are nested relying on Lemma 3.2 in Vuong (1989). Condition 2.4 ensures the consistency of the sample mean-squared error to the population mean-squared error. Condition 2.5 ensures the joint asymptotic normality of $\hat{\sigma}_\alpha(\beta_\alpha^*)$ and $\hat{\sigma}_\gamma(\beta_\gamma^*)$. We choose to present the conditions in terms of consistency and asymptotic normality in order to illustrate that the results can allow for dependence across i and t subject to the applicability of appropriate laws of large numbers and central limit theorems. If additional sampling requirements are imposed, it is straightforward to obtain more primitive conditions that imply Condition 2. For instance, if we impose the cross-sectional i.i.d. assumption, then the existence of D_α and D_γ , assuming they are both positive definite, would be sufficient for Condition 2.1. The existence of C_α and C_γ would imply Condition 2.2. As for Condition 2.3 (2.5), the existence of B_α and B_γ (V_α and V_γ) would be sufficient.

The following proposition gives sufficient conditions for $GIC_{\lambda_{nT}}$ to deliver (pseudo-)consistent model selection in our problem when considering three possible cases with two models. In the first two cases, both models are equal in terms of Kullback-Leibler divergence from the true data-generating distribution. In both cases, a (pseudo-) consistent GIC should select the more parsimonious model. The third case is when one model is strictly better in terms of Kullback-Leibler divergence, in which case this model should be chosen by a (pseudo-) consistent GIC. Recall that $x_{\omega_t,\alpha}$ is a realization of $X_{it,\alpha}$ given a particular realization of \mathcal{W}_{it} . Let $\tilde{\mathbf{x}}_{\{\omega_t\}_{t=1}^T,\alpha}$ denote the within-demeaned version of $x_{\omega_t,\alpha}$ given T realizations of \mathcal{W}_{it} , i.e. $\{\omega_t\}_{t=1}^T$.

Proposition 2. *Assume Condition 2 holds. The following statements hold as $n \rightarrow \infty$, holding T fixed.*

1. Suppose $\sigma_\alpha^2(\beta_\alpha^*) = \sigma_\gamma^2(\beta_\gamma^*)$ and $\tilde{\mathbf{x}}'_{\cdot,\alpha}\beta_\alpha^* = \tilde{\mathbf{x}}'_{\cdot,\gamma}\beta_\gamma^*$ hold. Then

$$P(\widehat{\mathbf{M}}_{\lambda_{nT}} = \mathbf{M}_\alpha) = P(GIC_{\alpha,\lambda_{nT}} > GIC_{\gamma,\lambda_{nT}}) = P(LR_n^{\alpha,\gamma} > \lambda_{nT}(k_\alpha - k_\gamma)) \rightarrow 1,$$

if $\lambda_{nT} \rightarrow \infty$.

2. Suppose $\sigma_\alpha^2(\beta_\alpha^*) = \sigma_\gamma^2(\beta_\gamma^*)$ and $\tilde{\mathbf{x}}'_{\cdot,\alpha}\beta_\alpha^* \neq \tilde{\mathbf{x}}'_{\cdot,\gamma}\beta_\gamma^*$ hold. Then

$$P(\widehat{\mathbf{M}}_{\lambda_{nT}} = \mathbf{M}_\alpha) = P(GIC_{\alpha,\lambda_{nT}} > GIC_{\gamma,\lambda_{nT}}) = P\left(\frac{1}{\sqrt{nT}}LR_n^{\alpha,\gamma} > \frac{\lambda_{nT}}{\sqrt{n}}(k_\alpha - k_\gamma)\right) \rightarrow 1,$$

if $\lambda_{nT}/\sqrt{n} \rightarrow \infty$.

3. a. Suppose that $\sigma_\alpha^2(\beta_\alpha^*) < \sigma_\gamma^2(\beta_\gamma^*)$ holds. Then

$$P(\widehat{\mathbf{M}}_{\lambda_{nT}} = \mathbf{M}_\alpha) = P(GIC_{\alpha,\lambda_{nT}} > GIC_{\gamma,\lambda_{nT}}) = P\left(\frac{1}{nT}LR_n^{\alpha,\gamma} > \frac{\lambda_{nT}}{n}(k_\alpha - k_\gamma)\right) \rightarrow 1,$$

if $\lambda_{nT}/n \rightarrow 0$.

b. Suppose that $\sigma_\alpha^2(\beta_\alpha^*) > \sigma_\gamma^2(\beta_\gamma^*)$ holds. Then

$$P(\widehat{\mathbf{M}}_{\lambda_{nT}} = \mathbf{M}_\gamma) = P(GIC_{\alpha,\lambda_{nT}} > GIC_{\gamma,\lambda_{nT}}) = P\left(\frac{1}{n}LR_n^{\alpha,\gamma} < \frac{\lambda_{nT}}{n}(k_\alpha - k_\gamma)\right) \rightarrow 1,$$

if $\lambda_{nT}/n \rightarrow 0$.

The proof of the above proposition is provided in Appendix A.3. It builds on Vuong (1989). The result is a special case of what has been shown in Sin and White (1996) and Hong and Preston (2012). The above theorem shows that for a GIC to be (pseudo-) consistent in all cases, then λ_{nT} has to fulfill three conditions as $n \rightarrow \infty$: (1) $\lambda_{nT} \rightarrow \infty$, (2) $\lambda_{nT}/\sqrt{n} \rightarrow \infty$, (3) $\lambda_{nT}/n \rightarrow 0$. The first two conditions ensure that when two models have the same population MSE, the smaller model is chosen. The third condition ensures that when one model dominates the other in terms of population MSE that the term that depends on the model dimension converges to zero, such that the best model in terms of smallest population MSE is chosen, whether it is \mathbf{M}_α or \mathbf{M}_γ .

The conditions on GIC provided in Proposition 2 are satisfied for the criteria proposed in Sin and White (1996) with $\lambda_{nT} = \sqrt{nT \log(\log(nT))}$ or $\lambda_{nT} = \sqrt{nT \log(nT)}$. However, $BIC_\alpha = GIC_{\alpha, \log(nT)}$ only satisfies (a) and (c), but not (b), which is required for consistency of model selection in Case 2. This pseudo-inconsistency of BIC occurs when $\tilde{\mathbf{x}}'_{\cdot,\alpha}\beta_\alpha^* \neq \tilde{\mathbf{x}}'_{\cdot,\gamma}\beta_\gamma^*$. In Section C.1 in the online appendix, we demonstrate that if the models considered contain the true DGP, then the predicted values at the pseudo-true parameters are equal given \mathcal{W}_i and hence we expect BIC

to be consistent. However, if model selection is conducted among models that do not contain \mathbf{M}_* , i.e. all the models under consideration are misspecified, then this issue may occur and BIC may therefore be pseudo-inconsistent. This analysis informs our simulation design.

We provide a set of simulations to evaluate the finite-sample performance of these existing model selection criteria in Section D in the online appendix. Specifically, we consider MCCV with fixed and vanishing training-to-full sample ratios (MCCV- p and MCCV-Shao, respectively), AIC, BIC, and two additional GICs following Sin and White (1996) (SW criteria). Our baseline simulation results confirm our theoretical predictions. When the true DGP is in the set of models under consideration, the MCCV with vanishing training-to-full sample ratios, BIC, and the SW criteria select it with (simulation) probability approaching one as n increases. AIC and MCCV with fixed training-to-full sample ratios tend to choose less parsimonious models that nest the true DGP with non-vanishing simulation probability as n increases. When all models under consideration are misspecified, however, only the SW criteria exhibit model selection pseudo-consistency. These results are consistent with our theoretical results as well as the results in Shao (1997) regarding the relationship between AIC, BIC and MCCV. We also examine the behavior of GICs in designs with varying levels of signal-to-noise ratio (SNR) (c.f. Hastie et al. 2020, for example). We find that for low SNR, the SW criteria may choose the null model, which is a model with fixed effects only and no temperature regressors, even though the true DGP is a nontrivial function of temperature. For these low SNR settings, our simulations indicate that BIC can choose the true DGP with high probability. These simulation results point to the importance of considering different model selection criteria as well as the SNR in practice.

Overall, this section formally underscores that the suitability of existing criteria for the policy objective of climate change projections is limited to cases where at least one model under consideration nests the true model. While this is possible in applications where the scientific literature can characterize the physical relationship between temperature and the outcome, the literature on climate change impacts examines a variety of economic outcomes for which the relationship with temperature is difficult to fully characterize. When all models are misspecified, some of the existing criteria minimize the MSE of the within-group transformed outcome, whereas others minimize the Kullback-Leibler divergence. Neither of these two targets ensures that the selected model would perform well in terms of the ideal target in (15). As a result, we next propose the PWMSE that seeks to mimic the ideal target.

3.2 Targeting the MSE of Projected Climate Change Impacts

In this section, we propose a new MSE criterion that targets the prediction of climate change impacts directly for a given climate scenario $\mathcal{W}_{i,T+\tau}$, which we refer to as proximity-weighted MSE

(PWMSE). We then propose an MCCV procedure to estimate the PWMSE and show that the model minimizing the estimated PWMSE is asymptotically minimizing its population analogue.

To motivate this criterion, note that under strict exogeneity and additional regularity conditions, minimizing the ideal MSE target in (15) is equivalent to minimizing

$$E[(\mu_\alpha(\mathcal{W}_{i,T+\tau}^f) - \mu_\alpha(\mathcal{W}_{i,T}) - (Y_{i,T+\tau} - Y_{iT}))^2] + E[(u_{i,T+\tau}^f - u_{iT})^2], \quad (25)$$

where $u_{i,T+\tau}^f = \mu_\star(\mathcal{W}_{i,T+\tau}) - \mu_\star(\mathcal{W}_{i,T+\tau}^f) + u_{i,T+\tau}$. Since the second term in (25) does not depend on \mathbf{M}_α , we can select the model based on the first term. In practice, the problem, as with other forecasting settings, is that we do not observe $Y_{i,T+\tau}$. The standard approach in forecasting would be to mimic the τ -step-ahead forecasting in the following way,

$$\frac{1}{T-\tau} \sum_{t=\tau+1}^T E[(\mu_\alpha(\mathcal{W}_{it}) - \mu_\alpha(\mathcal{W}_{i,t-\tau}) - (Y_{it} - Y_{i,t-\tau}))^2]. \quad (26)$$

This approach is not suitable in our setting since climate change implies that the distribution of weather is non-stationary. As a result, this criterion targets precision of the functional approximation of $\mu_\star(w_2) - \mu_\star(w_1)$ under the past as opposed to the future climate. For example, if in the past the climate was on average more moderate, while the projected climate is relatively hot, the above criterion will give relatively higher weight to moderate climates. Moreover, there is no guarantee that the projected changes in the climate will follow a linear trend that would make changes between $T - \tau$ and T comparable to changes between $T + \tau$ and T . Finally, this criterion can be infeasible in this setting, since τ/T tends to be close to or greater than 1 in practice.

We suggest the following criterion that relies on a weighting function that gives higher weights to historical years with climates that are more similar to the projected climate $\mathcal{W}_{i,T+\tau}^f$ and thereby mimics the ideal target more closely,

$$PWMSE_\alpha = \sum_{r=1}^{T-1} E[(\mu_\alpha(\mathcal{W}_{i,T-r}) - \mu_\alpha(\mathcal{W}_{iT}) - (\mu_\star(\mathcal{W}_{i,T-r}) - \mu_\star(\mathcal{W}_{iT})))^2 \pi(\mathcal{W}_{i,T-r}, \mathcal{W}_{i,T+\tau}^f)], \quad (27)$$

where $\pi(\mathcal{W}_{j,T-r}, \mathcal{W}_{i,T+\tau}^f)$ is a weighting function that gives higher weight to prior years with similar weather to the projected weather. The PWMSE can provide a good approximation to the ideal target in (15), if for each i there exists a year in the sample that resembles the corresponding projected climate. The two criteria trivially coincide if $T = 2$ and $\mathcal{W}_{i,1} = \mathcal{W}_{i,T+\tau}^f$ for all i . Intuitively, the weighting function $\pi(\cdot, \mathcal{W}_{i,T+\tau}^f)$ ensures that the selected model provides improved prediction of climate change impacts for years with climates that resemble the corresponding projected climate, $\mathcal{W}_{i,T+\tau}^f$.

In practice, the weighting function is a user-specified component in the PWMSE criterion. The function should be non-negative, bounded, and decrease with the distance between $\mathcal{W}_{i,T-r}$ and the target $\mathcal{W}_{i,T+\tau}^f$. A natural choice for the weighting function is $\pi(\mathcal{W}_{i,T-r}, \mathcal{W}_{i,T+\tau}^f) = e^{-\frac{\|\mathcal{W}_{i,T-r} - \mathcal{W}_{i,T+\tau}^f\|_p^2}{h}}$, which decays exponentially as the distance between $\mathcal{W}_{i,T-r}$ and $\mathcal{W}_{i,T+\tau}$ grows as measured by the norm, $\|\cdot\|_p$.

The choice of the norm should be guided by what aspects of the projected climate the researcher or policymaker would like to mimic. In the simulation section, we consider L^∞ and L^2 norms of the difference in annual and monthly mean temperature as well as daily temperature. We examine the impact of these different norms as well as the choice of the tuning parameter h in the simulation study in Section 3.2.1. We also provide guidance for practitioners in Appendix F.

In order to estimate the PWMSE in practice, we propose the following MCCV procedure,

1. For each s randomly split individuals $i = 1, \dots, n$ into a training sample \mathcal{I}_s^c of size n_c and a testing sample \mathcal{I}_s^v of size n_v . Use training sample \mathcal{I}_s^c to estimate $\hat{\mu}_\alpha^s(\cdot)$ and use the testing sample n_v to compute the out-of-sample MSE,

$$PW\widehat{MSE}_\alpha^s = \sum_{r=1}^{T-1} \frac{1}{n_v} \sum_{i \in \mathcal{I}_s^v} (\hat{\mu}_\alpha^s(\mathcal{W}_{iT}) - \hat{\mu}_\alpha^s(\mathcal{W}_{i,T-r}) - (Y_{iT} - Y_{i,T-r}))^2 \pi(\mathcal{W}_{i,T-r}, \mathcal{W}_{i,T+\tau}^f), \quad (28)$$

where $\pi(\mathcal{W}_{i,T-r}, \mathcal{W}_{i,T+\tau}^f) = e^{-\frac{\|\mathcal{W}_{i,T-r} - \mathcal{W}_{i,T+\tau}^f\|_p^2}{h}}$.

2. Repeat Step 1 S times,

$$PW\widehat{MSE}_\alpha = \frac{1}{S} \sum_{s=1}^S PW\widehat{MSE}_\alpha^s. \quad (29)$$

Next, we show that the model that minimizes $PW\widehat{MSE}_\alpha$ minimizes $PWMSE_\alpha$ with probability one as $n \rightarrow \infty$. Before we proceed to the proposition, we introduce the required conditions.

Condition 3. *The following conditions hold:*

1. $n_c \rightarrow \infty$ and $n_v \rightarrow \infty$, as $n \rightarrow \infty$ holding T fixed.
2. $(\{\tilde{Y}_{it}, \mathcal{W}_{it}\}_{t=1}^T, \mathcal{W}_{i,T+\tau}^f)$ are i.i.d across i .
3. $E[u_{it} | \mathcal{W}_{i1}, \dots, \mathcal{W}_{iT}, \mathcal{W}_{i,T+\tau}^f, a_i] = 0$.

4. $E[Y_{it}^{2+\varepsilon}] < M$ and $E[(X'_{it,\alpha}X_{it,\alpha})^{1+\varepsilon}] < M$ for all $t = 1, \dots, T$, $i = 1, \dots, N$, and $\alpha = 1, \dots, A$ for some $\varepsilon > 0$ and $M < \infty$.

5. $E[\tilde{X}_{i,\alpha}\tilde{X}'_{i,\alpha}]$ is invertible for all $\alpha = 1, \dots, A$.

The first part of Condition 3.1, $n_c \rightarrow \infty$, is required for consistency of each estimator $\hat{\beta}_\alpha^s$, while the second part, $n_v \rightarrow \infty$, is necessary for consistency of \widehat{PWMSE}_α . In practical terms, it means that when designing MCCV procedure, both n_c and n_v should be chosen sufficiently large. We do not impose any restriction on their relative rate for our purposes. The cross-sectional i.i.d. assumption (Condition 3.2) is imposed on the within-demeaned outcome, weather time series as well as the forecast climate. It is one of the sufficient conditions for the consistency of $\hat{\beta}_\alpha^s$ and application of the uniform law of large numbers to PWMSE. This condition can potentially be replaced by a weak-dependence assumption across i at a cost of changing the resampling scheme of the MCCV procedure. Condition 3.3 is an augmented version of the strict exogeneity assumption that includes the projected climate $\mathcal{W}_{i,T+\tau}^f$. Condition 3.4 is a sufficient condition for the applicability of a law of large numbers that results in the consistency of $\hat{\beta}_\alpha^s$ and \widehat{PWMSE}_α for all α . It is a rather mild moment restriction that is commonly assumed. Finally, Condition 3.5, no multicollinearity in approximate models, is required for the consistency of $\hat{\beta}_\alpha^s$.

Proposition 3. *Consider a finite class of models $\mathbb{M} = \{\mathbf{M}_\alpha\}_{\alpha=1}^A$. Suppose that Condition 3 holds. Then the model that minimizes \widehat{PWMSE}_α also minimizes $PWMSE_\alpha$ in the class of models with probability approaching 1.*

The proof is provided in Appendix A.4. If the model with minimal error $PWMSE_\alpha$ is unique, Proposition 3 implies that \widehat{PWMSE}_α selects that model as the training and validation sample sizes grow.

3.2.1 Simulation Study

We design a simulation study to illustrate the finite-sample performance of the PWMSE criterion under different tuning parameter choices. We consider three DGPs of an outcome-temperature relationship: (i) the annual mean model (A), (ii) the quadratic in annual mean model (*QinA*), and (iii) the quarterly mean model (Q), and we evaluate the performance of our proposed strategy based on minimizing the PWMSE for selecting among a broader set of models.

The following functions generate the outcome Y_{it} for the three DGPs we consider which correspond to the examples we provide in Example 1:

- Annual Mean (A): $Y_{it} = \bar{W}_{it} + a_{i,\alpha} + u_{it,\alpha}$,

- Quadratic in Annual Mean (*QinA*): $Y_{it} = 0.2\bar{W}_{it} - 0.05\bar{W}_{it}^2 + a_{i,\delta} + u_{it,\delta}$,
- Quarterly Mean (*Q*): $Y_{it} = -0.25\bar{W}_{it}^{Q_1} + 0.75\bar{W}_{it}^{Q_3} + a_{i,\gamma} + u_{it,\gamma}$,

For each of the DGPs we consider, we use a random sample of counties from the National Climatic Data Center (NCDC) temperature dataset for the years 1968-1977 as \mathcal{W}_{it} for $i = 1, \dots, n$ and $t = 1, \dots, T$, where $T = 10$. For each simulation replication, we generate $a_i | \mathcal{W}_{i1}, \mathcal{W}_{i2}, \dots, \mathcal{W}_{iT} \stackrel{i.i.d.}{\sim} N(0.5\bar{W}_i, 1)$, where $\bar{W}_i = \sum_{t=1}^T \sum_{\tau=1}^H W_{it\tau} / (TH)$. The idiosyncratic shocks u_{it} are generated as a bivariate mixture normal that is heteroskedastic and serially correlated as follows. Let $u_i = (u_{i1}, \dots, u_{iT}) = \epsilon_i^1 + \epsilon_i^2$, where $\epsilon_i^1 | \mathcal{W}_{i1}, \dots, \mathcal{W}_{iT}, a_i \stackrel{i.i.d.}{\sim} N(-0.5, \Sigma_1)$ and $\epsilon_i^2 | \mathcal{W}_{i1}, \dots, \mathcal{W}_{iT}, a_i \stackrel{i.i.d.}{\sim} N(0.5, \Sigma_2)$, with

$$\Sigma_1 = \begin{pmatrix} 1 & 0.5 & 0.1 & 0 & 0 & 0 & 0 & 0 & 0 & 0 \\ 0.5 & 1 & 0.5 & 0.1 & 0 & 0 & 0 & 0 & 0 & 0 \\ 0.1 & 0.5 & 1 & 0.5 & 0.1 & 0 & 0 & 0 & 0 & 0 \\ 0 & 0.1 & 0.5 & 1 & 0.5 & 0.1 & 0 & 0 & 0 & 0 \\ 0 & 0 & 0.1 & 0.5 & 1 & 0.5 & 0.1 & 0 & 0 & 0 \\ 0 & 0 & 0 & 0.1 & 0.5 & 1 & 0.5 & 0.1 & 0 & 0 \\ 0 & 0 & 0 & 0 & 0.1 & 0.5 & 1 & 0.5 & 0.1 & 0 \\ 0 & 0 & 0 & 0 & 0 & 0.1 & 0.5 & 1 & 0.5 & 0.1 \\ 0 & 0 & 0 & 0 & 0 & 0 & 0.1 & 0.5 & 1 & 0.5 \\ 0 & 0 & 0 & 0 & 0 & 0 & 0 & 0.1 & 0.5 & 1 \end{pmatrix}, \quad \Sigma_2 = \begin{pmatrix} 1 & 0.5 & 0.1 & 0 & 0 & 0 & 0 & 0 & 0 & 0 \\ 0.5 & 0.75 & 0.5 & 0.1 & 0 & 0 & 0 & 0 & 0 & 0 \\ 0.1 & 0.5 & 1 & 0.5 & 0.1 & 0 & 0 & 0 & 0 & 0 \\ 0 & 0.1 & 0.5 & 0.75 & 0.5 & 0.1 & 0 & 0 & 0 & 0 \\ 0 & 0 & 0.1 & 0.5 & 1 & 0.5 & 0.1 & 0 & 0 & 0 \\ 0 & 0 & 0 & 0.1 & 0.5 & 0.75 & 0.5 & 0.1 & 0 & 0 \\ 0 & 0 & 0 & 0 & 0.1 & 0.5 & 1 & 0.5 & 0.1 & 0 \\ 0 & 0 & 0 & 0 & 0 & 0.1 & 0.5 & 0.75 & 0.5 & 0.1 \\ 0 & 0 & 0 & 0 & 0 & 0 & 0.1 & 0.5 & 1 & 0.5 \\ 0 & 0 & 0 & 0 & 0 & 0 & 0 & 0.1 & 0.5 & 0.75 \end{pmatrix}.$$

For each DGP, we consider the following set of models for model selection:

- Annual Mean (*A*): $Y_{it} = \beta_1 \bar{W}_{it} + a_i + u_{it}$,
- Bi-annual Mean (*B*): $Y_{it} = \sum_{k=1}^2 \beta_k \bar{W}_{it}^{B_k} + a_i + u_{it}$,
- Quarterly Mean (*Q*): $Y_{it} = \sum_{k=1}^4 \beta_k \bar{W}_{it}^{Q_k} + a_i + u_{it}$,
- Monthly Mean (*M*): $Y_{it} = \sum_{k=1}^{12} \beta_k \bar{W}_{it}^{M_k} + a_i + u_{it}$,
- Quadratic in Annual Mean (*QinA*): $Y_{it} = \beta_1 \bar{W}_{it} + \beta_2 \bar{W}_{it}^2 + a_i + u_{it}$,
- 10°F Bins (*Bins*): $Y_{it} = \sum_{k=1}^9 \beta_k \text{Bin}^k_{it} + a_i + u_{it}$.

We use the year of 1997 as the future period, twenty years after the last period of the 1968-1977 sample (i.e., $\tau = 20$). In addition, we also conduct our simulation analyses by treating 1992 and 2002 as alternative future periods (i.e., $\tau = 15, 25$), respectively. Data for these three years come from the same county-level NCDC temperature dataset.

Given the importance of the pseudo-true parameter values as well as our proposed PWMSE evaluated at these values in our theoretical analysis, we simulate these quantities for models *A*, *B*, *Q*, *M*, *QinA*, and *Bins* using 2000 simulation replications using the sample of all counties in

our dataset ($n = 3,074$) to ensure that our simulated quantities are as close as possible to their population analogues.

Table 2 presents simulated pseudo-true parameter values $\bar{\beta}_\alpha$.¹⁹ We also simulate the ideal target for our sample $\frac{1}{n} \sum_{i=1}^n (\bar{\mu}_\alpha(\mathcal{W}_{i,T+\tau}^f) - \bar{\mu}_\alpha(\mathcal{W}_{iT}) - (\mu_\star(\mathcal{W}_{i,T+\tau}^f) - \mu_\star(\mathcal{W}_{iT})))^2$ for $\tau = 20$, where $\bar{\mu}_\alpha(\mathcal{W}_{it}) = X'_{it,\alpha} \bar{\beta}_\alpha$. The results indicate that the ideal target is minimized when the model being considered is the DGP (true model). However, we note that the ideal target is very close to that of the true model for models that nest it. In Appendix Table A2, we also report the ideal targets calculated for $\tau = 15$ and $\tau = 25$, respectively. The results are qualitatively similar.

Using simulated pseudo-true parameter values, we also compute the (population) PWMSE in (28) with different specifications of the weights $\pi(\mathcal{W}_{i,T-r}, \mathcal{W}_{i,T+\tau}^f)$ for $r = 1, \dots, T-1$. In constructing the weights, we consider six different norms of the temperature differences between $T-r$ and $T+\tau$: L^∞ norm of daily differences (D1), L^2 norm of daily differences (D2), L^∞ norm of monthly differences (M1), L^2 norm of monthly differences (M2), L^∞ norm of annual differences (Y1), and L^2 norm of annual differences (Y2). We provide precise definitions of these norms in Appendix E. Based on each of these norms, we form the weights with different tuning parameters $h = 1, 10, 100$. In addition, we consider a case where no weight is applied (N).

Table 3 presents the models that minimize the feasible targets under each DGP using different weight specifications for $\tau = 20$. We also present similar results for $\tau = 15, 25$ in Appendix Table A3. In most cases, the feasible target is minimized by the true model. In a few occasions, however, the feasible target is minimized by a less parsimonious model that nests the true model. This occurs when the norm is based on temperature differences at a finer temporal resolution (e.g., D1 and D2) and the tuning parameter is small (e.g., $h = 1$). In these situations, the calculation essentially puts much higher weight on historical observations with daily realizations that highly resemble those of the future year.

We then examine the finite-sample performance of the estimated PWMSE criteria based on a random sample of $n = 3000$ counties from the NCDC sample. We follow the Monte Carlo cross-validation procedure as described in Section 3.2 with $n_c/n = 0.75$ and $S = 100$ across 500 simulation replications. In each simulation design, we select the model that has the minimum \widehat{PWMSE}_α among a set of models being considered.

Figure 3 summarizes the simulation selection frequencies for $\tau = 20$. The figure is arranged in three blocks with each corresponding to a different DGP (i.e., A , $QinA$, and Q). Within each block, we generally consider two groups of model comparisons. The panels on the left are five sets of comparisons across nested models (i.e., A , B , Q , M), and the panels on the right are

¹⁹We compute these values by taking the simulation mean of the estimated coefficients using the entire NCDC sample for each model across 2,000 simulations.

another five sets of comparisons across non-nested models (i.e., A , $QinA$, Q , Bin). Within the nested/non-nested models, we compare across the four models as well as across all combinations of every three out of the four models. This systematic comparison design allows us to evaluate model selection performance when the true model is either included or excluded in the set of models being considered under each DGP. Within each panel, we show the simulation proportion of a model being selected with a colored bar using different weights defined using various norms (N, D1, D2, M1, M2, Y1, Y2) and tuning parameters ($h = 1, 10, 100$).

Several patterns emerge from the results. First, when the true model is considered in a set of candidate models, in general, the true model is much more likely to be selected. This is particularly evident in cases when the DGP is $QinA$ or Q . The results are slightly weaker when DGP is A . Specifically, models that nest A are selected for a non-negligible proportion of times even if A is among the candidate models, especially when the norms are based on daily differences and the adopted tuning parameters h are small.

Second, when the true model is not considered in a set of models, the candidate models that correspond to smaller values of the ideal target tend to be selected. This result can be seen in cases where (i) B is selected from $\{B, Q, M\}$ and $QinA$ is selected from $\{QinA, Q, Bin\}$ when the DGP is A , (ii) B/M is selected from $\{A, B, Q, M\}$ and Q is selected from $\{A, Q, Bin\}$ when the DGP is $QinA$, and (iii) M is selected from $\{A, B, M\}$ and Bin is selected from $\{A, QinA, Bin\}$ when the DGP is Q .

Comparing across different tuning parameters, we note that the choice of norm is inconsequential for high values of the tuning parameter. This is unsurprising given that $h = 100$ yields relatively equal weights across years no matter which norm is considered, rendering a situation that is very similar to the case of specifying no weight. In contrast, $h = 1$ produces very small weights on those observations that do not resemble their future counterparts in terms of the norm definition. Since different norms characterize similarities between the past and future realizations from different aspects, with small h , the observations that have been weighted more in calculating PWMSE could also vary across the different norms adopted, potentially resulting in different model selection outcomes. This phenomenon is reflected in our simulation results when comparing model selection outcomes between D1/D2 versus Y1/Y2 under $h = 1$.

This finding also indicates that the choice of norms can matter for the use of PWMSE especially if we assign much higher weights on those past realizations that are highly similar to their future counterparts. Among the six norms in our simulation study, the norms based on daily temperature differences tend to select larger models, which is most evident from the simulation results when DGP is A with small h . Since the true model in our simulation design does not exploit data variation at a very fine temporal scale, we conjecture that this may help explain why the norms

Y1/Y2 result in higher simulation probabilities of selecting A when it is the true model.

We also present the simulation results for different future climates $\tau = 15$ and $\tau = 25$ in Appendix Figures A5 and A6, respectively. For these different future climates, the model selection results do not vary much when the true model or a model that nests it is under consideration. However, the selection results vary across τ substantially when all models are misspecified. This is particularly true when h is small, which leads to bigger differences in the weighting function depending on the value of the norm. This is most evident when comparing results of DGP= $QinA$ with $h = 1$ across different τ . In particular, some results based on the norms of daily and monthly differences are substantially different for the different values of τ we consider. Based on these insights from the simulation results, we provide guidance for practitioners in Appendix F on how to specify the weighting function when using our proposed PWMSE criterion in practice.

Overall, our simulation results underscore the advantage of the PWMSE approach relative to existing model selection criteria that do not incorporate the climate scenario into model selection and therefore would choose the same model regardless of the climate scenario in question. By contrast, the PWMSE chooses the best approximate model for a given climate scenario. Consistent with our theoretical predictions, the advantage from the PWMSE relative to existing criteria is greater when all models under consideration are misspecified.

4 Empirical Application: Temperature and Crop Yields

We carry out an application of model selection in a classic context of the empirical literature — identifying nonlinear temperature effects on crop yields. The agronomic studies have documented that the accumulation of heat is only beneficial to crop growth over certain ranges of the temperature and becomes detrimental otherwise (Ritchie and Nesmith 1991). Previous statistical analyses also find evidence of nonlinearity in crop yield response to temperature under different estimation specifications (e.g., Burke and Emerick 2016; Gammans et al. 2017; Schlenker and Roberts 2009). However, the qualitative similarity of nonlinearity does not diminish the importance of exploring the quantitative difference between alternative specifications, especially considering that nuances in the estimation results could be substantially magnified when it comes to projecting future climate impacts.

In this empirical application, we consider different specifications of temperature variables in the following model,

$$\log(Y_{it}) = \mu_{\alpha}(\mathcal{T}_{it}) + \theta_1 P_{it} + \theta_2 P_{it}^2 + \delta_{1,s}t + \delta_{2,s}t^2 + a_i + \epsilon_{it},$$

where Y_{it} represents corn yield (bushels/acre) in county i in crop year t . The response function $\mu_{\alpha}(\mathcal{T}_{it}) = X'_{it,\alpha}\beta_{\alpha}$ is a linear function of regressors constructed from the daily temperature time

series over the growing season $\mathcal{T}_{it} \equiv \{T_{ith}\}_{h=1}^H$.²⁰ P_{it} represents growing-season total precipitation, $\delta_{1,s}$ and $\delta_{2,s}$ characterize state-level quadratic trends, a_i represents county fixed effect and ϵ_{it} is the error term.

We consider the following set of temperature specifications: (a) reference model with no temperature variables, (b) monthly average temperatures, (c) 1°C daily temperature bins, (d) 3°C step function, (e) degree days in the fashion of Schlenker et al. (2006) (SHF degree days, hereafter), (f) piecewise linear function with one knot, and (g) piecewise linear function with two knots. Models (a)-(f) are model candidates considered in Schlenker and Roberts (2009), and model (g) is a more flexible variant of (f).²¹ All the models above only consider growing-season temperatures. The two piecewise linear specifications rely on knots selected by minimizing MSE.²² Although the specifications considered here are not exhaustive, we believe they are sufficiently rich to illustrate the differentiated performances among different model selection criteria.

We obtain county-level corn yield data covering 1950-2015 from USDA Quick Stats. The source of historical weather information is the PRISM dataset, which provides spatially gridded daily data at 4km-by-4km resolution. We follow the data managing procedure in Schlenker and Roberts (2009) and obtain county-level daily temperature and precipitation over 1950-2015. Based on the merged county-level data, we first conduct estimation using an unbalanced panel of all available observations. This unbalanced sample contains 2,278 counties with a total of 120,995 observations. The estimation results, as reported in Appendix Table A5, are in line with previous findings.²³ We also implement the estimations based on a balanced panel of 679 counties in the core region of the corn belt, with a total of 44,814 observations. The estimation results, presented in Appendix Table A6, are qualitatively similar.

We illustrate the differentiated prediction outcomes based on these empirical estimates in the mid-century. Specifically, we recalculate all relevant temperature variables for the 2050 climate at the county level using projected climate data from the HadCM3-B1 model. We then calculate the predicted changes in these temperature variables at the county level by differencing their 2050 values with their 2015 counterparts, and form predicted changes in log yields by applying different sets of the empirical estimates. The predicted changes in log yields based on different models are

²⁰Previous studies have shown the importance of considering within-season temperature variation in modeling the response of crop yields since the seminal work in Schlenker et al. (2006) and Schlenker and Roberts (2009).

²¹Model (c) uses bins constructed based on daily average temperatures, while (d) further utilizes diurnal variation in temperature by employing a sinusoidal interpolation between daily maximum and minimum temperatures before forming relevant bins.

²²We present the smallest ten MSEs in Appendix Table A4.

²³We also report the SNR for each model, and these ratios are mostly close to 0.40. When calculating, we consider all weather variables as the signal component, and we obtain the SNRs by projecting out all the time trends and fixed effects.

mapped in Figure 4.

As for model selection, we first apply the existing model selection criteria, including the two MCCV and the four GICs. Table 4 shows that, evaluated on the unbalanced panel, AIC and BIC select the 3°C step function, the two cross-validation procedures and SW_1 select the two-knot piecewise function (knots at 24°C and 26°C), and SW_2 selects the one-knot piecewise linear function (knot at 29°C). When evaluated on the balanced panel, both AIC and BIC still select the 3°C step function, while the two SW criteria and the two MCCV procedures all choose the one-knot piecewise function for which the MSE-minimizing knot is at 30°C. We visualize these selected nonlinear temperature response functions in Figure 5. Although the nonlinear patterns are qualitatively similar for these selected models, those piecewise models selected by MCCV and SW criteria are more parsimonious while the step function selected by AIC and BIC is more complex.

As we discussed earlier, none of the criteria above are specifically tailored for the policy objective of better understanding potential future impacts of climate change. Therefore, we apply our proposed PWMSE criteria that incorporate projected future climatic conditions to the seven candidate models with $S = 1000$. Since the finest temporal resolution of our HadCM3-B1 projection data is at the monthly level, we only consider the norms based on monthly and annual differences when forming weights. In Table 5, we present the PWMSE for each model evaluated with different weights for the unbalanced panel and the balanced panel, respectively. Specifically, we consider the case with no weight specified, and the cases with weights based on M1, M2, Y1, Y2, scaled by $h = 1, 10, 100$, respectively. For the unbalanced panel, the PWMSEs are minimized by the model of 3°C step function except for the cases of $h = 1$ where the selected model is degree days in the fashion of Schlenker et al. (2006) (i.e., SHF degree days).²⁴ But we note that setting $h = 1$ in this unbalanced panel exercise may have assigned much higher weights to some of the historical observations that correspond to less frequent growing counties on the peripheral regions of the corn belt. For the balanced panel, the model of 3°C step function delivers the lowest PWMSE regardless of how we specify the weights.

Compared with the models selected by the SW criteria, the PWMSE criterion selects models that result in a qualitatively similar damage function, as we illustrated visually in Figure 5. We also note that the piecewise functions selected by the SW criteria deliver PWMSEs that are only slightly larger than those of the 3°C step function. These similarities may reflect that both models are fairly close approximations of the underlying DGP, especially considering that they deliver

²⁴The SHF degree days include three variables: the growing degree days (GDD), the square of GDD, and the square-root of heat degree days (HDD). GDD accumulates degree-by-days in the range of 8-32°C and HDD accumulates degree-by-days above 34°C.

damage functions that are consistent qualitatively with agronomic predictions.

The models selected by the SW criteria are more parsimonious compared with those selected by PWMSE criterion. This result is consistent with our theoretical discussion and simulation illustration. Nevertheless, we highlight that only the PWMSE criterion takes the future climate scenario into account directly through specifying the weights, while the SW criteria only depend on the historical observations. Our results indicate that the larger model of the 3°C step function provides higher flexibility that potentially improves the scenario-specific prediction for the policy objective of climate change projection. This tailored model selection has quantitative implications since the predicted outcomes under HadCM3-B1, although similar in their spatial gradient, have noticeable differences in their extents of yield reductions across the piecewise and 3°C step functions, as illustrated in Appendix Figure A7. These quantitative differences matter for the policy arrangements of investment activities and adaptation efforts that target specific areas toward a given future climate scenario.

5 Conclusion

This paper formalizes the model selection problem as well as the policy target faced by applied researchers and policymakers interested in examining climate change impacts on outcomes of interest. Building on this crucial first step, the paper first provides conditions under which existing criteria, specifically MCCV and GICs, are appropriate for the policy objective. We show that consistent model selection criteria are suitable if at least one of the models under consideration nests the truth. Since this requirement is restrictive for economic outcomes for which the relationship with temperature is not well understood, we propose a proximity-weighted MSE criterion that targets the MSE of projected climate change impacts directly. We illustrate that these criteria choose models that minimize the ideal target with high probability in a simulation analysis. We demonstrate the empirical relevance of our theoretical analysis in the context of an application on climate change projection of agricultural yields.

While this paper constitutes an important first step toward principled model selection in this policy-relevant empirical context, there are several interesting directions for future research. In light of recent work on exogeneity in climate econometrics (Pretis 2021), developing methods that relax the strict exogeneity assumption is an important direction for future work. More flexible procedures to estimate the response functions would also be a good substitute to the model selection approach taken in this literature. Furthermore, allowing for possible nonlinearities between regressors and fixed effects is another important departure from the setup in this paper. Finally, providing valid post-selection inference for the aforementioned methods constitutes a priority for future work.

A Derivations and Proofs

A.1 MSPE Derivation

Let $\tilde{\mathbf{Z}}$ denote a vector of n “future” values of the within-demeaned outcome whereas $\hat{\beta}_\alpha$ was estimated using the sample $\tilde{\mathbf{Y}}$ and $\tilde{\mathbf{X}}_\alpha$.

$$\begin{aligned}\hat{\Gamma}_{\alpha,nT} &= \frac{1}{nT} \left\| \tilde{\mathbf{Z}} - \tilde{\mathbf{X}}_\alpha \hat{\beta}_\alpha \right\|^2 \\ &= \frac{1}{nT} \left\| \tilde{\mathbf{U}}_z + \tilde{\mathbf{X}}_{\star} \beta_{\star,o} - \underbrace{\tilde{\mathbf{X}}_\alpha (\tilde{\mathbf{X}}_\alpha' \tilde{\mathbf{X}}_\alpha)^{-1} \tilde{\mathbf{X}}_\alpha' \tilde{\mathbf{Y}}}_{\equiv P_\alpha} \right\|^2 \\ &= \frac{1}{nT} \left\| \tilde{\mathbf{U}}_z + (I_{nT} - P_\alpha) \tilde{\mathbf{X}}_{\star} \beta_{\star,o} - P_\alpha \tilde{\mathbf{U}} \right\|^2\end{aligned}\tag{30}$$

where $\tilde{\mathbf{U}}_z$ denotes the within-individual demeaned error term of the observations $\tilde{\mathbf{Z}}$.

Let $\Gamma_{\alpha,nT}$ denote the expectation of $\hat{\Gamma}_{\alpha,nT}$ conditional on $\{\mathcal{W}_i\}_{i=1}^n$

$$\Gamma_{\alpha,nT} = \frac{1}{nT} E[\tilde{\mathbf{U}}_z' \tilde{\mathbf{U}}_z | \{\mathcal{W}_i\}_{i=1}^n] + E[\tilde{\mathbf{U}}' P_\alpha \tilde{\mathbf{U}} | \{\mathcal{W}_i\}_{i=1}^n] + \frac{1}{nT} \beta_{\star,o}' \tilde{\mathbf{X}}_{\star}' (I_{nT} - P_\alpha) \tilde{\mathbf{X}}_{\star} \beta_{\star,o} \tag{31}$$

The first term on the right hand side of the equality equals $E \left[\sum_{i=1}^n \sum_{t=1}^T \tilde{u}_{it}^2 \right] / nT = E[\tilde{u}_{it}^2] = \sigma^2(T-1)/T$. The second term can be simplified as follows

$$\begin{aligned}& \frac{1}{nT} E \left[\tilde{\mathbf{U}}' \tilde{\mathbf{X}}_\alpha (\tilde{\mathbf{X}}_\alpha' \tilde{\mathbf{X}}_\alpha)^{-1} \tilde{\mathbf{X}}_\alpha' \tilde{\mathbf{U}} | \{\mathcal{W}_i\}_{i=1}^n \right] = \frac{1}{nT} \text{tr} \left(E \left[\tilde{\mathbf{U}} \tilde{\mathbf{U}}' \tilde{\mathbf{X}}_\alpha (\tilde{\mathbf{X}}_\alpha' \tilde{\mathbf{X}}_\alpha)^{-1} \tilde{\mathbf{X}}_\alpha' | \{\mathcal{W}_i\}_{i=1}^n \right] \right) \\ &= \frac{1}{nT} \sigma^2 \text{tr} \left(\underbrace{(I_n \otimes (I_T - \mathcal{J}_T/T))}_{\equiv I_n \otimes Q_T} \tilde{\mathbf{X}}_\alpha (\tilde{\mathbf{X}}_\alpha' \tilde{\mathbf{X}}_\alpha)^{-1} \tilde{\mathbf{X}}_\alpha' \right) = \frac{1}{nT} \sigma^2 k_\alpha.\end{aligned}\tag{32}$$

where the last equality follows by noting $(I_n \otimes Q_T) \tilde{\mathbf{X}}_\alpha = \tilde{\mathbf{X}}_\alpha$ as well as properties of the trace.

A.2 Proof of Proposition 1

Proof. The proof is adapted from Shao (1993) to the setting of a fixed effects model with stochastic high-frequency regressors. Following Shao (1993), we first show the results for Balanced Incomplete Cross-Validation (BICV) with stochastic regressors, then we extend the results to MCCV. Let \mathbf{B} be a collection of b subsets of $\{1, \dots, n\}$ that have size n_v such that (i) for each i , $1 \leq i \leq n$, the same number of subsets of \mathbf{B} include it, (ii) for each pair (i, j) for $i, j \in \{1, \dots, n\}$, the same number of subsets of \mathbf{B} include it. From (3.1) in Shao (1993) and the balance property of \mathbf{B} ,

$$\hat{\Gamma}_{\alpha,nT}^{BICV} \geq \frac{1}{n_v T b} \sum_{s \in \mathbf{B}} \left\| \tilde{\mathbf{Y}}_s - \tilde{\mathbf{X}}_{s,\alpha} \hat{\beta}_\alpha \right\|^2 = n^{-1} \left\| \tilde{\mathbf{Y}} - \tilde{\mathbf{X}}_\alpha \hat{\beta}_\alpha \right\|^2 = (nT)^{-1} \tilde{\mathbf{U}}' \tilde{\mathbf{U}} + \Delta_{\alpha,nT} + o_p(1) \tag{33}$$

where the last equality follows from the proof of (3.5) in Shao (1993). (i) in this proposition follows by letting $R_n = \hat{\Gamma}_{\alpha,nT}^{BICV} - \left\| \tilde{\mathbf{Y}} - \tilde{\mathbf{X}}_\alpha \hat{\beta}_\alpha \right\|^2 / n$.

By Condition 1.3.(iii) with $s \in \mathbf{B}$ in lieu of $s \in \mathcal{R}$, it follows for every $s \in \mathbf{B}$,

$$\begin{aligned}
& \frac{1}{n} \tilde{\mathbf{X}}'_\alpha \tilde{\mathbf{X}}_\alpha - \frac{1}{n_v} \tilde{\mathbf{X}}'_{\alpha,s} \tilde{\mathbf{X}}_{\alpha,s} = \frac{1}{n} \left[\tilde{\mathbf{X}}'_{\alpha,s^c} \tilde{\mathbf{X}}_{\alpha,s^c} + \tilde{\mathbf{X}}'_{\alpha,s} \tilde{\mathbf{X}}_{\alpha,s} - \frac{n}{n_v} \tilde{\mathbf{X}}'_{\alpha,s} \tilde{\mathbf{X}}_{\alpha,s} \right] \\
&= \frac{1}{n} \left[\tilde{\mathbf{X}}'_{\alpha,s^c} \tilde{\mathbf{X}}_{\alpha,s^c} + \tilde{\mathbf{X}}'_{\alpha,s} \tilde{\mathbf{X}}_{\alpha,s} - \frac{n_c + n_v}{n_v} \tilde{\mathbf{X}}'_{\alpha,s} \tilde{\mathbf{X}}_{\alpha,s} \right] = \frac{1}{n} \left[\tilde{\mathbf{X}}'_{\alpha,s^c} \tilde{\mathbf{X}}_{\alpha,s^c} - \frac{n_c}{n_v} \tilde{\mathbf{X}}'_{\alpha,s} \tilde{\mathbf{X}}_{\alpha,s} \right] \\
&= \frac{n_c}{n} \left[\frac{1}{n_c} \tilde{\mathbf{X}}'_{\alpha,s^c} \tilde{\mathbf{X}}_{\alpha,s^c} - \frac{1}{n_v} \tilde{\mathbf{X}}'_{\alpha,s} \tilde{\mathbf{X}}_{\alpha,s} \right] = o_p \left(\frac{n_c}{n} \right)
\end{aligned} \tag{34}$$

With some further manipulations,

$$\begin{aligned}
& \left(\frac{1}{n_v} \tilde{\mathbf{X}}'_{\alpha,s} \tilde{\mathbf{X}}_{\alpha,s} \right)^{-1} \frac{1}{n} \tilde{\mathbf{X}}'_\alpha \tilde{\mathbf{X}}_\alpha - I = o_p \left(\frac{n_c}{n} \right) \left(\frac{1}{n_v} \tilde{\mathbf{X}}'_{\alpha,s} \tilde{\mathbf{X}}_{\alpha,s} \right)^{-1} \\
& \left(\frac{1}{n_v} \tilde{\mathbf{X}}'_{\alpha,s} \tilde{\mathbf{X}}_{\alpha,s} \right)^{-1} - \left(\frac{1}{n} \tilde{\mathbf{X}}'_\alpha \tilde{\mathbf{X}}_\alpha \right)^{-1} = o_p \left(\frac{n_c}{n} \right) \left(\frac{1}{n_v} \tilde{\mathbf{X}}'_{\alpha,s} \tilde{\mathbf{X}}_{\alpha,s} \right)^{-1} \left(\frac{1}{n} \tilde{\mathbf{X}}'_\alpha \tilde{\mathbf{X}}_\alpha \right)^{-1} \\
& \left(\tilde{\mathbf{X}}'_{\alpha,s} \tilde{\mathbf{X}}_{\alpha,s} \right)^{-1} - \frac{n}{n_v} \left(\tilde{\mathbf{X}}'_\alpha \tilde{\mathbf{X}}_\alpha \right)^{-1} = o_p \left(\frac{n_c}{n} \right) \left(\tilde{\mathbf{X}}'_{\alpha,s} \tilde{\mathbf{X}}_{\alpha,s} \right)^{-1} \underbrace{\left(\frac{1}{n} \tilde{\mathbf{X}}'_\alpha \tilde{\mathbf{X}}_\alpha \right)^{-1}}_{=O_p(1) \text{ by (3.3)}}
\end{aligned} \tag{35}$$

Hence, together with Condition 1.3.i, the above implies that

$$\left(\tilde{\mathbf{X}}'_{\alpha,s} \tilde{\mathbf{X}}_{\alpha,s} \right)^{-1} - \frac{n}{n_v} \left(\tilde{\mathbf{X}}'_\alpha \tilde{\mathbf{X}}_\alpha \right)^{-1} = o_p \left(\frac{n_c}{n} \right) \left(\tilde{\mathbf{X}}'_{\alpha,s} \tilde{\mathbf{X}}_{\alpha,s} \right)^{-1} \tag{36}$$

For $P_{\alpha,s} = \tilde{\mathbf{X}}_{\alpha,s} (\tilde{\mathbf{X}}'_{\alpha,s} \tilde{\mathbf{X}}_{\alpha,s})^{-1} \tilde{\mathbf{X}}'_{\alpha,s}$,

$$\begin{aligned}
P_{\alpha,s} &= \frac{n}{n_v} \tilde{\mathbf{X}}_{\alpha,s} \left(\tilde{\mathbf{X}}'_\alpha \tilde{\mathbf{X}}_\alpha \right)^{-1} \tilde{\mathbf{X}}'_{\alpha,s} + \frac{n}{n_v} \tilde{\mathbf{X}}_{\alpha,s} \left(\tilde{\mathbf{X}}'_\alpha \tilde{\mathbf{X}}_\alpha \right)^{-1} \tilde{\mathbf{X}}'_{\alpha,s} + o \left(\frac{n_c}{n} \right) \tilde{\mathbf{X}}_{\alpha,s} (\tilde{\mathbf{X}}'_{\alpha,s} \tilde{\mathbf{X}}_{\alpha,s})^{-1} \tilde{\mathbf{X}}'_{\alpha,s} \\
&= \frac{n}{n_v} Q_{\alpha,s} + o_p \left(\frac{n_c}{n} \right) P_{\alpha,s}
\end{aligned} \tag{37}$$

Given that $n_v/n = O(1)$, it follows that

$$Q_{\alpha,s} = P_{\alpha,s} \left(\frac{n_v}{n} + o_p \left(\frac{n_c}{n} \right) \right) \tag{38}$$

From the balance property of \mathbf{B} ,

$$\begin{aligned}
& \frac{1}{n_v T b} \sum_{s \in \mathbf{B}} \mathbf{r}'_{\alpha,s} Q_{\alpha,s} \nabla_{\alpha,s} = \frac{1}{n_v T b} \sum_{s \in \mathbf{B}} \sum_{i \in s} \sum_{t=1}^T w_{it,\alpha} r_{it,\alpha}^2 = \frac{1}{n_v T b} \left(\frac{n_v b}{n} - \frac{n_v b}{n} \frac{n_v - 1}{n - 1} \right) \sum_{i=1}^n \sum_{t=1}^T w_{it,\alpha} r_{it,\alpha}^2 \\
&= \frac{1}{T} \left(\frac{1}{n} - \frac{n_v - 1}{n(n-1)} \right) \sum_{i=1}^n \sum_{t=1}^T w_{it,\alpha} r_{it,\alpha}^2
\end{aligned}$$

where $\mathbf{r}_{\alpha,s} = \tilde{\mathbf{Y}}_s - \tilde{\mathbf{X}}_{\alpha,s}\hat{\beta}_\alpha$ and $r_{it,\alpha} = \tilde{Y}_{it} - \tilde{X}'_{it,\alpha}\hat{\beta}_\alpha$.

By (38) and $n_v/n \rightarrow 1$ and $n_c \rightarrow \infty$, let $c_n = n_v(n + n_c)n_c^{-2}$,

$$\begin{aligned} \frac{c_n}{n_v T b} \|P_{\alpha,s} \mathbf{r}_{\alpha,s}\|^2 &= \left[\frac{n_v}{n} + o_p\left(\frac{n_c}{n}\right) \right]^{-1} \frac{c_n}{n_v T b} \sum_{s \in \mathbf{B}} \mathbf{r}'_{\alpha,s} Q_{\alpha,s} \mathbf{r}_{\alpha,s} \\ &= \left[\frac{n}{n_v} + o_p\left(\frac{n_c}{n}\right) \right] \frac{n_v(n + n_c)n_c^{-2}}{n_v T b} \sum_{s \in \mathbf{B}} \mathbf{r}'_{\alpha,s} Q_{\alpha,s} \mathbf{r}_{\alpha,s} \\ &= \left[1 + o_p\left(\frac{n_c}{n}\right) \right] \frac{n + n_c}{n_c(n - 1)T} \sum_{i=1}^n \sum_{t=1}^T w_{it,\alpha} r_{it,\alpha}^2 \end{aligned} \quad (39)$$

Now we can write $\hat{\Gamma}_{\alpha,n}^{BICV} = D_\alpha + B_\alpha$, where

$$\begin{aligned} \hat{\Gamma}_{\alpha,n}^{BICV} &= \frac{1}{n_v T b} \sum_{s \in \mathbf{B}} \|(I_{n_v T} - Q_{\alpha,s})^{-1} (Y_s - \tilde{\mathbf{X}}_{\alpha,s} \hat{\beta}_\alpha)\|^2 = \frac{1}{n_v T b} \sum_{s \in \mathbf{B}} \mathbf{r}'_{\alpha,s} (I_{n_v T} - Q_{\alpha,s})^{-2} \mathbf{r}_{\alpha,s} \\ &= \frac{1}{n_v T b} \sum_{s \in \mathbf{B}} \|(I_{n_v T} - Q_{\alpha,s})^{-1} (Y_s - \tilde{\mathbf{X}}_{\alpha,s} \hat{\beta}_\alpha)\|^2 \\ &= \underbrace{\frac{1}{n_v T b} \sum_{s \in \mathbf{B}} \mathbf{r}'_{\alpha,s} (I_{n_v T} - Q_{\alpha,s})^{-1} U_{\alpha,s} (I_{n_v T} - Q_{\alpha,s})^{-1} \mathbf{r}_{\alpha,s}}_{\equiv D_\alpha} \\ &\quad + \underbrace{\frac{1}{n_v T b} \sum_{s \in \mathbf{B}} \mathbf{r}'_{\alpha,s} (I_{n_v T} - Q_{\alpha,s})^{-1} (I_{n_v T} - U_{\alpha,s}) (I_{n_v T} - Q_{\alpha,s})^{-1} \mathbf{r}_{\alpha,s}}_{\equiv B_\alpha} \end{aligned}$$

where

$$Z_{\alpha,s} = (I_{n_v T} - Q_{\alpha,s})(I + c_n P_{\alpha,s})(I_{n_v T} - Q_{\alpha,s})$$

From the balance property of \mathbf{B} and (39)

$$\begin{aligned} D_\alpha &= \frac{1}{n_v T b} \sum_{s \in \mathbf{B}} \|\mathbf{r}_{\alpha,s}\|^2 + \frac{c_n}{n_v T b} \sum_{s \in \mathbf{B}} P_{\alpha,s} \|\mathbf{r}_{\alpha,s}\|^2 \\ &= \frac{1}{nT} \|\tilde{\mathbf{Y}} - \tilde{\mathbf{X}}_\alpha \hat{\beta}_\alpha\|^2 + \left[1 + o_p\left(\frac{n_c}{n}\right) \right] \frac{n + n_c}{n_c(n - 1)T} \sum_{i=1}^n \sum_{t=1}^T w_{it,\alpha} r_{it,\alpha}^2 \end{aligned} \quad (40)$$

Assume \mathbf{M}_α is in Category II. Then by (40) and $\sum_{i=1}^n \sum_{t=1}^T w_{it,\alpha} r_{it,\alpha}^2 = k_\alpha \sigma^2 + o_p(1)$

$$\begin{aligned} D_\alpha &= \frac{1}{n} \tilde{\mathbf{U}}' (I - P_\alpha) \tilde{\mathbf{U}} + \left[1 + o_p\left(\frac{n_c}{n}\right) \right] \frac{n + n_c}{n_c(n - 1)T} [k_\alpha \sigma^2 + o_p(1)] \\ &= \frac{1}{n} \tilde{\mathbf{U}}' \tilde{\mathbf{U}} - \frac{1}{n} \tilde{\mathbf{U}}' P_\alpha \tilde{\mathbf{U}} + \left[1 + o_p\left(\frac{n_c}{n}\right) \right] \frac{n + n_c}{n_c(n - 1)T} [k_\alpha \sigma^2 + o_p(1)] \\ &= \frac{1}{n} \tilde{\mathbf{U}}' \tilde{\mathbf{U}} + \frac{k_\alpha \sigma^2}{n_c T} + o_p\left(\frac{1}{n_c}\right) \end{aligned}$$

It remains to show that $B_\alpha = o_p(n_c^{-1})$. From (38)

$$\begin{aligned} (I_{n_v T} - Q_{\alpha,s})P_{\alpha,s}(I_{n_v T} - Q_{\alpha,s}) &= \left(1 - \frac{n_v}{n} + o\left(\frac{n_c}{n}\right)\right) P_{\alpha,s}(I_{n_v T} - Q_{\alpha,s}) = \left(1 - \frac{n_v}{n} + o\left(\frac{n_c}{n}\right)\right)^2 P_{\alpha,s} \\ &= \left(\frac{n_c}{n} + o_p\left(\frac{n_c}{n}\right)\right)^2 P_{\alpha,s} \end{aligned} \quad (41)$$

Thus,

$$\left(\frac{n}{n_c}\right)^2 (I_{n_v T} - Q_{\alpha,s})P_{\alpha,s}(I_{n_v T} - Q_{\alpha,s}) = (1 + o(1))^2 P_{\alpha,s} \geq \frac{1}{2} P_{\alpha,s} \quad (42)$$

for $s \in \mathbf{B}$ and n sufficiently large. Pre- and post-multiplying the above by $(I_{n_v T} - Q_{\alpha,s})^{-1}$ yields

$$(I_{n_v T} - Q_{\alpha,s})^{-1} P_{\alpha,s} (I_{n_v T} - Q_{\alpha,s})^{-1} \leq 2 \left(\frac{n}{n_c}\right)^2 P_{\alpha,s} \quad (43)$$

Similarly by (38)

$$\begin{aligned} Z_{\alpha,s} &= \left\{ I_{n_v T} - \left[\frac{n_v}{n} + o_p\left(\frac{n_c}{n}\right) \right] P_{\alpha,s} \right\} (I_{n_v T} + c_n P_{\alpha,s}) \left\{ I_{n_v T} - \left[\frac{n_v}{n} + o_p\left(\frac{n_c}{n}\right) \right] \right\} \\ &= I_{n_v T} + \left[o_p\left(\frac{n_c}{n}\right) \right]^2 (1 + c_n) P_{\alpha,s} \end{aligned} \quad (44)$$

since $c_n(1 - n_v/n)^2 = (2 - n_v/n)n_v/n$. Using (40)

$$\begin{aligned} &(I_{n_v T} - Q_{\alpha,s})^{-1} (I_{n_v T} - Z_{\alpha,s}) (I_{n_v T} - Q_{\alpha,s})^{-1} \\ &= \left[o_p\left(\frac{n_c}{n}\right) \right]^2 (1 + c_n) (I_{n_v T} - Q_{\alpha,s})^{-1} P_{\alpha,s} (I_{n_v T} - Q_{\alpha,s})^{-1} \leq o_p(1) (1 + c_n) P_{\alpha,s}. \end{aligned}$$

Thus,

$$B_\alpha \leq o_p(1)(1 + c_n) \left(\frac{1}{n_v T b} \sum_{s \in \mathbf{B}} \|P_{\alpha,s} \mathbf{r}_{\alpha,s}\|^2 \right) = o_p\left(\frac{1}{n_c}\right) \quad (45)$$

since from the above $(c_n/n_v T b) \sum_{s \in \mathbf{B}} \|P_{\alpha,s} \mathbf{r}_{\alpha,s}\|^2 = O_p(n_c^{-1})$, which proves (ii) in the proposition for BICV. (iii) follows in a straightforward manner from (i) and (ii).

The extension of the proof to MCCV is straightforward from Theorem 2 in Shao (1993) assuming the sufficient conditions given in Condition 1. \square

A.3 Proof of Proposition 2

First, note that Conditions 2.1-2.3 imply that

$$\begin{aligned} \sqrt{n} \begin{pmatrix} \hat{\beta}_\alpha - \beta_\alpha^* \\ \hat{\beta}_\gamma - \beta_\gamma^* \end{pmatrix} &= \sqrt{n} \begin{pmatrix} \hat{D}_\alpha^{-1} & \mathbf{0}_{k_\alpha \times k_\gamma} \\ \mathbf{0}_{k_\gamma \times k_\alpha} & \hat{D}_\gamma^{-1} \end{pmatrix} \begin{pmatrix} \hat{b}_\alpha \\ \hat{b}_\gamma \end{pmatrix} \\ &= \begin{pmatrix} D_\alpha^{-1} & \mathbf{0}_{k_\alpha \times k_\gamma} \\ \mathbf{0}_{k_\gamma \times k_\alpha} & D_\gamma^{-1} \hat{b}_\gamma \end{pmatrix} \sqrt{n} \begin{pmatrix} \hat{b}_\alpha \\ \hat{b}_\gamma \end{pmatrix} + o_p(1) \xrightarrow{d} N \left(0, \begin{pmatrix} \Sigma_\alpha & \Sigma_{\alpha,\gamma} \\ \Sigma_{\gamma,\alpha} & \Sigma_\gamma \end{pmatrix} \right) \end{aligned} \quad (46)$$

where $\Sigma_\alpha = D_\alpha^{-1}B_\alpha D_\alpha^{-1}$, $\Sigma_{\alpha,\gamma} = D_\alpha^{-1}B_{\alpha,\gamma}D_\gamma^{-1}$, $\Sigma_\gamma = D_\gamma^{-1}B_\gamma D_\gamma^{-1}$. The first equality follows by definition of the fixed effects estimators and their pseudo-true parameter values. The second equality follows by Conditions 2.1 and 2.3. The convergence in distribution follows by Condition 2.3.

Next, we perform the following Taylor series expansion of $\ell_{nT}(\beta_\alpha) \equiv \ell_{nT}(\beta_\alpha, \sigma^2(\beta_\alpha))$

$$\begin{aligned}\ell_{nT}^\alpha(\beta_\alpha^*) &= \ell_{nT}^\alpha(\hat{\beta}_\alpha) + \frac{1}{2} \left(\hat{\beta}_\alpha - \beta_\alpha^* \right)' \frac{\partial^2 \ell_{nT}^\alpha(\beta_\alpha)}{\partial \beta_\alpha \partial \beta_\alpha'} \Big|_{\beta_\alpha = \hat{\beta}_\alpha} \left(\hat{\beta}_\alpha - \beta_\alpha^* \right) + o_p(1) \\ &= \ell_{nT}^\alpha(\hat{\beta}_\alpha) - n \left(\hat{\beta}_\alpha - \beta_\alpha^* \right)' \frac{D_\alpha}{\sigma_\alpha^2(\beta_\alpha^*)} \left(\hat{\beta}_\alpha - \beta_\alpha^* \right) + o_p(1)\end{aligned}\quad (47)$$

where the last equality follows by Lemma 1. By similar arguments,

$$\ell_{nT}^\gamma(\beta_\gamma^*) = \ell_{nT}^\gamma(\hat{\beta}_\gamma) - n \left(\hat{\beta}_\gamma - \beta_\gamma^* \right)' \frac{D_\gamma}{\sigma_\gamma^2(\beta_\gamma^*)} \left(\hat{\beta}_\gamma - \beta_\gamma^* \right) + o_p(1)\quad (48)$$

As a result,

$$LR_{nT}^{\alpha,\gamma} = \ell_{nT}^\alpha(\beta_\alpha^*) - \ell_{nT}^\gamma(\beta_\gamma^*) + n \left(\hat{\beta}_\alpha - \beta_\alpha^* \right)' \frac{D_\alpha}{\sigma_\alpha^2(\beta_\alpha^*)} \left(\hat{\beta}_\alpha - \beta_\alpha^* \right) - n \left(\hat{\beta}_\gamma - \beta_\gamma^* \right)' \frac{D_\gamma}{\sigma_\gamma^2(\beta_\gamma^*)} \left(\hat{\beta}_\gamma - \beta_\gamma^* \right) + o_p(1).\quad (49)$$

1. Note that in this case, $\ell_{nT}^\alpha(\beta_\alpha^*) = \ell_{nT}^\gamma(\beta_\gamma^*)$, since $\tilde{x}'_{\cdot,\alpha}\beta_\alpha^* = \tilde{x}'_{\cdot,\gamma}\beta_\gamma^*$. By Lemma 3.2 in Vuong (1989), with a symmetric real Q given by

$$Q = \begin{pmatrix} \frac{D_\alpha}{\sigma_\alpha^2(\beta_\alpha^*)} & \mathbf{0} \\ \mathbf{0} & -\frac{D_\gamma}{\sigma_\gamma^2(\beta_\gamma^*)} \end{pmatrix},$$

$LR_{nT}^{\alpha,\gamma}$ converges in distribution to a weighted sum of chi-squares with parameters $k_\alpha + k_\gamma$ and λ , the vector of eigenvalues of

$$Q \begin{pmatrix} \Sigma_\alpha & \Sigma_{\alpha,\gamma} \\ \Sigma_{\gamma,\alpha} & \Sigma_\gamma \end{pmatrix}.$$

As a result, $LR_{nT}^{\alpha,\gamma} = O_p(1)$, whereas $\lambda_{nT} \rightarrow \infty$. Since $k_\alpha < k_\gamma$ by definition, $\lambda_{nT}(k_\alpha - k_\gamma) \rightarrow -\infty$. It follows that $P(LR_{nT}^{\alpha,\gamma} > \lambda_{nT}(k_\alpha - k_\gamma)) \rightarrow 1$.

2. Recall that in this case, $\sigma_\alpha^2(\beta_\alpha^*) = \sigma_\gamma^2(\beta_\gamma^*)$, but $\tilde{x}'_{\cdot,\alpha}\beta_\alpha^* \neq \tilde{x}'_{\cdot,\gamma}\beta_\gamma^*$. As a result, from (49) we have

$$\frac{1}{\sqrt{n}} LR_{nT}^{\alpha,\gamma} = -\frac{(T-1)}{\sqrt{n}} (\ell_{nT}^\alpha(\beta_\alpha^*) - \ell_{nT}^\gamma(\beta_\gamma^*)) + o_p(1) = \sqrt{n}(T-1) (\log(\hat{\sigma}_\gamma^2(\beta_\gamma^*)) - \log(\hat{\sigma}_\alpha^2(\beta_\alpha^*))) + o_p(1)\quad (50)$$

By Conditions 2.4-2.5 and the δ -method, it follows that $\frac{1}{\sqrt{n}} LR_{nT}^{\alpha,\gamma} = O_p(1)$. The result follows from noting that since $k_\alpha < k_\gamma$, $\frac{\lambda_{nT}}{\sqrt{n}}(k_\alpha - k_\gamma) \rightarrow -\infty$ as $\lambda_{nT}/\sqrt{n} \rightarrow \infty$.

3.a. Here, we note that by definition

$$\frac{1}{n}LR_{nT}^{\alpha,\gamma} = -(T-1) \left(\log(\hat{\sigma}_\alpha^2(\hat{\beta}_\alpha)) - \log(\hat{\sigma}_\gamma^2(\hat{\beta}_\gamma)) \right) = (T-1) \left(\log(\sigma_\gamma^2(\beta_\gamma^*)) - \log(\sigma_\alpha^2(\beta_\alpha^*)) \right) + o_p(1), \quad (51)$$

where the second equality follows by Condition 2.4 and the continuous mapping theorem. Since in this case $\sigma_\alpha^2(\beta_\alpha^*) < \sigma_\gamma^2(\beta_\gamma^*)$, $(T-1) \left(\log(\sigma_\gamma^2(\beta_\gamma^*)) - \log(\sigma_\alpha^2(\beta_\alpha^*)) \right) > 0$. The result follows from noting that $\frac{\lambda_{nT}}{n}(k_\alpha - k_\gamma) \rightarrow 0$ and $\frac{1}{n}LR_{nT}^{\alpha,\gamma} \xrightarrow{p} (T-1) \left(\log(\sigma_\gamma^2(\beta_\gamma^*)) - \log(\sigma_\alpha^2(\beta_\alpha^*)) \right) > 0$.

3.b. The result follows by similar arguments as in 3.a noting that in this case the result follows from $\frac{1}{n}LR_{nT}^{\alpha,\gamma} \xrightarrow{p} (T-1) \left(\log(\sigma_\gamma^2(\beta_\gamma^*)) - \log(\sigma_\alpha^2(\beta_\alpha^*)) \right) < 0$. \square

A.4 Proof of Proposition 3

The proof proceeds in 5 steps.

Step 1 (Decomposition of PWMSE). Consider the PWMSE estimate based on a single sample split s .

$$\widehat{PWMSE}_\alpha^s = \sum_{r=1}^{T-1} \frac{1}{n_v} \sum_{i \in \mathcal{I}_s^v} (\hat{\mu}_\alpha^s(\mathcal{W}_{iT}) - \hat{\mu}_\alpha^s(\mathcal{W}_{i,T-r}) - (Y_{iT} - Y_{i,T-r}))^2 \pi(\mathcal{W}_{i,T-r}, \mathcal{W}_{i,T+\tau}^f) \quad (52)$$

and its component for an individual time period r ,

$$\frac{1}{n_v} \sum_{i \in \mathcal{I}_s^v} (\hat{\mu}_\alpha^s(\mathcal{W}_{iT}) - \hat{\mu}_\alpha^s(\mathcal{W}_{i,T-r}) - (Y_{iT} - Y_{i,T-r}))^2 \pi(\mathcal{W}_{i,T-r}, \mathcal{W}_{i,T+\tau}^f). \quad (53)$$

This component can be rewritten as

$$\frac{1}{n_v} \sum_{i \in \mathcal{I}_s^v} (\hat{\mu}_\alpha^s(\mathcal{W}_{iT}) - \hat{\mu}_\alpha^s(\mathcal{W}_{i,T-r}) - (\mu_\star(\mathcal{W}_{iT}) - \mu_\star(\mathcal{W}_{i,T-r})))^2 \pi_{ir} \quad (54)$$

$$+ \frac{2}{n_v} \sum_{i \in \mathcal{I}_s^v} (\hat{\mu}_\alpha^s(\mathcal{W}_{iT}) - \hat{\mu}_\alpha^s(\mathcal{W}_{i,T-r}) - (\mu_\star(\mathcal{W}_{iT}) - \mu_\star(\mathcal{W}_{i,T-r}))) (u_{iT} - u_{i,T-r}) \pi_{ir} \quad (55)$$

$$+ \frac{1}{n_v} \sum_{i \in \mathcal{I}_s^v} (u_{iT} - u_{i,T-r})^2 \pi_{ir}, \quad (56)$$

where we use a shorthand notation $\pi_{ir} = \pi(\mathcal{W}_{i,T-r}, \mathcal{W}_{i,T+\tau}^f)$ for each i, r . The term (54) can be

further decomposed as follows,

$$\frac{1}{n_v} \sum_{i \in \mathcal{I}_s^v} (\hat{\mu}_\alpha^s(\mathcal{W}_{iT}) - \hat{\mu}_\alpha^s(\mathcal{W}_{i,T-r}) - (\mu_\star(\mathcal{W}_{iT}) - \mu_\star(\mathcal{W}_{i,T-r})))^2 \pi_{ir} \quad (57)$$

$$= \frac{1}{n_v} \sum_{i \in \mathcal{I}_s^v} (\hat{\mu}_\alpha^s(\mathcal{W}_{iT}) - \hat{\mu}_\alpha^s(\mathcal{W}_{i,T-r}) - (\mu_\alpha^s(\mathcal{W}_{iT}) - \mu_\alpha^s(\mathcal{W}_{i,T-r})))^2 \pi_{ir} \quad (58)$$

$$+ \frac{1}{n_v} \sum_{i \in \mathcal{I}_s^v} (\mu_\alpha^s(\mathcal{W}_{iT}) - \mu_\alpha^s(\mathcal{W}_{i,T-r}) - (\mu_\star(\mathcal{W}_{iT}) - \mu_\star(\mathcal{W}_{i,T-r})))^2 \pi_{ir} \quad (59)$$

$$+ 2 \frac{1}{n_v} \sum_{i \in \mathcal{I}_s^v} (\mu_\alpha^s(\mathcal{W}_{iT}) - \mu_\alpha^s(\mathcal{W}_{i,T-r}) - (\mu_\star(\mathcal{W}_{iT}) - \mu_\star(\mathcal{W}_{i,T-r}))) \times (\hat{\mu}_\alpha^s(\mathcal{W}_{iT}) - \hat{\mu}_\alpha^s(\mathcal{W}_{i,T-r}) - (\mu_\alpha^s(\mathcal{W}_{iT}) - \mu_\alpha^s(\mathcal{W}_{i,T-r}))) \pi_{ir} \quad (60)$$

Step 2 (Consistency of FE estimator). Consider the fixed effect estimator for a subsample with split index s for the model α ,

$$\hat{\beta}_\alpha^s = \left(\frac{1}{T n_c} \sum_{t=1}^T \sum_{i \in \mathcal{I}_s^c} [\tilde{X}_{it,\alpha} \tilde{X}'_{it,\alpha}] \right)^{-1} \frac{1}{T n_c} \sum_{t=1}^T \sum_{i \in \mathcal{I}_s^c} [\tilde{X}_{it,\alpha} \tilde{Y}_{it}]. \quad (61)$$

Under Condition 3, the corresponding population analog β_α^* exists,

$$\beta_\alpha^* = \left(\bar{E}[\tilde{X}_{i,\alpha} \tilde{X}'_{i,\alpha}] \right)^{-1} \bar{E}[\tilde{X}_{i,\alpha} \tilde{Y}_i]. \quad (62)$$

Further, the law of large numbers implies $\hat{\beta}_\alpha^s \xrightarrow{p} \beta_\alpha^*$ as $n_c \rightarrow \infty$ for each s and α under consideration.

Step 3 (Uniform LLN). Let \mathcal{B}_α be any compact subset of \mathbb{R}^{k_α} that contains β_α^* as an interior point. By Step 2, $\hat{\beta}_\alpha^s \in \mathcal{B}_\alpha$ with probability approaching 1 as n_c grows.

For each $\alpha = 1, \dots, A$, consider an empirical process indexed by a vector $b_\alpha \in \mathcal{B}_\alpha$.

$$\Xi_{\alpha, n_v}^{r,s}(b_\alpha) = (E_{n_v}^s - E)((X_{iT,\alpha} - X_{i,T-r,\alpha})' b_\alpha - (Y_{iT} - Y_{i,T-r}))^2 \pi_{ir}. \quad (63)$$

where operator notation $(E_{n_v}^s - E)f_i = E_{n_v}^s f_i - E f_i$ is used to define an empirical process indexed by f . Since the index set \mathcal{B}_α for the empirical process is a compact set in a finite-dimensional Euclidean space and Condition 3 holds,

$$\max_{b_\alpha \in \mathcal{B}_\alpha} |\Xi_{\alpha, n_v}^{r,s}(b)| \xrightarrow{p} 0 \quad \text{as } n_v \rightarrow \infty \quad (64)$$

by Corollary 2.7.2 and Theorem 2.4.3 in van der Vaart and Wellner (1996). It implies for each $\alpha = 1, \dots, A$ as $n_v \rightarrow \infty$

$$\begin{aligned} & \frac{1}{S} \sum_{s=1}^S \sum_{r=1}^{T-1} \frac{1}{n_v} \sum_{i \in \mathcal{I}_s^v} (\hat{\mu}_\alpha^s(\mathcal{W}_{iT}) - \hat{\mu}_\alpha^s(\mathcal{W}_{i,T-r}) - (Y_{iT} - Y_{i,T-r}))^2 \pi_{ir} \\ & - \frac{1}{S} \sum_{s=1}^S \sum_{r=1}^{T-1} E[(\hat{\mu}_\alpha^s(\mathcal{W}_{iT}) - \hat{\mu}_\alpha^s(\mathcal{W}_{i,T-r}) - (Y_{iT} - Y_{i,T-r}))^2 \pi_{ir} | \hat{\beta}_\alpha^s] \xrightarrow{p} 0. \end{aligned} \quad (65)$$

Step 4 (Conditional Expectation of PWMSE). The conditional expectation of the term (60) is given by

$$E\left[(\mu_\alpha^s(\mathcal{W}_{iT}) - \mu_\alpha^s(\mathcal{W}_{i,T-r}) - (\mu_\star(\mathcal{W}_{iT}) - \mu_\star(\mathcal{W}_{i,T-r})))\right] \quad (66)$$

$$\times (\hat{\mu}_\alpha^s(\mathcal{W}_{iT}) - \hat{\mu}_\alpha^s(\mathcal{W}_{i,T-r}) - \mu_\alpha^s(\mathcal{W}_{iT}) + \mu_\alpha^s(\mathcal{W}_{i,T-r}))|\hat{\beta}^s] \quad (67)$$

$$= E\left[(\mu_\alpha^s(\mathcal{W}_{iT}) - \mu_\alpha^s(\mathcal{W}_{i,T-r}) - (\mu_\star(\mathcal{W}_{iT}) - \mu_\star(\mathcal{W}_{i,T-r})))\right. \\ \left. \times (\tilde{X}_{iT,\alpha} - \tilde{X}_{i,T-r,\alpha})'\right](\hat{\beta}_\alpha^s - \beta_\alpha). \quad (68)$$

where the last equality follows from the independence of the training and validation samples. In addition, under strict exogeneity (Condition 3.2), we obtain the following,

$$E\left[(\hat{\mu}_\alpha^s(\mathcal{W}_{iT}) - \hat{\mu}_\alpha^s(\mathcal{W}_{i,T-r}) - (\mu_\star(\mathcal{W}_{iT}) - \mu_\star(\mathcal{W}_{i,T-r}))) (u_{iT} - u_{i,T-r}) \pi_{ir}\right] = 0. \quad (69)$$

Summarizing the previous steps and taking expectation conditional on $\hat{\beta}^s$ of the r -specific PWMSE component in (53),

$$E[(\hat{\mu}_\alpha^s(\mathcal{W}_{iT}) - \hat{\mu}_\alpha^s(\mathcal{W}_{i,T-r}) - (Y_{iT} - Y_{i,T-r}))^2 \pi_{ir} | \hat{\beta}_\alpha^s] \quad (70)$$

$$= E[(\mu_\alpha(\mathcal{W}_{i,T-r}) - \mu_\alpha(\mathcal{W}_{iT}) - (\mu_\star(\mathcal{W}_{i,T-r}) - \mu_\star(\mathcal{W}_{iT})))^2 \pi_{ir}] \quad (71)$$

$$+ (\hat{\beta}_\alpha^s - \beta_\alpha)' \Omega_{r,\alpha} (\hat{\beta}_\alpha^s - \beta_\alpha^*) \quad (72)$$

$$+ E[(\mu_\alpha^s(\mathcal{W}_{iT}) - \mu_\alpha^s(\mathcal{W}_{i,T-r}) - (\mu_\star(\mathcal{W}_{iT}) - \mu_\star(\mathcal{W}_{i,T-r}))) \quad (73)$$

$$\times (\tilde{X}_{iT,\alpha} - \tilde{X}_{i,T-r,\alpha})'] (\hat{\beta}_\alpha^s - \beta_\alpha^*) \quad (74)$$

$$+ E(u_{iT} - u_{i,T-r})^2 \pi_{ir}, \quad (75)$$

where $\Omega_{r,\alpha} = E(\tilde{X}_{iT,\alpha} - \tilde{X}_{i,T-r,\alpha})(\tilde{X}_{iT,\alpha} - \tilde{X}_{i,T-r,\alpha})' \pi_{ir}$. The fourth term does not depend on α so it will not affect the model selection.

Step 5 (Using continuous mapping theorem). As a result of Step 4 and (65), the model α that minimizes \widehat{PWMSE}_α with probability approaching 1 as $n_v \rightarrow \infty$ also minimizes

$$PWMSE_\alpha + \frac{1}{S} \sum_{s=1}^S (\hat{\beta}_\alpha^s - \beta_\alpha^*)' \Omega_\alpha (\hat{\beta}_\alpha^s - \beta_\alpha^*) + \frac{1}{S} \sum_{s=1}^S \Theta_\alpha (\hat{\beta}_\alpha^s - \beta_\alpha^*), \quad (76)$$

where $\Omega_\alpha = \sum_{r=1}^{T-1} \Omega_{r,\alpha}$ and

$$\Theta_\alpha = \sum_{r=1}^{T-1} E[(\mu_\alpha^s(\mathcal{W}_{iT}) - \mu_\alpha^s(\mathcal{W}_{i,T-r}) - (\mu_\star(\mathcal{W}_{iT}) - \mu_\star(\mathcal{W}_{i,T-r}))) \times (\tilde{X}_{iT,\alpha} - \tilde{X}_{i,T-r,\alpha})']$$

by the continuous mapping theorem. Since by Step 2 $\hat{\beta}_\alpha^s \xrightarrow{P} \beta_\alpha^*$, the model selected by \widehat{PWMSE}_α also minimizes $PWMSE_\alpha$ with probability approaching 1. \square

A.5 Supplementary Lemmas

Lemma 1. *Under Conditions 2.1, 2.2 and 2.4, as $n \rightarrow \infty$ holding T fixed*

$$(i) \quad \frac{1}{n} \frac{\partial^2 \ell_{nT}^\alpha(\beta_\alpha)}{\partial \beta_\alpha \partial \beta'_\alpha} \Big|_{\beta_\alpha = \hat{\beta}_\alpha} \xrightarrow{p} -\frac{2D_\alpha}{\sigma_\alpha^2(\beta_\alpha^*)}$$

$$(ii) \quad \frac{1}{n} \frac{\partial^2 \ell_{nT}^\gamma(\beta_\gamma)}{\partial \beta_\gamma \partial \beta'_\gamma} \Big|_{\beta_\gamma = \hat{\beta}_\gamma} \xrightarrow{p} -\frac{2D_\gamma}{\sigma_\gamma^2(\beta_\gamma^*)}.$$

Proof. (i)

$$\begin{aligned} \frac{1}{n} \frac{\partial^2 \ell_{nT}^\alpha(\beta_\alpha)}{\partial \beta_\alpha} &= (T-1) \frac{2}{\sum_{i=1}^n \sum_{t=1}^T (\tilde{Y}_{it} - \tilde{X}'_{it,\alpha} \beta_\alpha)^2 / (n(T-1))} \frac{1}{n(T-1)} \sum_{i=1}^n \sum_{t=1}^T \tilde{X}_{it,\alpha} (\tilde{Y}_{it} - \tilde{X}'_{it,\alpha} \beta_\alpha) \\ &= \frac{2}{\sum_{i=1}^n \sum_{t=1}^T (\tilde{Y}_{it} - \tilde{X}'_{it,\alpha} \beta_\alpha)^2 / (T-1)} \sum_{i=1}^n \sum_{t=1}^T \tilde{X}_{it,\alpha} (\tilde{Y}_{it} - \tilde{X}'_{it,\alpha} \beta_\alpha) \\ \frac{1}{n} \frac{\partial^2 \ell_{nT}^\alpha(\beta_\alpha)}{\partial \beta_\alpha \partial \beta'_\alpha} &= -\frac{2}{\sum_{i=1}^n \sum_{t=1}^T (\tilde{Y}_{it} - \tilde{X}'_{it,\alpha} \beta_\alpha)^2 / (T-1)} \sum_{i=1}^n \sum_{t=1}^T \tilde{X}_{it} \tilde{X}'_{it} \\ &\quad + \frac{4}{T-1} \frac{\sum_{i=1}^n \sum_{t=1}^T \tilde{X}_{it,\alpha} (\tilde{Y}_{it} - \tilde{X}'_{it,\alpha} \beta_\alpha) \sum_{i=1}^n \sum_{s=1}^T (\tilde{Y}_{it} - \tilde{X}'_{it,\alpha} \beta_\alpha) \tilde{X}'_{it,\alpha}}{\left(\sum_{i=1}^n \sum_{t=1}^T (\tilde{Y}_{it} - \tilde{X}'_{it,\alpha} \beta_\alpha)^2 \right)^2 / (T-1)} \end{aligned} \quad (77)$$

Note that under Conditions 2.1-2.2 and Slutsky's theorem, it follows that as $n \rightarrow \infty$,

$$\frac{1}{n} \sum_{i=1}^n \sum_{t=1}^T \tilde{X}_{it,\alpha} (\tilde{Y}_{it} - \tilde{X}'_{it,\alpha} \hat{\beta}_\alpha) \xrightarrow{p} C_\alpha - D_\alpha D_\alpha^{-1} C_\alpha = 0 \quad (78)$$

As a result, the second term in (77) is $o_p(1)$, since its numerator once scaled by n^{-2} is $o_p(1)$ and its denominator, once scaled by n^{-2} , converges in probability to $(\sigma_\alpha^2(\beta_\alpha^*))^2 > 0$ under Condition 2.4.

As a result, it follows that under Conditions 2.1, 2.2 and 2.4, as $n \rightarrow$

$$\frac{1}{n} \frac{\partial^2 \ell_{nT}^\alpha(\beta_\alpha)}{\partial \beta_\alpha \partial \beta'_\alpha} \Big|_{\beta_\alpha = \hat{\beta}_\alpha} \xrightarrow{p} -\frac{2D_\alpha}{\sigma_\alpha^2(\beta_\alpha^*)} \quad (79)$$

(ii) follows by symmetric arguments. \square

References

- J. M. Addoum, D. T. Ng, and A. Ortiz-Bobea. Temperature shocks and establishment sales. *The Review of Financial Studies*, 33(3):1331–1366, 2020.
- A. Adhvaryu, N. Kala, and A. Nyshadham. The light and the heat: Productivity co-benefits of energy-saving technology. *Review of Economics and Statistics*, 102(4):779–792, 2020.
- R. W. Anderson, N. D. Johnson, and M. Koyama. Jewish persecutions and weather shocks: 1100–1800. *The Economic Journal*, 127(602):924–958, 2017.

- E. Andreou and E. Ghysels. Sampling frequency and window length trade-offs in data-driven volatility estimation: appraising the accuracy of asymptotic approximations. In D. Terrell and T. B. Fomby, editors, *Econometric Analysis of Financial and Economic Time Series*, Advances in Econometrics, Volume 20 Part 1, pages 155–181. Emerald Group Publishing Limited, 2006.
- E. Andreou, E. Ghysels, and A. Kourtellis. Regression models with mixed sampling frequencies. *J. Econometrics*, 158(2):246–261, 2010. ISSN 0304-4076. doi: 10.1016/j.jeconom.2010.01.004. URL <http://dx.doi.org/10.1016/j.jeconom.2010.01.004>.
- F. M. Aragón, F. Oteiza, and J. P. Rud. Climate change and agriculture: Subsistence farmers’ response to extreme heat. *American Economic Journal: Economic Policy*, 13(1):1–35, 2021.
- M. Arellano. *Panel Data Econometrics*. Oxford: Oxford University Press, 2003.
- S. Arlot and A. Celisse. A survey of cross-validation procedures for model selection. *Statistics Surveys*, 4:40–79, 2010. doi: 10.1214/09-SS054.
- M. Auffhammer. Quantifying economic damages from climate change. *Journal of Economic Perspectives*, 32(4):33–52, 2018.
- M. Auffhammer, P. Baylis, and C. H. Hausman. Climate change is projected to have severe impacts on the frequency and intensity of peak electricity demand across the united states. *Proceedings of the National Academy of Sciences*, 114(8):1886–1891, 2017.
- A. Barreca, K. Clay, O. Deschenes, M. Greenstone, and J. S. Shapiro. Adapting to climate change: The remarkable decline in the US temperature-mortality relationship over the twentieth century. *Journal of Political Economy*, 124(1):105–159, 2016.
- M. Burke and K. Emerick. Adaptation to climate change: Evidence from US agriculture. *American Economic Journal: Economic Policy*, 8(3):106–40, 2016.
- M. Burke, S. M. Hsiang, and E. Miguel. Global non-linear effect of temperature on economic production. *Nature*, 527(7577):235–239, 2015.
- M. Burke, F. González, P. Baylis, S. Heft-Neal, C. Baysan, S. Basu, and S. Hsiang. Higher temperatures increase suicide rates in the united states and mexico. *Nature climate change*, 8(8):723–729, 2018.
- M. R. Busse, D. G. Pope, J. C. Pope, and J. Silva-Risso. The psychological effect of weather on car purchases. *The Quarterly Journal of Economics*, 130(1):371–414, 2015.

- C. Cattaneo and G. Peri. The migration response to increasing temperatures. *Journal of Development Economics*, 122:127–146, 2016.
- M. J. Chambers. The asymptotic efficiency of cointegration estimators under temporal aggregation. *Econometric Theory*, 19(1):49–77, 2003.
- M. J. Chambers. Cointegration and sampling frequency. *The Econometrics Journal*, 14(2):156–185, 2011.
- M. J. Chambers. The estimation of continuous time models with mixed frequency data. *Journal of Econometrics*, 193(2):390–404, 2016.
- M. J. Chambers and J. R. McCrorie. Frequency domain estimation of temporally aggregated gaussian cointegrated systems. *Journal of Econometrics*, 136(1):1–29, 2007.
- G. Claeskens and N. L. Hjort. *Model Selection and Model Averaging*. Cambridge Series in Statistical and Probabilistic Mathematics. Cambridge University Press, 2008. doi: 10.1017/CBO9780511790485.
- F. Cohen and A. Dechezleprêtre. Mortality, temperature, and public health provision: evidence from mexico. *American Economic Journal: Economic Policy*, Forthcoming.
- J. Colmer. Temperature, labor reallocation, and industrial production: Evidence from india. *American Economic Journal: Applied Economics*, 13(4):101–24, 2021.
- X. Cui. Beyond yield response: Weather shocks and crop abandonment. *Journal of the Association of Environmental and Resource Economists*, 7(5):901–932, 2020.
- M. Dell, B. F. Jones, and B. A. Olken. Temperature shocks and economic growth: Evidence from the last half century. *American Economic Journal: Macroeconomics*, 4(3):66–95, 2012.
- M. Dell, B. F. Jones, and B. A. Olken. What do we learn from the weather? the new climate-economy literature. *Journal of Economic Literature*, 52:740–798, 2014.
- T. Deryugina and S. Hsiang. The marginal product of climate. Technical report, National Bureau of Economic Research, 2017.
- O. Deschênes and M. Greenstone. The economic impacts of climate change: evidence from agricultural output and random fluctuations in weather. *American Economic Review*, 97(1):354–385, 2007.

- O. Deschênes and M. Greenstone. Climate change, mortality, and adaptation: Evidence from annual fluctuations in weather in the US. *American Economic Journal: Applied Economics*, 3(4):152–185, 2011.
- D. Diaz and F. Moore. Quantifying the economic risks of climate change. *Nature Climate Change*, 7(11):774–782, 2017.
- S. Feng, A. B. Krueger, and M. Oppenheimer. Linkages among climate change, crop yields and Mexico–US cross-border migration. *Proceedings of the National Academy of Sciences*, 107(32):14257–14262, 2010.
- M. Gammans, P. Mérel, and A. Ortiz-Bobea. Negative impacts of climate change on cereal yields: statistical evidence from France. *Environmental Research Letters*, 12(5):054007, 2017.
- T. Garg, M. Jagnani, and V. Taraz. Temperature and human capital in india. *Journal of the Association of Environmental and Resource Economists*, 7(6):1113–1150, 2020.
- E. Ghysels, P. Santa-Clara, and R. Valkanov. Predicting volatility: getting the most out of return data sampled at different frequencies. *J. Econometrics*, 131(1-2):59–95, 2006. ISSN 0304-4076. doi: 10.1016/j.jeconom.2005.01.004.
- E. Ghysels, A. Sinko, and R. Valkanov. MIDAS regressions: further results and new directions. *Econometric Rev.*, 26(1):53–90, 2007. ISSN 0747-4938. doi: 10.1080/07474930600972467.
- J. Graff Zivin, S. M. Hsiang, and M. Neidell. Temperature and human capital in the short and long run. *Journal of the Association of Environmental and Resource Economists*, 5(1):77–105, 2018.
- H. Groenvik and Y. Rho. A self-normalizing approach to the specification test of mixed-frequency models. *Communications in Statistics-Theory and Methods*, 47(8):1913–1922, 2018.
- M. Harari and E. L. Ferrara. Conflict, climate, and cells: a disaggregated analysis. *Review of Economics and Statistics*, 100(4):594–608, 2018.
- T. Hastie, R. Tibshirani, and R. Tibshirani. Best Subset, Forward Stepwise or Lasso? Analysis and Recommendations Based on Extensive Comparisons. *Statistical Science*, 35(4):579 – 592, 2020. doi: 10.1214/19-STS733. URL <https://doi.org/10.1214/19-STS733>.
- G. Heutel, N. H. Miller, and D. Molitor. Adaptation and the mortality effects of temperature across us climate regions. *Review of Economics and Statistics*, 103(4):740–753, 2021.
- A. Heyes and S. Saberian. Temperature and decisions: evidence from 207,000 court cases. *American Economic Journal: Applied Economics*, 11(2):238–65, 2019.

- H. Hong and B. Preston. Bayesian averaging, prediction and nonnested model selection. *Journal of Econometrics*, 167(2):358 – 369, 2012. ISSN 0304-4076. doi: <https://doi.org/10.1016/j.jeconom.2011.09.021>. Fourth Symposium on Econometric Theory and Applications (SETA).
- S. M. Hsiang. Temperatures and cyclones strongly associated with economic production in the Caribbean and Central America. *Proceedings of the National Academy of Sciences*, 107(35):15367–15372, 2010.
- S. M. Hsiang, K. C. Meng, and M. A. Cane. Civil conflicts are associated with the global climate. *Nature*, 476(7361):438–441, 2011.
- S. M. Hsiang, M. Burke, and E. Miguel. Quantifying the influence of climate on human conflict. *Science*, 341(6151):1235367, 2013.
- M. Jagnani, C. B. Barrett, Y. Liu, and L. You. Within-season producer response to warmer temperatures: Defensive investments by kenyan farmers. *The Economic Journal*, 131(633):392–419, 2021.
- K. Jessoe, D. T. Manning, and J. E. Taylor. Climate change and labour allocation in rural Mexico: Evidence from annual fluctuations in weather. *The Economic Journal*, 128(608):230–261, 2018.
- V. Kvedaras and V. Zemlys. Testing the functional constraints on parameters in regressions with variables of different frequency. *Economics Letters*, 116(2):250–254, 2012.
- A. Levinson. How much energy do building energy codes save? evidence from california houses. *American Economic Review*, 106(10):2867–94, 2016.
- Y. Li, W. A. Pizer, and L. Wu. Climate change and residential electricity consumption in the yangtze river delta, china. *Proceedings of the National Academy of Sciences*, 116(2):472–477, 2019.
- Z. Liao and X. Shi. A nondegenerate vuong test and post selection confidence intervals for semi/nonparametric models. *Quantitative Economics*, 11(3):983–1017, 2020.
- M. Y. Liu, Y. Shamdasani, and V. Taraz. Climate change and labor reallocation: Evidence from six decades of the indian census. *American Economic Journal: Economic Policy*, Forthcoming.
- Y. Liu and Y. Rho. On the choice of instruments in mixed frequency specification tests. *Communications in Statistics-Theory and Methods*, 48(24):6098–6118, 2019.
- M. LoPalo. Temperature, worker productivity, and adaptation: evidence from survey data production. *American Economic Journal: Applied Economics*, Forthcoming.

- R. Mendelsohn, W. D. Nordhaus, and D. Shaw. The impact of global warming on agriculture: a Ricardian analysis. *American Economic Review*, pages 753–771, 1994.
- J. I. Miller. Mixed-frequency cointegrating regressions with parsimonious distributed lag structures. *Journal of Financial Econometrics*, 12(3):584–614, 2014.
- J. I. Miller. Conditionally efficient estimation of long-run relationships using mixed-frequency time series. *Econometric Reviews*, 35(6):1142–1171, 2016.
- J. I. Miller. Simple robust tests for the specification of high-frequency predictors of a low-frequency series. *Econometrics and Statistics*, 5:45–66, 2018.
- F. C. Moore, U. Baldos, T. Hertel, and D. Diaz. New science of climate change impacts on agriculture implies higher social cost of carbon. *Nature Communications*, 8(1):1–9, 2017.
- V. Mueller, C. Gray, and K. Kosec. Heat stress increases long-term human migration in rural pakistan. *Nature climate change*, 4(3):182–185, 2014.
- National Academies of Sciences, Engineering, and Medicine. *Valuing climate damages: updating estimation of the social cost of carbon dioxide*. National Academies Press, 2017.
- K. Novan, A. Smith, and T. Zhou. Residential building codes do save energy: Evidence from hourly smart-meter data. *The Review of Economics and Statistics*, pages 1–45, Forthcoming.
- R. J. Park, J. Goodman, M. Hurwitz, and J. Smith. Heat and learning. *American Economic Journal: Economic Policy*, 12(2):306–39, 2020.
- F. Pretis. Exogeneity in climate econometrics. *Energy Economics*, 96:105122, 2021. ISSN 0140-9883. doi: <https://doi.org/10.1016/j.eneco.2021.105122>. URL <https://www.sciencedirect.com/science/article/pii/S014098832100027X>.
- K. Ricke, L. Drouet, K. Caldeira, and M. Tavoni. Country-level social cost of carbon. *Nature Climate Change*, 8(10):895–900, 2018.
- J. T. Ritchie and D. S. Nesmith. Temperature and crop development. In J. Hanks and J. T. Ritchie, editors, *Modeling Plant and Soil Systems, Agronomy 31*, pages 5–29. American Society of Agronomy, Crop Science Society of America, Soil Science Society of America, 1991.
- W. Schlenker and M. J. Roberts. Nonlinear temperature effects indicate severe damages to U.S. crop yields under climate change. *Proceedings of the National Academy of Sciences*, 106, 2009.

- W. Schlenker, W. M. Hanemann, and A. C. Fisher. The impact of global warming on us agriculture: an econometric analysis of optimal growing conditions. *Review of Economics and statistics*, 88(1):113–125, 2006.
- J. Shao. Linear model selection by cross-validation. *Journal of the American Statistical Association*, 88(422):486–494, 1993. ISSN 0162-1459.
- J. Shao. An asymptotic theory for linear model selection. *Statistica Sinica*, 7(2):221–264, 1997. ISSN 1017-0405. With comments and a rejoinder by the author.
- X. Shi. A nondegenerate vuong test. *Quantitative Economics*, 6(1):85–121, 2015.
- C.-Y. Sin and H. White. Information criteria for selecting possibly misspecified parametric models. *Journal of Econometrics*, 71(1):207 – 225, 1996. ISSN 0304-4076. doi: [https://doi.org/10.1016/0304-4076\(94\)01701-8](https://doi.org/10.1016/0304-4076(94)01701-8).
- E. Somanathan, R. Somanathan, A. Sudarshan, and M. Tewari. The impact of temperature on productivity and labor supply: Evidence from indian manufacturing. *Journal of Political Economy*, 129(6):1797–1827, 2021.
- A. W. van der Vaart and J. A. Wellner. *Weak Convergence and Empirical Processes: With Applications to Statistics*. Springer Science & Business Media, 1996.
- Q. H. Vuong. Likelihood ratio tests for model selection and non-nested hypotheses. *Econometrica*, 57(2):307–333, 1989.
- L. Wenz, A. Levermann, and M. Auffhammer. North–south polarization of european electricity consumption under future warming. *Proceedings of the National Academy of Sciences*, 114(38):E7910–E7918, 2017.
- Y. Yang. Can the strengths of aic and bic be shared? a conflict between model identification and regression estimation. *Biometrika*, 92(4):937–950, 2005. ISSN 00063444. URL <http://www.jstor.org/stable/20441246>.
- P. Zhang, J. Zhang, O. Deschenes, and K. Meng. Temperature effects on productivity and factor reallocation: Evidence from a half million Chinese manufacturing plants. *Journal of Environmental Economics and Management*, 88:1–17, 2018.

Table 2: Simulation Mean of Model Coefficients and Ideal Targets

DGP:	A			$QinA$		Q	
M_α	$X_{it,\alpha}^k$	β_α^k	Ideal target	β_α^k	Ideal target	β_α^k	Ideal target
A	A	1.000	$\}0.25 \times 10^{-6}$	-5.130	$\}1.32$	0.109	$\}5.60$
B	B1	0.496	$\}0.37 \times 10^{-6}$	-2.497	$\}1.25$	-0.382	$\}4.68$
	B2	0.504		-2.627		0.434	
Q	Q1	0.246	$\}1.03 \times 10^{-6}$	-1.244	$\}1.26$	-0.250	$\}1.03 \times 10^{-6}$
	Q2	0.249		-1.247		0.000	
	Q3	0.252		-1.304		0.750	
	Q4	0.252		-1.318		0.000	
M	M1	0.085	$\}1.19 \times 10^{-6}$	-0.451	$\}1.40$	-0.086	$\}1.19 \times 10^{-6}$
	M2	0.077		-0.380		-0.078	
	M3	0.085		-0.429		-0.086	
	M4	0.082		-0.361		0.000	
	M5	0.085		-0.472		0.000	
	M6	0.082		-0.439		0.000	
	M7	0.085		-0.396		0.253	
	M8	0.085		-0.381		0.253	
	M9	0.082		-0.487		0.245	
	M10	0.085		-0.377		0.000	
	M11	0.082		-0.481		0.000	
	M12	0.085		-0.430		0.000	
QinA	A	0.998	$\}0.28 \times 10^{-6}$	0.198	$\}0.28 \times 10^{-6}$	-0.519	$\}5.47$
	A ²	0.000		-0.050		0.006	
Bin	Bin1	-0.152	$\}0.07$	0.723	$\}4.07$	0.076	$\}0.99$
	Bin2	-0.103		0.513		0.075	
	Bin3	-0.083		0.414		0.048	
	Bin4	-0.055		0.288		0.023	
	Bin5	-0.028		0.157		0.013	
	Bin6	0.026		-0.146		-0.008	
	Bin7	0.054		-0.290		0.051	
	Bin8	0.076		-0.414		0.109	
	Bin9	0.120		-0.734		0.211	

Notes: The table presents simulated pseudo-true parameter values, $\bar{\beta}_\alpha^k$, which are computed as the simulation mean for each estimated element of the parameter vector in the models considered across 2,000 simulation replications for each DGP (A , $QinA$ and Q). In this design, $n = 3074$ (the total number of counties in the dataset) and $T = 10$. We use $\bar{\beta}_\alpha^k$ to calculate the ideal target $\frac{1}{n} \sum_{i=1}^n (\bar{\mu}_\alpha(\mathcal{W}_{i,T+\tau}^f) - \bar{\mu}_\alpha(\mathcal{W}_{iT}) - (\mu_\star(\mathcal{W}_{i,T+\tau}^f) - \mu_\star(\mathcal{W}_{iT})))^2$, where $\bar{\mu}_\alpha(\mathcal{W}_{it}) = X'_{it}\bar{\beta}_\alpha^k$ and $\tau = 20$.

Table 3: Models Minimizing Feasible Targets

DGP:	A			$QinA$			Q		
h :	1	10	100	1	10	100	1	10	100
Norm:									
N	A	A	A	QinA	QinA	QinA	Q	Q	Q
D1	M	A	A	QinA	QinA	QinA	M	Q	Q
D2	M	M	A	QinA	QinA	QinA	M	M	Q
M1	QinA	A	A	QinA	QinA	QinA	Q	Q	Q
M2	A	A	A	QinA	QinA	QinA	Q	Q	Q
Y1	A	A	A	QinA	QinA	QinA	Q	Q	Q
Y2	A	A	A	QinA	QinA	QinA	Q	Q	Q

Notes: The table presents the model that minimizes the feasible target $\sum_{s=1}^{T-1} \frac{1}{n} \sum_{i=1}^n (\bar{\mu}_\alpha(\mathcal{W}_{i,T}) - \bar{\mu}_\alpha(\mathcal{W}_{i,T-s}) - (Y_{i,T} - Y_{i,T-s}))^2 \pi(\mathcal{W}_{i,T-s}, \mathcal{W}_{i,T+\tau}^f)$, where $\bar{\mu}_\alpha(\mathcal{W}_{it}) = X'_{it} \bar{\beta}_\alpha^k$ and $\tau = 20$. N indicates no weight; D1 and D2 are L^∞ and L^2 norms of daily differences; M1 and M2 are L^∞ and L^2 norms of monthly differences; Y1 and Y2 are L^∞ and L^2 norms of annual differences.

Table 4: Existing Model Selection Criteria for the Temperature-Yield Relationship

Model	\widehat{R}^2	SNR	MCCV _{-p}	MCCV _{-Shao}	AIC	BIC	SW ₁	SW ₂
<i>Unbalanced Panel</i>								
(a) no temperature variable	9.18%	10.11%	71.26	73.69	-33.31	-33.25	-29.94	-25.94
(b) monthly averages	20.19%	25.29%	64.43	67.52	-34.84	-34.78	-31.15	-26.76
(c) 1°C daily bins	26.88%	36.76%	59.79	62.18	-35.88	-35.78	-30.49	-24.11
(d) 3°C step function	29.34%	41.52%	57.68	59.84	<i>-36.29</i>	<i>-36.21</i>	-32.16	-27.26
(e) SHF degree days	27.60%	38.13%	57.95	59.90	-36.11	-36.04	-32.57	-28.38
(f) piecewise: 0-29, 29+	28.99%	40.82%	57.78	59.54	-36.13	-36.06	-32.65	<i>-28.52</i>
(g) piecewise: 0-24, 24-26, 26+	28.24%	39.35%	<i>57.44</i>	<i>59.23</i>	-36.21	-36.15	<i>-32.68</i>	-28.49
<i>Balanced Panel</i>								
(a) no temperature variable	10.25%	11.42%	47.84	49.98	-13.82	-13.79	-12.65	-11.33
(b) monthly averages	23.19%	30.19%	42.45	45.85	-14.51	-14.47	-13.15	-11.61
(c) 1°C daily bins	36.18%	56.69%	35.30	37.97	-15.32	-15.26	-12.99	-10.34
(d) 3°C step function	39.27%	64.66%	33.22	35.49	<i>-15.54</i>	<i>-15.50</i>	-13.92	-12.09
(e) SHF degree days	38.25%	61.94%	35.83	37.87	-15.33	-15.30	-14.07	-12.64
(f) piecewise: 0-30, 30+	38.37%	62.25%	<i>33.10</i>	<i>34.86</i>	-15.47	-15.44	<i>-14.24</i>	<i>-12.85</i>
(g) piecewise: 0-29, 29-33, 33+	36.26%	56.88%	33.15	35.00	-15.48	-15.44	-14.22	-12.78

Notes: \widehat{R}^2 and SNR are calculated based on the following regression: $\widehat{\log(y_{it})} = \widehat{X'_{it,\alpha}}\beta_\alpha + \theta_1\widehat{P_{it}} + \theta_2\widehat{P_{it}^2} + \widehat{\epsilon_{it}}$, where the hatted variables are obtained by projecting the original variables out of county and year fixed effects and state quadratic trends. The SNR is formed by dividing the model sum of squares by the residual sum of squares. The columns for MCCV-p and MCCV-Shao presents MSE for cross-validation with 1,000 simulations. We italicize the smallest model selection criterion in each column for the unbalanced and balanced sample, respectively. For legibility, we scale up the MSE for MCCV by 1,000 times and scale down the MSE for GICs by 10,000 times.

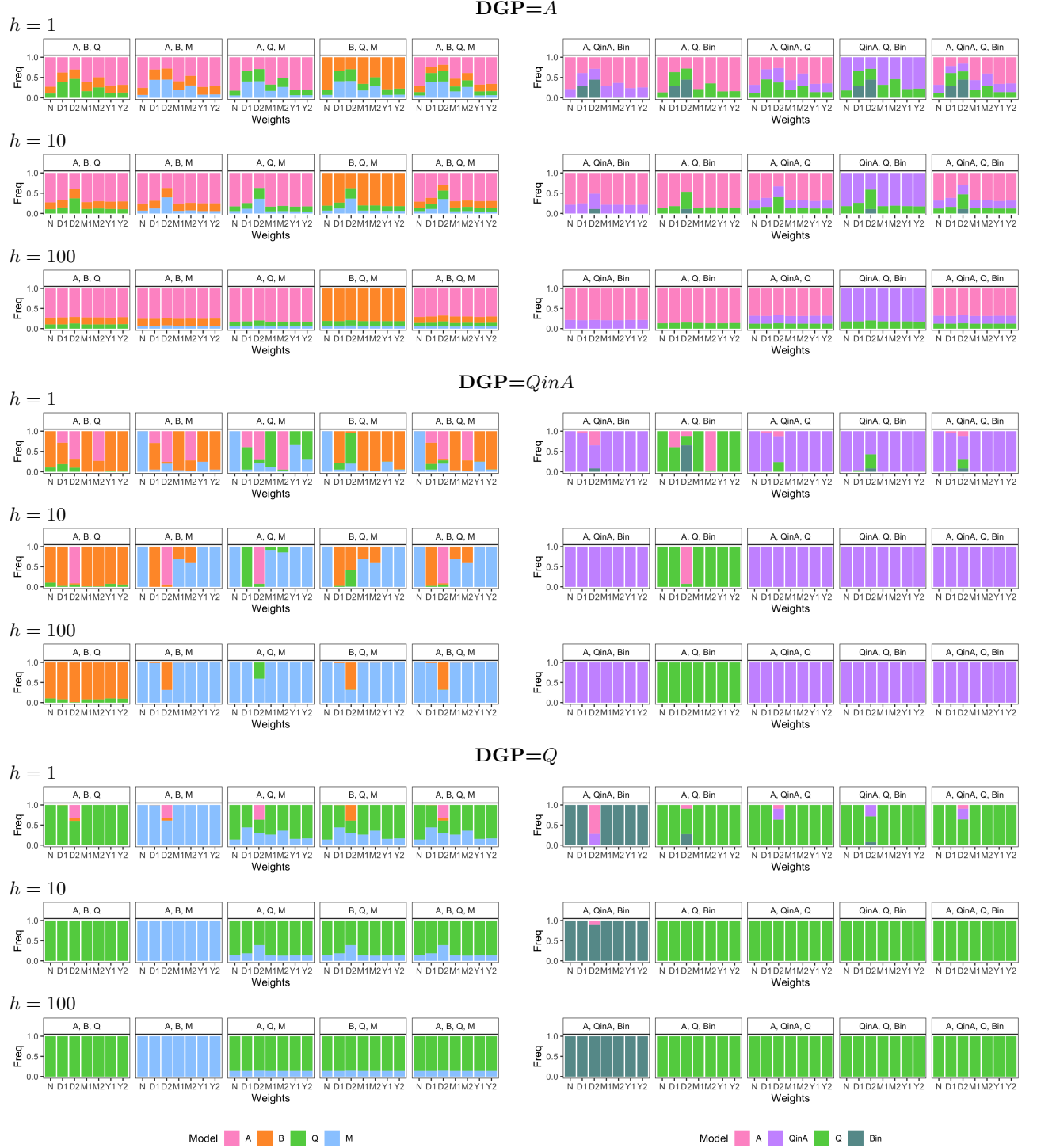


Figure 3: Simulated Model Selection Outcomes for $\tau = 20$.

Notes: In each panel, the title indicates the set of models being compared, the horizontal axis labels different norms being considered for forming weights, the height of a colored bar indicates the proportion of times that a particular model is selected among the set of models. The five panels on the left are for comparisons across nested models and the five on the right are for possibly non-nested models. The results are based on $\tau = 20$.

Table 5: Proximity-weighted MSE for the Temperature-Yield Relationship

Norm: h :	N			M1			M2			Y1			Y2		
	1	10	100	1	10	100	1	10	100	1	10	100	1	10	100
<i>Unbalanced Panel</i>															
(a) no temperature variable	105.39	7.13	77.08	102.09	8.88	68.88	100.60	32.13	90.14	103.71	24.03	78.21	101.92	101.92	101.92
(b) monthly averages	96.28	6.61	70.52	93.28	8.23	62.93	91.89	28.70	82.17	94.73	21.39	71.03	93.04	93.04	93.04
(c) 1°C daily bins	85.19	5.77	62.34	82.53	7.08	55.43	81.27	24.72	72.55	83.80	18.43	62.53	82.28	82.28	82.28
(d) 3°C step function	<i>82.52</i>	5.54	<i>60.33</i>	<i>79.93</i>	6.76	<i>53.56</i>	<i>78.70</i>	23.91	<i>70.24</i>	<i>81.17</i>	17.68	<i>60.45</i>	<i>79.68</i>	<i>79.68</i>	<i>79.68</i>
(e) SHF degree days	82.96	<i>5.50</i>	60.57	80.35	<i>6.68</i>	53.62	79.08	<i>23.67</i>	70.51	81.59	<i>17.43</i>	60.54	80.07	80.07	80.07
(f) piecewise: 0-29, 29+	83.37	5.56	60.89	80.75	6.80	53.91	79.47	23.90	70.88	81.99	17.71	60.85	80.46	80.46	80.46
(g) piecewise: 0-24, 24-26, 26+	83.77	5.63	61.24	81.15	6.90	54.32	79.88	24.17	71.27	82.40	17.92	61.28	80.88	80.88	80.88
<i>Balanced Panel</i>															
(a) no temperature variable	128.59	9.92	95.42	124.75	13.16	87.94	123.39	42.96	111.40	126.72	34.14	99.22	124.92	124.92	124.92
(b) monthly averages	125.17	9.89	93.21	121.48	13.17	86.08	120.17	41.48	108.35	123.34	32.92	96.41	121.57	121.57	121.57
(c) 1°C daily bins	94.71	7.41	70.47	91.91	9.74	64.94	90.90	30.34	81.80	93.30	23.98	72.66	91.95	91.95	91.95
(d) 3°C step function	<i>89.51</i>	<i>6.97</i>	<i>66.57</i>	<i>86.86</i>	<i>9.16</i>	<i>61.29</i>	<i>85.89</i>	<i>28.61</i>	<i>77.28</i>	<i>88.17</i>	<i>22.59</i>	<i>68.60</i>	<i>86.89</i>	<i>86.89</i>	<i>86.89</i>
(e) SHF degree days	91.29	7.06	67.81	88.57	9.27	62.47	87.60	29.44	78.88	89.93	23.22	70.09	88.63	88.63	88.63
(f) piecewise: 0-30, 30+	91.33	7.11	67.91	88.63	9.34	62.55	87.64	29.35	78.88	89.97	23.18	70.03	88.66	88.66	88.66
(g) piecewise: 0-29, 29-33, 33+	91.31	7.11	67.90	88.60	9.34	62.52	87.62	29.25	78.84	89.95	23.11	69.98	88.63	88.63	88.63

Notes: The PWMSEs are obtained from cross-validation with 1,000 simulations. We italicize the smallest PWMSE in each column for the unbalanced and balanced sample, respectively. M1 and M2 are L^∞ and L^2 norms of monthly differences; Y1 and Y2 are L^∞ and L^2 norms of annual differences. For legibility, we scale up the PWMSE by 1,000 times.

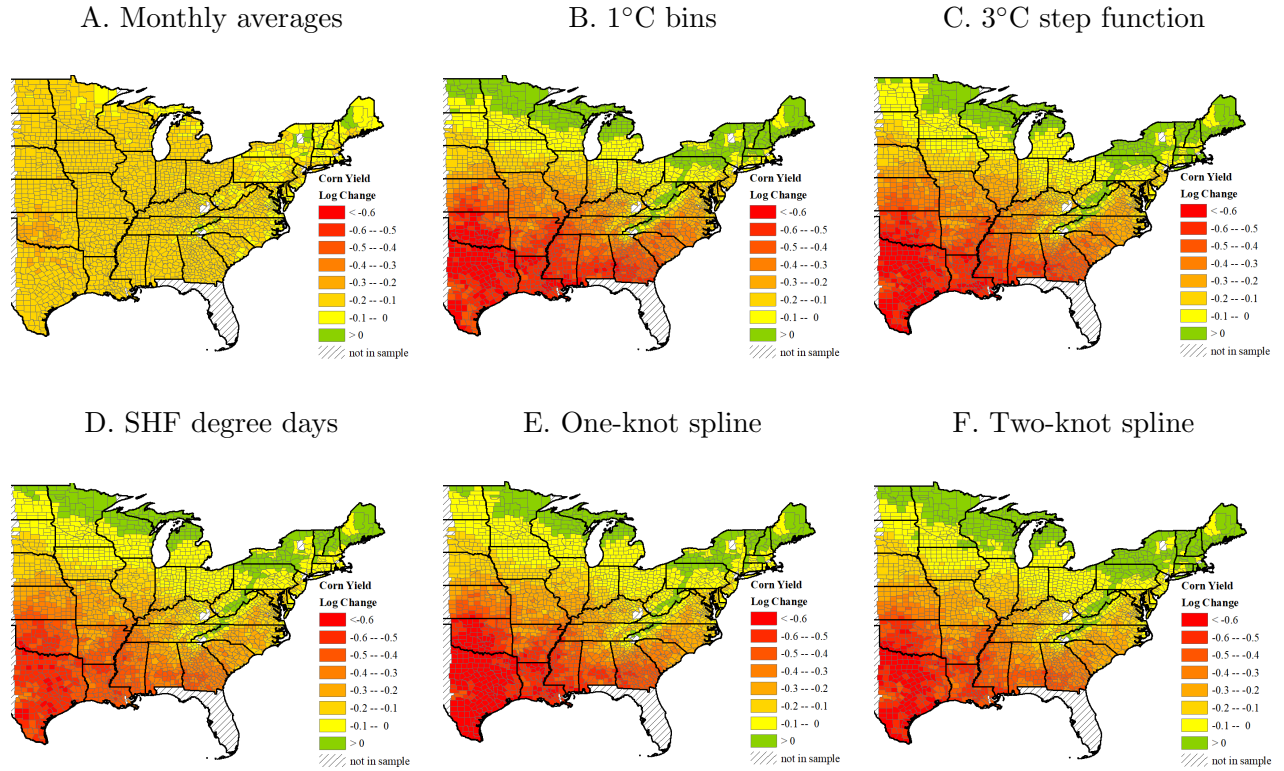


Figure 4: Yield Impacts Projected under Future Climate

Notes: The county-level log changes in corn yields are obtained by applying different yield-response functions to the climate of 2050 projected under HadCM3-B1. The yield-response functions considered here correspond to models (b)-(g) in the unbalanced case.

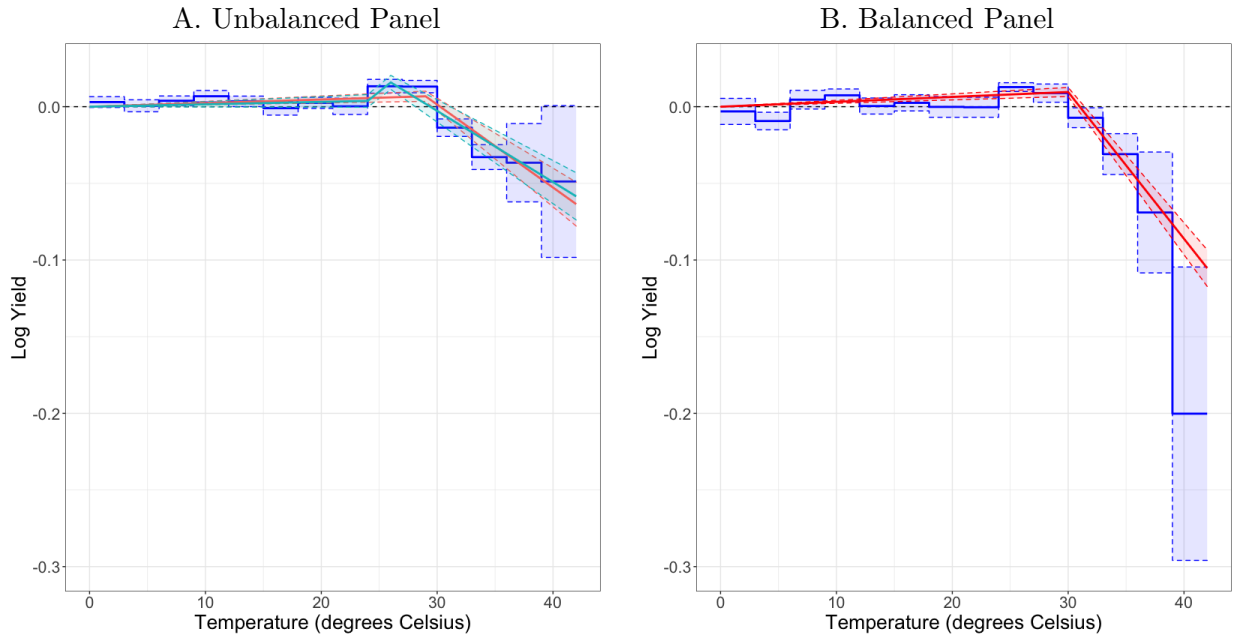


Figure 5: Yield Response to Growing-season Temperature: Selected Models
Notes: The solid lines represent point estimates of the yield response functions, and the shallow bands are 95% point-wise confidence intervals constructed by applying the delta method on state-clustered standard errors. We caution that these confidence intervals do not account for the model selection step.

Online Appendix

B Formal Definitions of Commonly Used Models in the Literature	2
C Probability Limits of Fixed Effects Estimators under Misspecification	3
C.1 Predicted Values at the Pseudo-True Parameters	4
D Simulation Study: MCCV and GICs	5
D.1 Baseline Results: Comparing MCCV and Generalized Information Criteria	6
D.2 Signal-to-noise Ratio and Model Selection Consistency	8
E Formal Definitions of the Norms used in PWMSE Simulations	9
F A Practitioner’s Guide on the Specification of the Weights in the PWMSE	10

B Formal Definitions of Commonly Used Models in the Literature

We provide formal definitions of some of the models commonly adopted in the empirical literature, based on the following representation of response functions:

$$\mu_\alpha(W_{it}) = X'_{it,\alpha}\beta_\alpha$$

$$X_{it,\alpha} = \psi_\alpha \left(\sum_{h=1}^H f_\alpha(W_{ith})' \phi_{\alpha,h} \right).$$

(1) Mean temperatures:

$$f_\alpha(W_{ith}) = W_{ith}, \phi_{\alpha,h} = \frac{1}{H}, \psi_\alpha = \sum_{h=1}^H W_{ith}/H.$$

(2) Maximum temperatures:

$$f_\alpha(W_{ith}) = W_{ith}, \phi_{\alpha,h} = 1\{W_{ith} = \max_h\{W_{ith}\}^H\}, \psi_\alpha = \max_h\{W_{ith}\}^H.$$

(3) Degree days:

$$f_\alpha(W_{ith}) = (\max\{W_{ith} - u, 0\}, \max\{\min\{W_{ith} - l, u - l\}, 0\})',$$

$$\phi_{\alpha,h} = (1, 1)', \psi_\alpha \text{ is the identity function and } u \text{ and } l \text{ are upper and lower thresholds } (u > l).$$

(4) Bins:

$$f_\alpha(W_{ith}) = (1\{W_{ith} \in [l_1, u_1]\}, 1\{W_{ith} \in [l_2, u_2]\}, \dots, 1\{W_{ith} \in [l_{d_{f_\alpha}}, l_{d_{f_\alpha}}]\})',$$

$$\phi_{\alpha,h} = (1, 1, \dots, 1)', \psi_\alpha \text{ is the identity function and } \{[l_j, u_j]\}_{j=1}^{d_{f_\alpha}} \text{ is a set of intervals.}$$

(5) Polynomials:

$$f_\alpha(W_{ith}) = (W_{ith}, W_{ith}^2, \dots, W_{ith}^k)' \text{ for } k\text{th polynomials,}$$

$$\phi_{\alpha,h} = (\frac{1}{H}, \frac{1}{H}, \dots, \frac{1}{H})', \psi_\alpha \text{ is the identity function.}$$

(6) Splines:

$$f_\alpha(W_{ith}) = (s_0(W_{ith}) \cdot 1\{W_{ith} \in [t_0, t_1]\}, s_1(W_{ith}) \cdot 1\{W_{ith} \in [t_1, t_2]\}, \dots, s_n(W_{ith}) \cdot 1\{W_{ith} \in [t_n, +\infty)\})',$$

$$\phi_{\alpha,h} = (1, 1, \dots, 1)', \psi_\alpha \text{ is the identity function and } s_0, s_1, \dots, s_n \text{ are a set of spline functions}$$

with associated knots of t_0, t_1, \dots, t_n .

(7) Heat index:

Heat index typically involves $\dim(W_{ith}) \geq 2$. For illustration, suppose we have $W_{ith} = (W_{1,ith}, W_{2,ith})$. $f_\alpha(W_{ith}) = g(W_{1,ith}, W_{2,ith})$ where g is a transformation function that interacts $W_{1,ith}$ and $W_{2,ith}$ in a specific manner. $\phi_{\alpha,h} = \frac{1}{H}$, $\psi_\alpha = \sum_{h=1}^H W_{ith}/H$.

C Probability Limits of Fixed Effects Estimators under Misspecification

Given that all models considered here use regressors that are functions of different summary statistics of the same time series, we formalize the (pseudo-)true parameter values of the models under consideration. We first introduce the within-demeaning notation for linear fixed effects estimation. For V_{it} , $\tilde{V}_{it} = V_{it} - \bar{V}_i$, where $\bar{V}_i = \sum_{t=1}^T V_{it}/T$. For \mathbf{M}_α , the within-transformation is given by

$$\begin{aligned} Y_{it} &= X'_{it,\alpha} \beta_\alpha + a_{i,\alpha} + u_{it,\alpha}, \\ \tilde{Y}_{it} &= \tilde{X}'_{it,\alpha} \beta_\alpha + \tilde{u}_{it,\alpha}. \end{aligned} \quad (80)$$

The probability limit of the fixed effects estimator of the above model, which we refer to as the pseudo-true parameter vector of \mathbf{M}_α , is denoted by β_α^* and is given in (81). We further assume that the estimation problem is sufficiently regular, and we also assume strict exogeneity of the high-frequency regressor, $E[u_{it}|\mathcal{W}_{i1}, \dots, \mathcal{W}_{iT}, a_i] = 0$. For a random variable W_i , let $\bar{E}[W_i] = \lim_{n \rightarrow \infty} \sum_{i=1}^n E[W_i]/n$. Then, assuming sufficient conditions for the application of a law of large numbers,

$$\begin{aligned} \beta_\alpha^* &= \text{plim}_{n \rightarrow \infty} \left(\sum_{i=1}^n \sum_{t=1}^T \tilde{X}_{it,\alpha} \tilde{X}'_{it,\alpha} \right)^{-1} \sum_{i=1}^n \sum_{t=1}^T \tilde{X}_{it,\alpha} \tilde{Y}_{it} \\ &= \left(\bar{E} \left[\sum_{t=1}^T \tilde{X}_{it,\alpha} \tilde{X}'_{it,\alpha} \right] \right)^{-1} \bar{E} \left[\sum_{t=1}^T \tilde{X}_{it,\alpha} \tilde{X}'_{it,\star} \right] \beta_{\star,o}. \end{aligned} \quad (81)$$

Equation (81) is the counterpart of the omitted variable bias formula in this problem. In the context of mixed-frequency time series, this issue has also been recognized as neglected nonlinearity in Miller (2014). To gain some intuition for (81), consider the case where both $X_{it,\star}$ and $X_{it,\alpha}$ are scalar. Then

$$\beta_\alpha^* = \frac{\bar{E}[\sum_{t=1}^T \tilde{X}_{it,\alpha} \tilde{X}_{it,\star}]}{\bar{E}[\sum_{t=1}^T \tilde{X}_{it,\alpha}^2]} \beta_{\star,o} = \rho_{*,\alpha} \sqrt{\frac{\bar{E}[\sum_{t=1}^T \tilde{X}_{it,\star}^2]}{\bar{E}[\sum_{t=1}^T \tilde{X}_{it,\alpha}^2]}} \beta_{\star,o}, \quad (82)$$

where $\rho_{*,\alpha} = \bar{E}[\sum_{t=1}^T \tilde{X}_{it,\alpha} \tilde{X}_{it,\star}] / \sqrt{\bar{E}[\sum_{t=1}^T \tilde{X}_{it,\alpha}^2] \bar{E}[\sum_{t=1}^T \tilde{X}_{it,\star}^2]}$ is the within-correlation coefficient between $X_{it,\alpha}$ and $X_{it,\star}$. Under the assumption that $\beta_{\star,o}$ is non-zero, the sign and the magnitude of $\beta_\alpha^*/\beta_{\star,o}$ will depend on the within-correlation between $X_{it,\alpha}$ and $X_{it,\star}$ as well as the ratio of their variances. If the within-correlation between the two variables is positive, then β_α^* and $\beta_{\star,o}$ will have the same sign, otherwise β_α^* will have the opposite sign of $\beta_{\star,o}$. Suppose that $X_{it,\alpha}$ and $X_{it,\star}$ have equal within-variance, then β_α^* will tend to be smaller in magnitude the weaker the within-correlation between $X_{it,\alpha}$ and $X_{it,\star}$. This example of attenuation bias is similar to the classical

measurement error problem. If $X_{it,\alpha}$ has greater within-variance than $X_{it,\star}$, then the attenuation is greater.

Returning to the general (non-scalar) case, if \mathbf{M}_α contains \mathbf{M}_\star , i.e. $X_{it,\star} = R_{\star,\alpha} X_{it,\alpha}$ for some $R_{\star,\alpha}$, then

$$\beta_\alpha^* = R'_{\star,\alpha} \beta_{\star,o}. \quad (83)$$

For instance, if \mathbf{M}_α is the quarterly mean model, and \mathbf{M}_\star is the annual mean model,

$$\beta_\alpha^* = \begin{pmatrix} \frac{|Q_1|}{H} \\ \vdots \\ \frac{|Q_4|}{H} \end{pmatrix} \beta_{\star,o}. \quad (84)$$

Since $X_{it,\alpha}$ and $X_{it,\star}$ are summary statistics of \mathcal{W}_{it} , if $\beta_{\star,o}$ is non-zero, then we expect all elements of β_α^* to be non-zero, unless $R_{\star,\alpha}$ has zero rows. This is different from the standard variable selection problem, where the pseudo-true parameter value for models that contain \mathbf{M}_\star will have zero elements for variables that are not in the DGP.

C.1 Predicted Values at the Pseudo-True Parameters

Let $\tilde{Y}_{it,\alpha}^*(\mathcal{W}_i) \equiv \tilde{X}'_{it,\alpha} \beta_\alpha^*$ denote the within-demeaned predicted value of the outcome for individual i in period t given \mathcal{W}_i using the pseudo-true parameter vector of \mathbf{M}_α . Consider two models, \mathbf{M}_α and \mathbf{M}_γ , where both models contain \mathbf{M}_\star , i.e. $\tilde{X}_{it,\star} = R_{\star,\alpha} \tilde{X}_{it,\alpha} = R_{\star,\gamma} \tilde{X}_{it,\gamma}$. By Eq. (83), $\beta_\alpha^* = R'_{\star,\alpha} \beta_{\star,o}$ for \mathbf{M}_α when \mathbf{M}_\star is nested in it. As a result,

$$\begin{aligned} \tilde{Y}_{it,\alpha}^*(\mathcal{W}_i) &= \tilde{X}'_{it,\alpha} \beta_\alpha^* = \tilde{X}'_{it,\alpha} R'_{\star,\alpha} \beta_{\star,o} = \tilde{X}'_{it,\star} \beta_{\star,o}, \\ \tilde{Y}_{it,\gamma}^*(\mathcal{W}_i) &= \tilde{X}'_{it,\gamma} \beta_\gamma^* = \tilde{X}'_{it,\gamma} R'_{\star,\gamma} \beta_{\star,o} = \tilde{X}'_{it,\star} \beta_{\star,o}. \end{aligned} \quad (85)$$

Hence, in this case, both models yield identical predictions given \mathcal{W}_i using their respective pseudo-true parameter vectors. This result holds regardless of the relationship between the two models as long as \mathbf{M}_\star is nested in both of them.

Note that if \mathbf{M}_α is nested in \mathbf{M}_γ , but the DGP is not contained in either model, they may still have different predictions using their respective pseudo-true parameter vectors. To see this, consider

$$\tilde{Y}_{it,\gamma}^*(\mathcal{W}_i) = \tilde{X}'_{it,\gamma} \beta_\gamma^* = \tilde{X}'_{it,\gamma} \left(E[\tilde{X}_{it,\gamma} \tilde{X}'_{it,\gamma}] \right)^{-1} E[\tilde{X}_{it,\gamma} X'_{it,\star}] \beta_{\star,o}, \quad (86)$$

$$\begin{aligned} \tilde{Y}_{it,\alpha}^*(\mathcal{W}_i) &= \tilde{X}'_{it,\alpha} \beta_\alpha^* = \tilde{X}'_{it,\alpha} \left(E[\tilde{X}_{it,\alpha} \tilde{X}'_{it,\alpha}] \right)^{-1} E[\tilde{X}_{it,\alpha} \tilde{X}'_{it,\star}] \beta_{\star,o} \\ &= \tilde{X}'_{it,\gamma} R'_{\alpha,\gamma} \left(R_{\alpha,\gamma} E[\tilde{X}_{it,\gamma} \tilde{X}'_{it,\gamma}] R'_{\alpha,\gamma} \right)^{-1} R_{\alpha,\gamma} E[\tilde{X}_{it,\gamma} \tilde{X}'_{it,\star}] \beta_{\star,o}. \end{aligned} \quad (87)$$

Note that $\tilde{Y}_{it,\gamma}^*(\mathcal{W}_i) = Y_{it,\alpha}^*(\mathcal{W}_i)$ is true if

$$R'_{\alpha,\gamma} \left(R_{\alpha,\gamma} E[\tilde{X}_{it,\gamma} \tilde{X}'_{it,\gamma}] R'_{\alpha,\gamma} \right)^{-1} R_{\alpha,\gamma} = \left(E[\tilde{X}_{it,\gamma} \tilde{X}'_{it,\gamma}] \right)^{-1}, \quad (88)$$

which would hold in general if $R_{\alpha,\gamma}$ were symmetric and invertible. However, by definition it is not a square matrix. As a result, $\tilde{Y}_{it,\gamma}^*(\mathcal{W}_i) \neq Y_{it,\alpha}^*(\mathcal{W}_i)$ in general if neither of the models contain the true DGP.

We now consider a simple example to illustrate this point. Suppose that \mathbf{M}_α is the annual mean model and \mathbf{M}_γ is the quarterly mean model. Then $E[\tilde{X}_{it,\gamma} \tilde{X}'_{it,\gamma}]$ is the within variance-covariance matrix of the quarterly means, and $E[\tilde{X}_{it,\alpha}^2]$ is the within-variance of the annual mean, which is a weighted average of the quarterly means. Clearly, the “variability” is not in general the same for the higher- and lower-frequency mean, unless we impose some restrictive assumptions. For instance, if we require that the within-variance is the same for all quarterly means and that there is no within-covariance between the quarterly means, then $E[\tilde{X}_{it,\gamma} \tilde{X}'_{it,\gamma}] = E[\tilde{X}_{it,\alpha}^2] I_{k_\gamma}$, where $E[\tilde{X}_{it,\alpha}^2] > 0$. This would imply that the within-variance of summer and winter average temperatures are the same and that there is no inter-seasonal correlation in temperature. These are unrealistic assumptions that we entertain to illustrate our point. In this example, (88) simplifies to

$$\begin{aligned} R'_{\alpha,\gamma} (R_{\alpha,\gamma} R'_{\alpha,\gamma})^{-1} R_{\alpha,\gamma} &= I_{k_\gamma}, \\ \frac{1}{\sum_{j=1}^4 |Q_j|^2 / H^2} R'_{\alpha,\gamma} R_{\alpha,\gamma} &= I_{k_\gamma}. \end{aligned} \quad (89)$$

The above equality is trivially fulfilled if $R_{\alpha,\gamma}$ is proportional to the identity matrix, which would imply that both models are identical. But this is not true in this simple example. If we further simplify the problem by assuming that $|Q_j| = H/4$ for $j = 1, \dots, 4$, then $\mathcal{R}_{\alpha,\gamma} = \frac{1}{4} \mathbf{1}'_k$, where $\mathbf{1}_k$ is a $k \times 1$ vector with all elements equal to one. It follows that the above equality clearly does not hold, since its left-hand side would simplify to $\frac{1}{4} \mathbf{1}_k \mathbf{1}'_k$. Hence, even in this simple example, it is difficult to show that it is possible to obtain identical predictions of the outcome variable given \mathcal{W}_i when considering two models that do not nest \mathbf{M}_\star . We use the above insights to inform our simulation design in the next section to show cases where BIC is (pseudo-)inconsistent.

D Simulation Study: MCCV and GICs

In this section, we first compare the finite-sample performance of the MCCV and GICs in a baseline design that exhibits a high signal-to-noise ratio. Then, we examine the performance of the model selection criteria for varying levels of signal-to-noise ratio.

D.1 Baseline Results: Comparing MCCV and Generalized Information Criteria

Here we illustrate the aforementioned theoretical results using a simple simulation study. We consider three DGPs of an outcome-temperature relationship: (i) the annual mean model (A), (ii) the quadratic in annual mean model ($QinA$), and (iii) the quarterly mean model (Q), and we evaluate the performance of model selection criteria for selecting among a broader set of models.

The following functions generate the outcome Y_{it} for the three DGPs that correspond to three of the models we consider in Example 1:

- Annual Mean (A): $Y_{it} = \bar{W}_{it} + a_{i,\alpha} + u_{it,\alpha}$,
- Quadratic in Annual Mean ($QinA$): $Y_{it} = 0.2\bar{W}_{it} - 0.05\bar{W}_{it}^2 + a_{i,\delta} + u_{it,\delta}$,
- Quarterly Mean (Q): $Y_{it} = -0.25\bar{W}_{it}^{Q_1} + 0.75\bar{W}_{it}^{Q_3} + a_{i,\gamma} + u_{it,\gamma}$,

For each of the DGPs we consider, we use a random sample of counties from the National Climatic Data Center (NCDC) temperature dataset for the years 1968-1972 as \mathcal{W}_{it} for $i = 1, \dots, n$ and $t = 1, \dots, T$, where $T = 5$. For each simulation replication, we generate $a_i | \mathcal{W}_{i1}, \mathcal{W}_{i2}, \dots, \mathcal{W}_{i5} \stackrel{i.i.d.}{\sim} N(0.5\bar{W}_i, 1)$, where $\bar{W}_i = \sum_{t=1}^T \sum_{h=1}^H W_{ith} / (TH)$. The idiosyncratic shocks u_{it} are generated as a bivariate mixture normal that is heteroskedastic and serially correlated as follows. Let $u_i = (u_{i1}, \dots, u_{iT}) = \epsilon_i^1 + \epsilon_i^2$, where $\epsilon_i^1 | \mathcal{W}_{i1}, \dots, \mathcal{W}_{i5}, a_i \stackrel{i.i.d.}{\sim} N(-0.5, \Sigma_1)$ and $\epsilon_i^2 | \mathcal{W}_{i1}, \dots, \mathcal{W}_{i5}, a_i \stackrel{i.i.d.}{\sim} N(0.5, \Sigma_2)$, with

$$\Sigma_1 = \begin{pmatrix} 1 & 0.5 & 0.1 & 0 & 0 \\ 0.5 & 1 & 0.5 & 0.1 & 0 \\ 0.1 & 0.5 & 1 & 0.5 & 0.1 \\ 0 & 0.1 & 0.5 & 1 & 0.5 \\ 0 & 0 & 0.1 & 0.5 & 1 \end{pmatrix}, \quad \Sigma_2 = \begin{pmatrix} 1 & 0.5 & 0.1 & 0 & 0 \\ 0.5 & 0.75 & 0.5 & 0.1 & 0 \\ 0.1 & 0.5 & 1 & 0.5 & 0.1 \\ 0 & 0.1 & 0.5 & 0.75 & 0.5 \\ 0 & 0 & 0.1 & 0.5 & 1 \end{pmatrix}. \quad (90)$$

We consider the following set of models for model selection:

- Annual Mean (A): $Y_{it} = \beta_1 \bar{W}_{it} + a_i + u_{it}$,
- Bi-annual Mean (B): $Y_{it} = \sum_{k=1}^2 \beta_k \bar{W}_{it}^{B_k} + a_i + u_{it}$,
- Quarterly Mean (Q): $Y_{it} = \sum_{k=1}^4 \beta_k \bar{W}_{it}^{Q_k} + a_i + u_{it}$,
- Monthly Mean (M): $Y_{it} = \sum_{k=1}^{12} \beta_k \bar{W}_{it}^{M_k} + a_i + u_{it}$,
- Quadratic in Annual Mean ($QinA$): $Y_{it} = \beta_1 \bar{W}_{it} + \beta_2 \bar{W}_{it}^2 + a_i + u_{it}$,
- 10°F Bins ($Bins$): $Y_{it} = \sum_{k=1}^9 \beta_k Bin^k_{it} + a_i + u_{it}$.

Given the importance of the pseudo-true parameter values as well as the MSE evaluated at these values in our theoretical analysis, we simulate these quantities for models A , B , Q , M , $QinA$, and $Bins$ using 2000 simulation replications using the sample of all counties in our dataset ($n = 3074$) to ensure that our simulated quantities are as close as possible to their population analogues.

Table A1 presents the simulation mean of coefficients ($\bar{\beta}_\alpha$) and MSE estimated using $\bar{\beta}_\alpha$ for our entire sample, i.e. $MSE(\bar{\beta}_\alpha) = \sum_{i=1}^n \sum_{t=1}^T (\tilde{y}_{it} - \tilde{x}'_{it,\alpha} \bar{\beta}_\alpha)^2 / (nT)$, for all six models we consider when the DGP is A , Q , and $QinA$, respectively. Note that when $QinA$ is the DGP, the annual mean (A) and quarterly mean (Q) models yield very similar MSEs at $\bar{\beta}_\alpha$. Similarly, when Q is the DGP, the MSE at $\bar{\beta}_\alpha$ is similar for models A and $QinA$. However, the predicted values of the outcome given the models' pseudo-true parameter values are quite different. Hence, our theoretical results would predict BIC to be pseudo-inconsistent when selecting between A and Q (A and $QinA$) when the DGP is $QinA$ (Q), i.e. BIC will choose the larger model among the two models under consideration.

We use the same random sample of n counties from the full NCDC sample of 3,074 counties and use the temperature data for these counties between 1968-72 as our high-frequency regressor $\{\mathcal{W}_i\}_{i=1}^n$ in all the simulation designs. The outcome variable is generated using the DGP in question. All regression models are implemented on the generated data and the six model selection criteria presented below are calculated for each model:

- MCCV (n_c/n)
 - $n_c/n = p = 0.75$ (MCCV with fixed training-to-full sample ratios, hereinafter MCCV- p),
 - $n_c = n^{-1/4}$ (MCCV with vanishing training-to-full sample ratios, hereinafter MCCV-Shao);
- $GIC_{\alpha, \lambda_{nT}} = -n(T-1) \log(\hat{\sigma}_\alpha^2) - \lambda_{nT} k_\alpha$, where $\hat{\sigma}^2 = \sum_{i=1}^n \sum_{t=1}^T (\tilde{y}_{it} - \tilde{x}'_{it,\alpha} \hat{\beta}_\alpha)^2 / (nT)$,
 - $\lambda_{nT} = 2$ (AIC),
 - $\lambda_{nT} = \log(nT)$ (BIC),
 - $\lambda_{nT} = \sqrt{nT \log(\log(nT))}$ (SW₁),
 - $\lambda_{nT} = \sqrt{nT \log(nT)}$ (SW₂).

The simulation probabilities (proportions) of selecting a particular model using each of the criteria are computed using 500 simulation replications.

In Figure A2, we show simulation probabilities of selecting different models when the DGP is A , $QinA$, and Q in Panels A-C for $n = 3000$, respectively.²⁵ In each panel, we report results in different

²⁵We also report the simulations results for $n = 500$ in Appendix Figure A3.

model selection problems with the specific problem defined in the title of each sub-panel. Under each DGP, the model selection problems in the first row of sub-panels consider nested models, and those in the second row consider possibly non-nested models.

We highlight a few important findings. As suggested in Panel A of Figure A2, AIC and MCCV- p are not model selection consistent as our theoretical results predict; they specifically select overfit models, such as Q or $QinA$, even when \mathbf{M}_\star (corresponding to A) is among the models under consideration. In this setting, MCCV-Shao, BIC, SW_1 and SW_2 select the most parsimonious correctly specified model with simulation probability very close to or equal to 1.

To study the pseudo-consistency of the model selection criteria, we examine two designs: (1) choose between A and Q where DGP = $QinA$, (2) choose between A and $QinA$ where DGP = Q . Since in both cases the two models under consideration have similar $MSE(\bar{\beta}_\alpha)$, A should be chosen in both cases. In our simulation results, BIC and MCCV-Shao choose the larger model, Q in (1) and $QinA$ in (2), with probability almost equal to 1 when $n = 3000$, whereas SW_1 and SW_2 choose A . Hence, the former criteria exhibit pseudo-inconsistency of model selection. The BIC's pseudo-inconsistency is predicted by our theoretical results. According to Shao (1997), MCCV-Shao and BIC are asymptotically equivalent, hence it is not surprising that they both behave similarly in the simulations.

D.2 Signal-to-noise Ratio and Model Selection Consistency

Given the potential sensitivity of the finite-sample performance of model selection procedures to the signal-to-noise ratio (SNR) in the DGP,²⁶ we examine the behavior of the model selection criteria when we vary the signal-to-noise ratio in our design. To do so, we let a given DGP \mathbf{M}_\star be in the form of $Y_{it} = X'_{it,\star}\beta_\star + \alpha_i + v_{it}$. To generate v_{it} , we first generate u_{it} as in our baseline design and obtain \tilde{X}_{it} and \tilde{u}_{it} which are demeaned versions of X_{it} and u_{it} . We then construct the rescaled error term v_{it} such that its demeaned version \tilde{v}_{it} satisfies

$$\tilde{v}_{it} = \sqrt{\frac{1}{\rho} \cdot \frac{Var(\tilde{\mathbf{X}}_{it}\beta_\star)}{Var(\tilde{u}_{it})}} \times \tilde{u}_{it},$$

where ρ is the value of SNR we use in a given design.

Figure A4 presents the simulation probability of selecting each model under consideration for two model selection problems from the baseline design: (1) the full set of nested models, (2) the full set of possibly non-nested models. Since we vary the SNR between 0.1 and 10, we also include the null model (with no temperature variable) for the two model selection problems we consider.

²⁶For instance, Hastie et al. (2020) compare the finite-sample performance of best subset selection, LASSO and forward step-wise regression via simulations and illustrate how their relative performance depends on the SNR.

To simplify illustration, we only include results for AIC, BIC, SW_1 and SW_2 , omitting the MCCV procedures.

Overall, the results for high SNRs are consistent with our baseline results. For low SNRs, however, we find that SW_1 and SW_2 can underfit, even if the true DGP is under consideration. For instance, in the second row of Panel B in Figure A4, for SNRs of up to 1.0 or 2.0, the SW criteria tend to select the annual mean model with simulation probability equal or close to one, whereas the AIC and BIC choose the true DGP with high probability. In the third row of Panel B in Figure A4, the SW criteria select the null model with probability close to one for very low SNRs (0.1-0.2).

A practical implication of these simulation results is that the SNR is an important quantity to report when interpreting the results of model selection criteria. In addition, they suggest that rather than reporting the results of a single model selection criterion chosen by the empirical researcher as in current empirical practice, different model selection criteria should be reported to aid in the interpretation of their results.

E Formal Definitions of the Norms used in PWMSE Simulations

We formally define the different norms used in specifying the PWMSE in Section 3.2.1. To be precise, we first introduce additional notation.

- $W_{i,T-r,h}$: the historical realization in location i in day h in the r th year before the last observable year T .
- $W_{i,T-r,m}$: the historical realization in location i in month m in the r th year before the last observable year T , averaged over daily realizations within the month, i.e., $W_{i,T-r,m} = \sum_{h_m=1,\dots,H_m} W_{i,T-r,h_m} / H_m$ where h_m denotes the days within month m .
- $W_{i,T-r}$: represent the historical realization in location i in the r th year before the last observable year T , averaged over daily realizations within the year, i.e., $W_{i,T-r} = \sum_{h=1,\dots,H} W_{i,T-r,h} / H$.
- $\mathcal{W}_{i,T+\tau,h}$, $\mathcal{W}_{i,T+\tau,m}$, $\mathcal{W}_{i,T+\tau}$: τ years forward projected future counterparts of $W_{i,T-r,h}$, $W_{i,T-r,m}$, and $W_{i,T-r}$.

Based on the notations above, we define the six norms considered in our simulation study.

- (1) L^∞ norm of daily differences (D1): $\max_h |W_{i,T-r,h} - \mathcal{W}_{i,T+\tau,h}|$
- (2) L^2 norm of daily differences (D2): $\sqrt{\sum_h (W_{i,T-r,h} - \mathcal{W}_{i,T+\tau,h})^2}$
- (3) L^∞ norm of monthly differences (M1): $\max_m |W_{i,T-r,m} - \mathcal{W}_{i,T+\tau,m}|$
- (4) L^2 norm of monthly differences (M2): $\sqrt{\sum_m (W_{i,T-r,m} - \mathcal{W}_{i,T+\tau,m})^2}$

(5) L^∞ norm of daily differences (Y1): $|W_{i,T-r} - \mathcal{W}_{i,T+\tau}|$

(6) L^2 norm of daily differences (Y2): $(W_{i,T-r} - \mathcal{W}_{i,T+\tau})^2$

F A Practitioner’s Guide on the Specification of the Weights in the PWMSE

In our proposed PWMSE, the weight consists of a norm and a tuning parameter. The norm measures the distance between past and future realizations. How we construct this norm reflects the specific dimension we would like to characterize proximity by. In our simulations, we consider three sets of norms based on temperature differences at the daily, monthly, and annual level, respectively. The measured proximity can be substantially different with norms constructed based on different temporal scales. For example, norms based on annual mean temperature ignore the within-year temperature variability, whereas such information would be incorporated in daily norms. Put simply, two years that have the same annual mean temperature may still be very different in terms of the daily norm.

The chosen aggregation level used for the norm pins down the temporal scale at which the differences between past and future realizations will be measured. Therefore, we recommend choosing the level such that it matches the temporal resolution of the empirical context. For instance, the DGPs in our simulations only leverage data variation at the annual (or seasonal) level. As reflected from our simulation results, the model selection results tend to be more consistent when we opt for norms based on differences at the annual level, holding the tuning parameters constant. However, if the empirical setting examines an outcome variable at a finer temporal scale, using norms based on monthly or even daily differences may be more appropriate.

For any norm adopted, the tuning parameter determines the relative weights on years with different degrees of similarity to the projected climate scenario. We plot a set of functions of $y = e^{-x/h}$ in Figure A1 to illustrate the difference between different levels of h . Referring to the three levels of h we considered in our simulation, $h = 1$ would assign much higher weights only to those with little differences in their past and future realizations. In contrast, $h = 100$ would produce relatively equal weights across observations. It is important to note that the relative differences between different levels of h have to be examined under a particular empirical context, since the magnitude of the norms is not unit free and varies across different settings. For the empirical context of temperature impacts, like the one in this paper, we recommend choosing tuning parameters no lower than one and no higher than 100. Nevertheless, we remind the practitioners that there is essentially a trade-off to be made. The practitioner has to balance between relying on more representative historical data and focusing only on those past realizations that are highly similar

to their future counterparts.

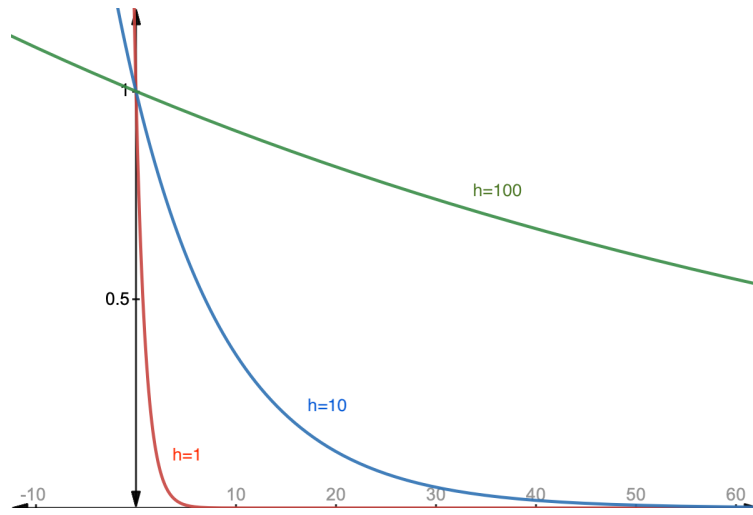


Figure A1: Weights under Different Tuning Parameters

Notes: The figure plots the function $y = e^{-x/h}$ on the space of (x, y) with $h = 1, 10, 100$, respectively.

Table A1: Simulation Mean of Model Coefficients and Mean Squared Error

DGP:		A		$QinA$		Q	
M_α	$X_{it,\alpha}^k$	$\bar{\beta}_\alpha^k$	MSE	$\bar{\beta}_\alpha^k$	MSE	$\bar{\beta}_\alpha^k$	MSE
A	A	1.000	}0.59	-5.218	}1.05	0.112	}1.56
B	B1	0.498	}0.59	-2.594	}1.06	-0.399	}1.21
	B2	0.498		-2.598		0.361	
Q	Q1	0.249	}0.59	-1.314	}1.05	-0.250	}0.59
	Q2	0.246		-1.206		0.000	
	Q3	0.248		-1.307		0.750	
	Q4	0.249		-1.305		0.000	
M	M1	0.085	}0.59	-0.463	}0.97	-0.083	}0.59
	M2	0.077		-0.411		-0.083	
	M3	0.085		-0.454		-0.083	
	M4	0.082		-0.312		0.000	
	M5	0.085		-0.509		0.000	
	M6	0.082		-0.444		0.000	
	M7	0.085		-0.411		0.250	
	M8	0.085		-0.396		0.250	
	M9	0.082		-0.500		0.250	
	M10	0.085		-0.391		0.000	
	M11	0.082		-0.471		0.000	
	M12	0.085		-0.437		0.000	
QinA	A	1.002	}0.59	0.202	}0.59	0.545	}1.56
	A ²	0.000		-0.050		-0.004	
Bins (10°F)	Bin(-∞,10]	-0.153	}0.62	0.715	}1.60	0.054	}1.13
	Bin[10,20]	-0.105		0.527		0.081	
	Bin[30,40]	-0.083		0.422		0.045	
	Bin[40,50]	-0.055		0.290		0.014	
	Bin[50,60]	-0.028		0.159		0.017	
	Bin[60,70]	0.026		-0.151		0.002	
	Bin[70,80]	0.053		-0.294		0.045	
	Bin[80,90]	0.073		-0.403		0.095	
	Bin[90,∞]	0.116		-0.704		0.253	

Notes: The table presents $\bar{\beta}_\alpha^k$, the simulation mean for each estimated element of the parameter vector in the models considered across 2000 simulation replications for each DGP (A , $QinA$ and Q). In this design, $n = 3074$ (the total number of counties in the dataset) and $T = 5$. We use $\bar{\beta}_\alpha^k$ to calculate the mean squared error $MSE(\bar{\beta}_\alpha) = \sum_{i=1}^n \sum_{t=1}^T (\tilde{y}_{it} - \tilde{x}'_{it,\alpha} \bar{\beta}_\alpha)^2 / (nT)$.



Figure A2: Simulation Results for the Model Selection Criteria

Notes: For each DGP, the figure plots the simulation probability (proportion) that a particular model (A , B , Q , M , $QinA$, or $Bins$) is chosen by a model selection criterion in a given model selection problem. The model selection problems we consider are labeled in the shaded sub-panel titles. The model selection criteria are listed on the left side of the sub-panels. The simulations are based on $n = 3000$, and the number of simulation replications is 500.



Figure A3: Simulation Results for the Model Selection Criteria ($n = 500$)

Notes: For each DGP, the figure plots the simulation probability (proportion) that a particular model (A , B , Q , M , $QinA$, or $Bins$) is chosen by a model selection criterion in a given model selection problem. The model selection problems we consider are labeled in the shaded sub-panel titles. The model selection criteria are listed on the left side of the sub-panels. The simulations are based on $n = 500$, and the number of simulation replications is 500.

Table A2: Ideal Targets Evaluated at Simulation Mean of Coefficients for $\tau = 15, 25$						
DGP:	A		QinA		Q	
	$\tau = 15$	$\tau = 25$	$\tau = 15$	$\tau = 25$	$\tau = 15$	$\tau = 25$
M_α :						
A	1.87×10^{-7}	2.15×10^{-7}	0.98	1.10	14.44	1.84
B	1.85×10^{-7}	3.17×10^{-7}	0.92	1.10	8.42	0.74
Q	2.77×10^{-7}	4.93×10^{-7}	0.94	1.11	2.77×10^{-7}	4.93×10^{-7}
M	4.27×10^{-7}	11.67×10^{-7}	0.92	1.54	4.27×10^{-7}	11.67×10^{-7}
QinA	2.10×10^{-7}	2.26×10^{-7}	2.10×10^{-7}	2.26×10^{-7}	14.27	1.83
Bin	0.07	0.09	4.27	4.89	1.81	1.13

Notes: The table presents the calculated ideal target $\frac{1}{n} \sum_{i=1}^n (\bar{\mu}_\alpha(\mathcal{W}_{i,T+\tau}^f) - \bar{\mu}_\alpha(\mathcal{W}_{iT}) - (\mu_\star(\mathcal{W}_{i,T+\tau}^f) - \mu_\star(\mathcal{W}_{iT})))^2$, where $\bar{\mu}_\alpha(\mathcal{W}_{iT}) = X_{iT}' \bar{\beta}_\alpha^k$ for the simulated $\bar{\beta}_\alpha^k$ in Table 2.

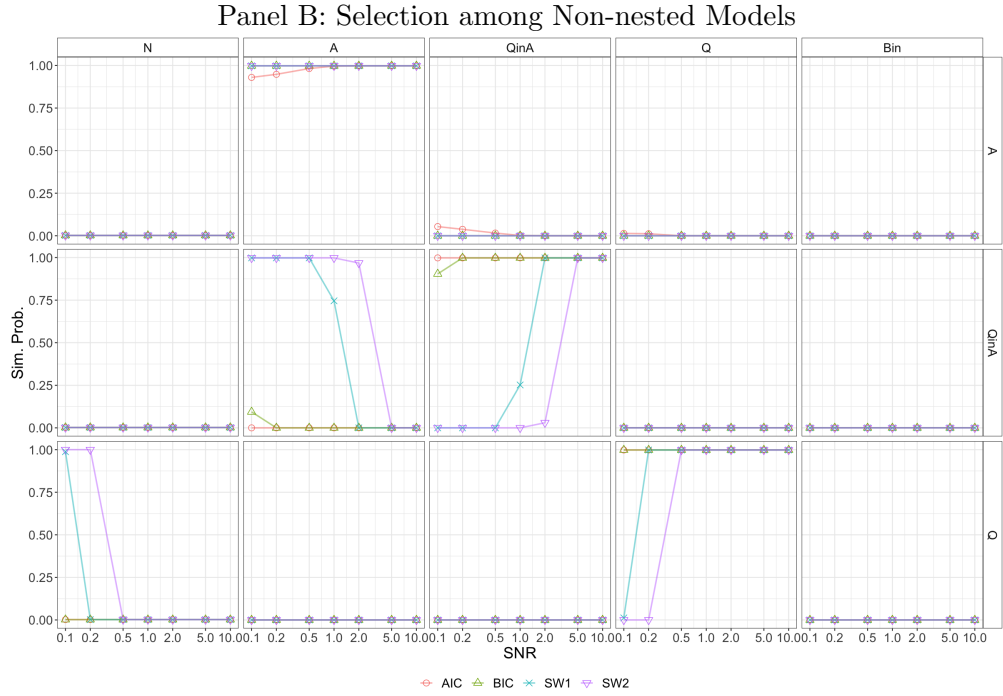
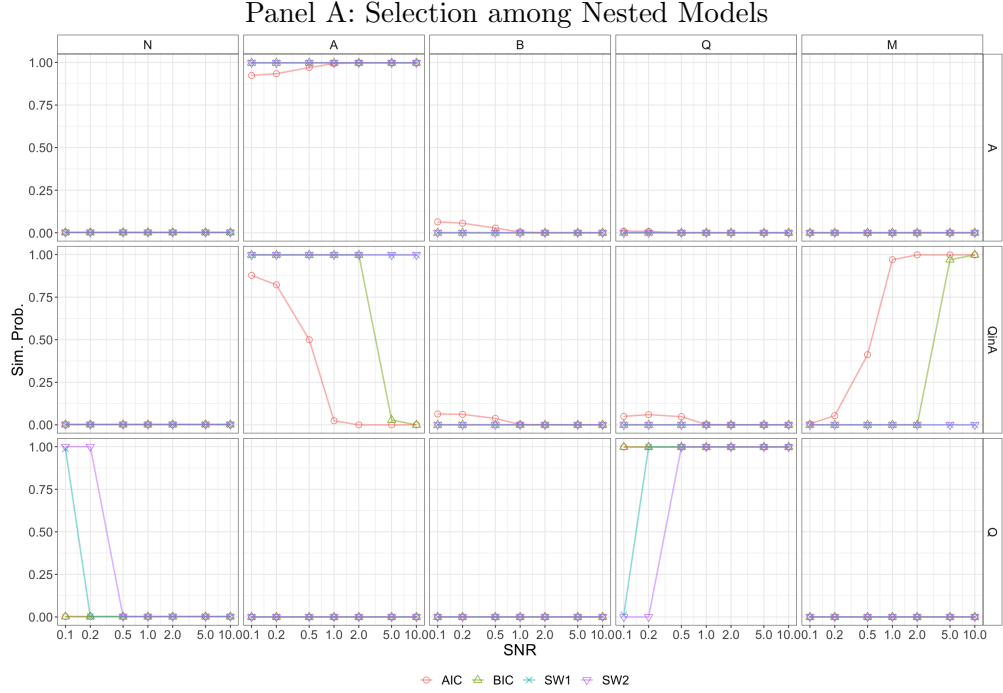


Figure A4: Simulation Results for the Model Selection Criteria under Different SNR

Notes: For each DGP (indicated on the right), the figure plots the simulation probability (proportion) that a particular model (indicated on the top) is chosen by a model selection criterion in a given model selection problem under a specific signal-to-noise ratio (SNR). Four information criteria are considered: AIC, BIC, SW1, and SW2. The scale of the horizontal axis is log-transformed.

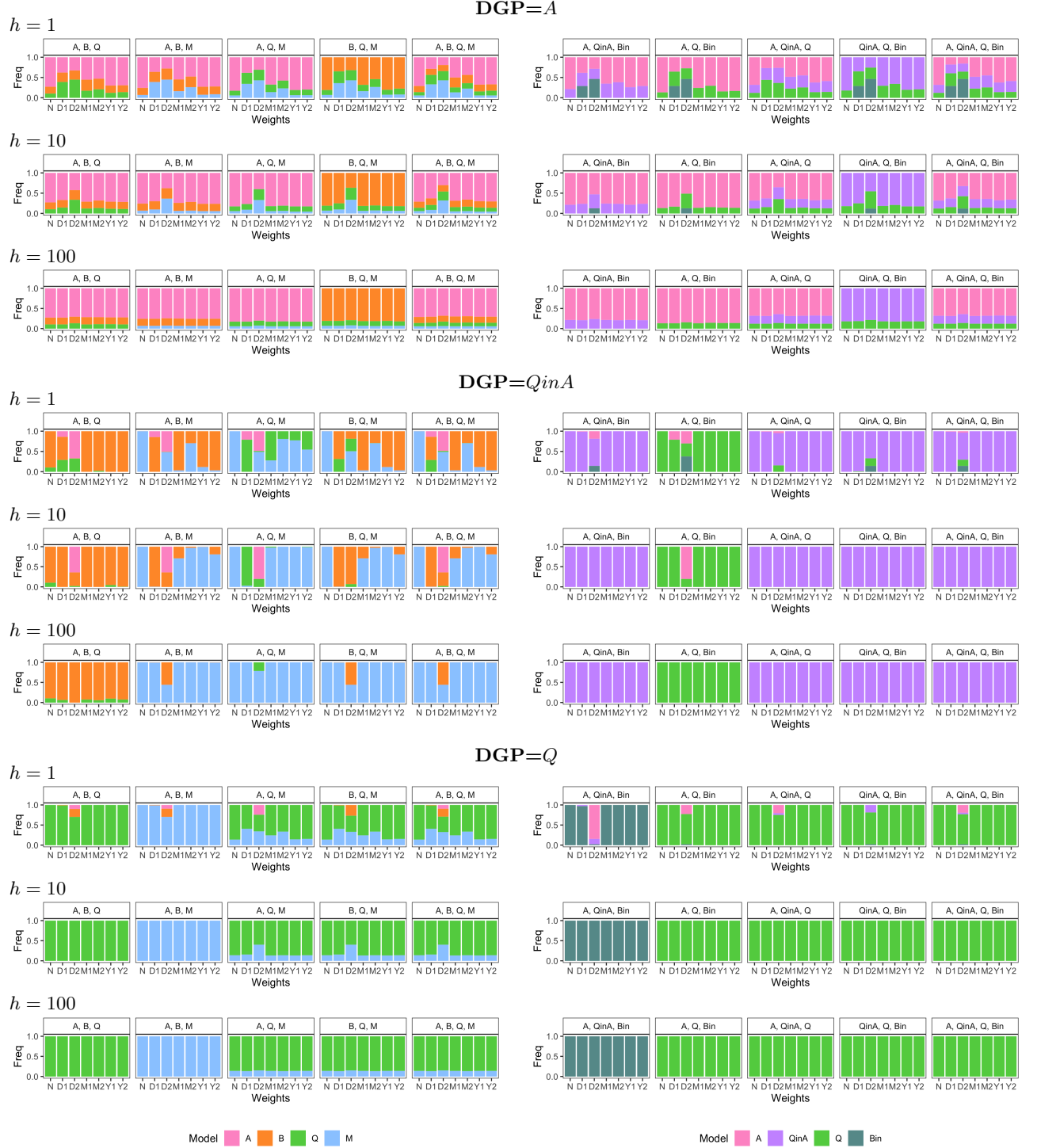


Figure A5: Simulated Model Selection Outcomes for $\tau = 15$

Notes: In each panel, the title indicates the set of models being compared, the horizontal axis labels different norms being considered for forming weights, the height of a colored bar indicates the proportion of times that a particular model is selected among the set of models. The five panels on the left are for comparisons across nested models and the five on the right are for possibly non-nested models. The results are based on $\tau = 15$.

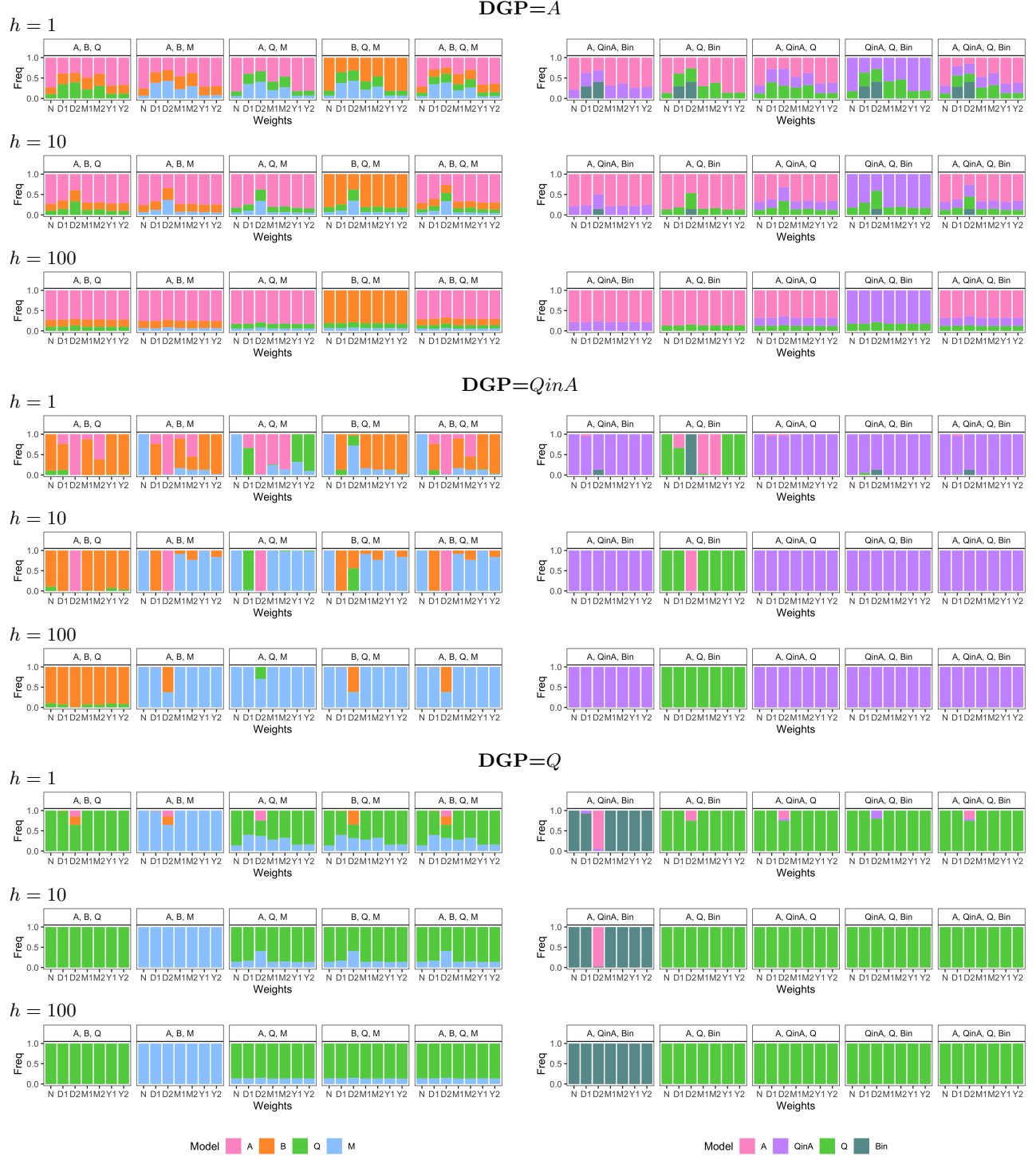


Figure A6: Simulated Model Selection Outcomes for $\tau = 25$

Notes: In each panel, the title indicates the set of models being compared, the horizontal axis labels different norms being considered for forming weights, the height of a colored bar indicates the proportion of times that a particular model is selected among the set of models. The five panels on the left are for comparisons across nested models and the five on the right are for possibly non-nested models. The results are based on $\tau = 25$.

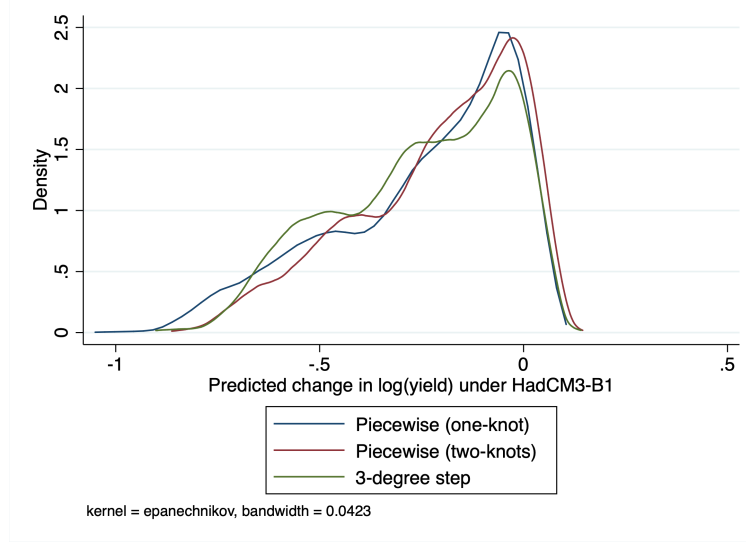


Figure A7: Distribution of Predicted Yield Changes under HadCM3-B1

Notes: The figure plots the kernel density estimates of the county-level predicted yield changes under the HadCM3-B1 climate scenario, based on the estimated one-knot, two-knots piecewise functions, and the 3°C step function.

Table A3: Models Minimizing Feasible Targets for $\tau = 15, 25$

DGP: h :	A			$QinA$			Q		
	1	10	100	1	10	100	1	10	100
$\tau = 15$									
N	A	A	A	QinA	QinA	QinA	Q	Q	Q
D1	QinA	A	A	QinA	QinA	QinA	Q	Q	Q
D2	M	M	A	Bin	QinA	QinA	B	M	Q
M1	A	A	A	QinA	QinA	QinA	Q	Q	Q
M2	A	A	A	QinA	QinA	QinA	Q	Q	Q
Y1	A	A	A	QinA	QinA	QinA	Q	Q	Q
Y2	A	A	A	QinA	QinA	QinA	Q	Q	Q
$\tau = 25$									
N	A	A	A	QinA	QinA	QinA	Q	Q	Q
D1	QinA	A	A	QinA	QinA	QinA	Q	Q	Q
D2	QinA	M	A	QinA	QinA	QinA	B	M	Q
M1	A	A	A	QinA	QinA	QinA	M	Q	Q
M2	M	A	A	QinA	QinA	QinA	M	Q	Q
Y1	A	A	A	QinA	QinA	QinA	Q	Q	Q
Y2	A	A	A	QinA	QinA	QinA	M	Q	Q

Notes: The table presents the model that minimizes the feasible target $\sum_{s=1}^{T-1} \frac{1}{n} \sum_{i=1}^n (\bar{\mu}_\alpha(\mathcal{W}_{i,T}) - \bar{\mu}_\alpha(\mathcal{W}_{i,T-s}) - (Y_{i,T} - Y_{i,T-s}))^2 \pi(\mathcal{W}_{i,T-s}, \mathcal{W}_{i,T+\tau})$, where $\bar{\mu}_\alpha(\mathcal{W}_{it}) = X'_{it} \bar{\beta}_\alpha^k$ and $\tau = 15, 25$. N indicates no weight; D1 and D2 are L^∞ and L^2 norms of daily differences; M1 and M2 are L^∞ and L^2 norms of monthly differences; Y1 and Y2 are L^∞ and L^2 norms of annual differences.

Table A4: Selecting Knots in Piecewise Yield Function Based on Minimized MSE

Unbalanced Panel				Balanced Panel			
One-knot Piecewise		Two-knot Piecewise		One-knot Piecewise		Two-knot Piecewise	
Knot	MSE	Knots	MSE	Knot	MSE	Knots	MSE
29	0.046905	24, 26	0.046478	30	0.029987	29, 33	0.047226
28	0.046959	23, 27	0.046483	31	0.030061	30, 32	0.047235
30	0.047258	25, 26	0.046488	29	0.030243	29, 34	0.047239
27	0.047331	24, 27	0.046497	32	0.030493	30, 31	0.047239
26	0.047903	31, 32	0.046499	28	0.030736	29, 32	0.047244
31	0.048043	30, 33	0.046499	33	0.031261	29, 35	0.047269
25	0.048573	22, 27	0.046505	27	0.031377	30, 33	0.047282
32	0.049233	23, 26	0.046507	26	0.032090	29, 31	0.047285
24	0.049271	30, 32	0.046536	34	0.032273	24, 26	0.047301
23	0.049950	25, 27	0.046538	25	0.032816	28, 36	0.047301

Notes: For illustration purpose, in each case, only the smallest ten MSEs and their corresponding knots are presented.

Table A5: Weather Impacts on Corn Yields: Unbalanced Sample

	(1)	(2)	(3)	(4)
Average temperature: April	0.0110*** [0.0020]			
Average temperature: May	0.0033 [0.0029]			
Average temperature: June	-0.0093 [0.0057]			
Average temperature: July	-0.0586*** [0.0084]			
Average temperature: August	-0.0305*** [0.0036]			
Average temperature: September	0.0021 [0.0047]			
GDD (8-32C, in 100C)		0.0802* [0.0316]		
GDD, squared		-0.0018* [0.0007]		
HDD (34C+), squared root		-0.1240*** [0.0123]		
Degrees accumulated above 0C			0.0002*** [0.0001]	0.0002 [0.0001]
Degrees accumulated above 24C				0.0059** [0.0017]
Degrees accumulated above 26C				-0.0107*** [0.0022]
Degrees accumulated above 29C			-0.0056*** [0.0007]	
Precipitation	0.1794*** [0.0169]	0.1141*** [0.0189]	0.1055*** [0.0201]	0.1068*** [0.0205]
Precipitation, squared	-0.0115*** [0.0012]	-0.0087*** [0.0014]	-0.0082*** [0.0015]	-0.0084*** [0.0015]
Signal-to-noise ratio	0.2529	0.3813	0.4082	0.3935
Observations	120,995	120,995	120,995	120,995

Notes: Standard errors (in brackets) are state-clustered. Significance: * .05, ** .01, *** .001.

Table A6: Weather Impacts on Corn Yields: Balanced Sample

	(1)	(2)	(3)	(4)
Average temperature: April	0.0126*** [0.0021]			
Average temperature: May	0.0008 [0.0028]			
Average temperature: June	0.0014 [0.0038]			
Average temperature: July	-0.0453*** [0.0082]			
Average temperature: August	-0.0320*** [0.0028]			
Average temperature: September	0.0075 [0.0050]			
GDD (8-32C, in 100C)		0.1768*** [0.0284]		
GDD, squared		-0.0041*** [0.0007]		
HDD (34C+), squared root		-0.1491*** [0.0101]		
Degrees accumulated above 0C			0.0003*** [0.0000]	0.0003*** [0.0000]
Degrees accumulated above 29C				-0.0055*** [0.0007]
Degrees accumulated above 30C			-0.0099*** [0.0006]	
Degrees accumulated above 33C				-0.0084** [0.0024]
Precipitation	0.2245*** [0.0293]	0.1498*** [0.0316]	0.1380*** [0.0294]	0.1347*** [0.0293]
Precipitation, squared	-0.0156*** [0.0025]	-0.0123*** [0.0026]	-0.0117*** [0.0025]	-0.0114*** [0.0025]
Signal-to-noise ratio	0.3019	0.6194	0.6225	0.5688
Observations	44,814	44,814	44,814	44,814

Notes: Standard errors (in brackets) are state-clustered. Significance: * .05, ** .01, *** .001.